Importance of African horse sickness virus NS2 protein phosphorylation for the formation of viral inclusion bodies

by

Gina Roebuck
(15281737)

Submitted in fulfilment of the requirements for the degree
Magister Scientiae
in the Faculty of Natural and Agricultural Sciences
Department of Biochemistry, Genetics, and Microbiology
University of Pretoria
April 2023

Under the supervision of Prof Jacques Theron

UNIVERSITEIT VAN PRETORIA
UNIVERSITY OF PRETORIA
YUNIBESITHI YA PRETORIA

DECLARATION

I, Gina Roebuck, declare that the dissertation, which I hereby submit for the degree MSc Microbiology at the University of Pretoria, is my own work and has not previously been submitted by me for a degree at this or any other tertiary institution.

Signature: ……

Date: April 2023

ACKNOWLEDGEMENTS

I would like to thank the following people for their direct and indirect contributions to this dissertation:

My supervisor, Prof Theron, for his guidance, patience, and belief in me to undertake this project. It has been a privilege to work under your supervision for these past few years.

My lab mates, past and present, for their assistance, and knowledge, and for providing a fun work environment.

Prof Vida van Staden for her support and advice, and for serving on the research committee.

The University of Pretoria and the Poliomyelitis Research Foundation for the financial support.

My Oupa who constantly believed in me and would always ask for updates on how my research was going, and his constant reminder of "nose to the grindstone" when things got hard.

My friends whose words of encouragement and support have been invaluable.

And finally, my husband, Dave Roebuck, for his unwavering support, encouragement, and love, as well as the many cups of tea, glasses of wine, and slabs of chocolate, to get me through the difficult moments. This would not have been possible without you by my side.

Dedicated to my Oupa,
Prof Daniel Jacobus Joubert Botha
1928 – 2022

SUMMARY

Importance of African horse sickness virus NS2 protein phosphorylation for the formation of viral inclusion bodies

by

Gina Roebuck

Supervisor: Prof. J. Theron
Department of Biochemistry, Genetics and Microbiology
University of Pretoria

for the degree MSc

African horse sickness virus (AHSV) is a member of the *Orbivirus* genus (family *Sedoreoviridae*, order *Reovirales*) and has a segmented double-stranded RNA genome that encodes seven structural proteins and four non-structural proteins. The non-structural protein NS2 has several properties that suggest it may play an important role in the virus replication cycle. Not only is NS2 the only virus-specified phosphoprotein, but it is also capable of binding single-stranded RNA and is the main component of the characteristic virus inclusion bodies (VIBs) observed in the cytoplasm of orbivirus-infected cells. Although VIBs are considered the sites at which virus replication and assembly occur, the factors that govern their formation are still poorly understood in the case of AHSV. Consequently, the aim of this study was to determine the importance of AHSV-4 NS2 protein phosphorylation for its ability to form intracellular inclusion bodies.

To identify the cellular kinase responsible for NS2 protein phosphorylation, *in vitro* phosphorylation assays were performed on an unphosphorylated version of the protein that was expressed in *Escherichia coli*. The NS2 protein could be phosphorylated by a protein kinase present in the cell lysate of *Spodoptera frugiperda* insect cells and by making use of a kinase-specific inhibitor, it was established that casein kinase 2 (CK2) is responsible for phosphorylating the NS2 protein. Previous studies reported that NS2 of different orbiviruses is phosphorylated on serine residues within its carboxyl (C) terminus. Consequently, the NS2 protein of AHSV-4 was subjected to bioinformatics analyses and four serine residues were

identified at positions 256, 258, 262 and 270 that were predicted target sites for CK2 phosphorylation. The importance of these serine residues for NS2 phosphorylation was investigated by making use of engineered recombinant baculoviruses expressing NS2 or NS2 mutants in which the serine residues were substituted with either alanine or with negatively charged aspartate residues to mimic phosphoserine residues. The phosphorylation state of the recombinant proteins expressed in *S. frugiperda* cells was determined by phosphoprotein staining, following electrophoresis of purified protein samples on SDS-polyacrylamide gels. The results indicated that NS2 is predominantly phosphorylated at serine residues 256 and 258 since the substitution of these residues severely diminished the phosphorylation signal. To evaluate the importance of NS2 protein phosphorylation for inclusion body formation, immunofluorescence confocal microscopy was performed on *S. frugiperda* cells infected with recombinant baculoviruses expressing NS2 or the NS2 mutant proteins. Analysis of the micrographs indicated that a mutant NS2 protein in which the serine residues at both positions 256 and 258 were substituted with alanine was unable to form intracellular inclusion bodies. However, when both of these residues were substituted with aspartate residues, inclusion bodies could be observed and thus suggested that the negative charges imparted by NS2 protein phosphorylation is important for inclusion body formation.

Overall, the results obtained in this study indicate that NS2 of AHSV-4 is phosphorylated by CK2 at serine residues 256 and 258 and that phosphorylation of the NS2 protein is required for the formation of intracellular inclusion bodies. This information may be combined in future studies with a reverse genetics approach to generate an AHSV-4 strain that expresses a phosphorylation-deficient NS2 protein, and thus provide a means whereby the importance of VIBs for virus replication and assembly can be investigated.

TABLE OF CONTENTS

LIST OF ABBREVIATIONS

A	absorbance
AHS	African horse sickness
AHSV	African horse sickness virus
Ala (A)	alanine
AP2	adaptor protein 2
Asp (D)	aspartic acid/aspartate
ATP	adenosine-5'-triphosphate
ATPase	adenosine triphosphatase
bp	base pair
BSA	bovine serum albumin
BTV	Bluetongue virus
°C	degrees Celsius
C	carboxyl
Ca^{2+}	calcium
cDNA	complementary DNA
CK2	Casein kinase 2
CLP	core-like particle
cm^2	cubic centimetre
CTD	C-terminal domain
CTP	cytidine 5'-triphosphate
DAPI	4',6-diamidino-2'-phenylindole dihydrochloride
DIVA	differentiating infected from vaccinated animals
DNA	deoxyribonucleic acid
dNTP	deoxyribonucleoside-5'-triphosphate
ds	double-stranded
DTT	1,4-dithiothreitol
EDTA	ethylenediaminetetra-acetic acid
EHDV	Epizootic haemorrhagic disease virus
EMSA	electrophoretic mobility shift assays
ERK	extracellular signal-regulated kinase
et al.	*et alia* (and others)
FBS	foetal bovine serum
Fig.	figure
FRAP	fluorescence recovery after photobleaching
GTP	guanosine 5'-triphosphate
h	hour
H_2O_2	hydrogen peroxide
i.e.	*id est* (that is)
IB	inclusion body
IKKε	I-kappa-B-kinase epsilon
IMAC	immobilized metal affinity chromatography
IPTG	isopropyl-β-D-thiogalactopyranoside
JAK/STAT	Janus kinase/signal transducers and activators of transcription
kb	kilobase pairs

kDa	kilodalton
KOAc	potassium acetate
LB	Lysogeny broth
LLPS	liquid-liquid phase separation
M	molar
MAPK	mitogen-activated protein kinase
MAVS	mitochondrial antiviral-signaling protein
mg	milligram
min	minute
ml	millilitre
mM	millimolar
MOI	multiplicity of infection
mRNA	messenger ribonucleic acid
MTT	3-(4,5-dimethylthiazol-2-yl)-2,5-diphenyltetrazolium bromide
MVA	modified vaccinia Ankara
MVBs	multivesicular bodies
N	amino
N7MTase	N7-methyltransferase
NaOAc	sodium acetate
ng	nanogram
nm	nanometre
no.	number
nt	nucleotides
NTD	N-terminal domain
NTPase	nucleoside triphosphate phosphohydrolase/nucleoside triphosphatase
NTPs	nucleoside triphosphates
OD	optical density
OIE	Office International des Epizootics
2’ O MTase	nucleoside-2’-O-methyltransferase
ORF	open reading frame
ORN	nuclease-resistant oligoribonucleotide
PAGE	polyacrylamide gel electrophoresis
PBS	phosphate-buffered saline
PCR	polymerase chain reaction
PD	polymerase domain
PEG	polyethylene glycol
pfu	plaque forming unit
PML-NBs	promyelocytic leukaemia nuclear bodies
poly(A)	poly(adenylate)
poly(U)	poly(uridylate)
PP2A	protein phosphatase 2A
PSB	protein solvent buffer
RdRP	RNA-dependent RNA polymerase
RLR	RIG-I-like receptor
RNA	ribonucleic acid
RNase	ribonuclease
rpm	revolutions per minute
s	second

S	Svedberg unit
SAXS	small-angle X-ray scattering measurements
SDS	sodium dodecyl sulphate
Ser (S)	serine
Sf-9	*Spodotera frugiperda* clone 9
ss	single-stranded
TBB	4, 5, 6, 7-tetrabromobenzotriazole
TEMED	N',N',N',N'-tetramethylethylenediamine
Tris	Tris-hydroxymethyl-aminomethane
TX-100	Triton X-100
U	units
µg	microgram
µl	microlitre
µm	micrometre
µM	micromolar
UTP	uridine 5'-triphosphate
UTR	untranslated region
UV	ultraviolet
V	volts
v.	version
v/v	volume per volume
VIB	viral inclusion body
VLP	virus-like particle
w/v	weight per volume
X-Gal	5-bromo-4-chloro-3-indolyl β-D-galactopyranoside
α	alpha
β	beta
γ	gamma

LIST OF FIGURES

LIST OF TABLES

CHAPTER ONE

PREFACE

The genus *Orbivirus* (family *Sedoreoviridae*, order *Reovirales*) includes several animal pathogens that are of economic importance such as Bluetongue virus (BTV), African horse sickness virus (AHSV) and Epizootic haemorrhagic disease virus (EHDV). Unlike other *Sedoreoviridae* family members, orbiviruses are transmitted to their vertebrate host by *Culicoides* biting midges (Diptera, Ceratopogonidae) and are capable of replicating within both the vector insect and mammalian host (Gorman *et al.*, 1983; Carpenter *et al.*, 2017). African horse sickness (AHS), of which AHSV is the causative agent, is remarkably variable in its clinical manifestation and can range from a mild fever form to an acute (pulmonary) form with a mortality rate of up to 95% in naïve horse populations (Coetzer and Guthrie, 2004). The disease is listed as a notifiable equine disease by the World Organization of Animal Health (OIE: Office International des Epizooties) due to its negative impact on animal welfare, considerable economic losses to the equestrian industry, the risk of rapid global spread, and its impact on the international trade of horses (MacLachlan and Guthrie, 2010; Clemmons *et al.*, 2021). AHS is endemic to sub-Saharan Africa; however, outbreaks outside the endemic region have occurred in the Persian Gulf, the Middle East, Europe and, more recently, Thailand (Zientara *et al.*, 2015; King *et al*., 2020).

Similar to the Bluetongue virus (BTV), the prototype orbivirus species, AHSV has a genome of 10 linear double-stranded (ds) RNA segments (S1 to S10) that are enclosed within two protein capsids (Manole *et al.*, 2012). The inner capsid is composed of five highly conserved proteins (VP1, VP3, VP4, VP6 and VP7), whereas the outer capsid comprises two variable proteins (VP2 and VP5). In addition, the viral genome also encodes four non-structural proteins (NS1, NS2, NS3/3A and NS4) in virus-infected cells that are produced at different stages of the infectious cycle. The NS4 protein has been shown to be dispensable for virus replication (Ratinier *et al.*, 2011), but it is considered to be a key determinant of viral virulence (Ratinier *et al.*, 2016; Li *et al.*, 2021). In contrast, the other non-structural proteins are involved in virus morphogenesis processes that lead to the assembly and release of progeny virions from infected cells. The NS1 and NS2 proteins are synthesized abundantly in virus-infected cells and their synthesis coincides with the appearance of two virus-specific structures, *i.e.*, tubules and granular viral inclusion bodies (VIBs), respectively (Huismans and Els, 1979; Brookes *et al*., 1993). Although the function of the tubules is not yet understood fully, the NS1 protein has nevertheless been implicated as playing a role in morphogenesis and release of progeny virions (Eaton *et al.*, 1990; Owens *et al.*, 2004). The VIBs, of which NS2 is a major component, are believed to be the sites in which virus assembly occurs and are considered to be of central

importance in the virus replication strategy (Kar *et al.*, 2007; Patel and Roy, 2014). The two closely related NS3 and NS3A proteins, which are synthesized in low abundance in orbivirus-infected cells (Huismans, 1979), play a role in the final stages of viral morphogenesis by facilitating the release of progeny virions from infected cells (Hyatt *et al.*, 1993; Celma and Roy, 2009).

Investigations of the NS2 protein of BTV have indicated that it is a multifunctional protein and several properties of NS2 suggest that it might play an important role in the virus replication cycle. The NS2 protein forms multimers and the size of the NS2 oligomers is likely to be between six and eight subunits (Taraporewala *et al.*, 2001), with more recent structural investigations favouring a decameric composition (Mumtsidu *et al.*, 2007). Unlike other BTV proteins, NS2 has a strong affinity for single-stranded (ss) RNA, but not for dsRNA (Huismans *et al.*, 1987; Thomas *et al.*, 1990; Taraporewala *et al.*, 2001). It has subsequently been reported that NS2 displays preferential and specific binding to viral ssRNA (Theron and Nel, 1997; Lymperopoulos *et al.*, 2003). The NS2 protein is therefore of particular interest, because of its possible involvement in genome recognition (preference for viral ssRNA versus cellular RNA), which is known to be an early essential step in the assembly process of viruses. Indeed, during the assembly of progeny orbivirus virions, the positive-strand ssRNA is packaged and then replicated to form a dsRNA genome segment by the RNA-dependent RNA polymerase (VP1) inside the progeny virions (Mertens and Diprose, 2004; Matsuo and Roy, 2013). Moreover, the NS2 protein also has the enzymatic activity of hydrolyzing nucleotide triphosphates (NTPs) to their corresponding nucleotide monophosphates (Horscroft and Roy, 2000; Taraporewala *et al.*, 2001). Although the significance of the enzymatic activity is not clear, it has been suggested that the NTPase action of NS2 may play a role in providing energy for the assortment, movement, packaging, or condensation of bound ssRNA (Horscroft and Roy, 2000).

As highlighted previously, the NS2 protein is the predominant component of VIBs observed in virus-infected cells (Brookes *et al.*, 1993; Uitenweerde *et al.*, 1995). Expression of BTV NS2, in the absence of other viral proteins in both insect and mammalian cells, results in the formation of inclusion bodies (IBs) that are indistinguishable from VIBs found in virus-infected cells and thus indicates that NS2 is solely responsible for the formation of VIBs (Thomas *et al.*, 1990; Uitenweerde *et al.*, 1995). Notably, the presence of BTV structural

proteins and ssRNA, as well as newly assembled subcore and core particles in and around the periphery of VIBs has led to the proposal that virus assembly and replication occur at these sites (Hyatt and Eaton, 1988; Kar *et al.*, 2007; Patel and Roy, 2014). Unique features of NS2 are that it is capable of binding Ca^{2+} (Rahman *et al.*, 2020) and it is the only virus-specific protein that is phosphorylated in BTV-infected cells (Huismans *et al.*, 1987; Devaney *et al.*, 1988) or when expressed in insect cells using a baculovirus recombinant (Thomas *et al.*, 1990). Initial studies indicated that BTV NS2 purified to homogeneity could be phosphorylated *in vitro* without the addition of an exogenous kinase (Huismans *et al.*, 1987), but subsequent studies demonstrated that NS2 lacks autophosphorylation activity (Theron *et al.*, 1994; Taraporewala *et al.*, 2001). More recently, it was reported that BTV NS2 is phosphorylated at two serine residues in the carboxyl (C)-terminal region of the protein by the ubiquitous cellular kinase Casein kinase 2 (Modrof *et al.*, 2005). The functional importance of NS2 phosphorylation has been investigated for BTV, and it was reported that phosphorylation of the NS2 protein is important for VIB formation but not for ssRNA binding (Thomas *et al.*, 1990; Modrof *et al.*, 2005; Mohl and Roy, 2016).

In contrast to BTV, the properties and biological importance of the AHSV NS2 protein have not yet been investigated in great detail. Studies regarding AHSV NS2 have reported that it is phosphorylated (Devaney *et al.*, 1988; Theron *et al.*, 1994), able to self-associate to form multimeric assemblies in complex with ssRNA (Uitenweerde *et al.*, 1995) and is responsible for the formation of VIBs (Uitenweerde *et al.*, 1995). Studies regarding the structure-function relationships of different AHSV genes and encoded proteins, as well as mapping of the function of some of these proteins, have been facilitated greatly by the baculovirus expression system (Uitenweerde *et al.*, 1995; Maree and Huismans, 1997; de Waal and Huismans, 2005; Stassen *et al.*, 2011; Bekker *et al.*, 2014; Boughan *et al.*, 2020). These types of investigations generally rely on a combination of mutagenesis and expression of the AHSV mutant proteins by appropriately constructed baculovirus recombinants in *Spodoptera frugiperda* insect cell culture, followed by studies to assess the effect(s) of the newly introduced mutations on protein function. It can therefore be envisaged that a similar strategy would allow for a greater understanding of the functional importance of AHSV NS2 phosphorylation. Consequently, this dissertation reports on investigations undertaken to identify phosphate-acceptor residues within the AHSV NS2 protein and to determine the functional significance of NS2 phosphorylation concerning the formation of intracellular inclusion bodies.

CHAPTER TWO

LITERATURE REVIEW

2.1 GENERAL INTRODUCTION

African horse sickness (AHS), which is caused by the African horse sickness virus (AHSV), is an infectious but non-contagious disease that most commonly affects horses. The disease can also occur in other equids such as donkeys, mules, and zebra, but they rarely exhibit clinical symptoms (Coetzer and Guthrie, 2004; Mellor and Hamblin, 2004). AHS can manifest different symptoms in infected animals. These symptoms can include fever, lack of appetite, and lesions that are associated with damage to the circulatory and respiratory systems and result in oedema of the lungs, pleura, and subcutaneous tissues, as well as haemorrhages in various organs and tissues (Thompson *et al.*, 2012). The mortality rate of AHS is dependent on which form of the disease occurs but has been reported to be as high as 95% in naïve horse populations (Coetzer and Guthrie, 2004). AHS is considered to be economically important due to its potential for high mortality rates in naïve horse populations and its economic impact on the trade and movement of animals between AHS-affected and AHS-free areas. In addition, morbidity and mortality from AHS within working equids may also constrain the draft power that these horses and donkeys provide in low-income countries and consequently, may affect food security and poverty alleviation (De Vos *et al.*, 2012; Carpenter *et al.*, 2017; Clemmons *et al.*, 2021). As a result, AHS has been listed as a notifiable equine disease by the World Organization for Animal Health (WOAH, 2022) and has also been declared a state-controlled disease in South Africa (Animal Diseases Act No. 35 of 1984).

The first historical account of AHS is found in an Arabian document that describes an outbreak of the disease in 1327 in Yemen (Mellor and Hamblin, 2004). However, the first description of the disease on the African continent dates back to the 16th century. Father Monclaro, in his account of the journey of Francisco Baro in 1569 to East Africa, described a disease outbreak among the horses that were imported from India. Almost a century later, in 1652, the first settlers arrived at the then Cape of Good Hope and this was soon followed, in 1657, by the importation of horses and mules from Europe and the Far East. In 1719 the first severe outbreak of AHS occurred and led to the death of 1 700 horses. Over the subsequent 217 years following this outbreak, at least 10 major and several lesser outbreaks have been recorded in South Africa. The most severe AHS outbreak in South Africa occurred in 1854-1855, which led to the death of an estimated 70 000 horses that represented 40% of the horse droves (Mellor and Hamblin, 2004). Over the last century, the frequency and severity of the outbreaks have declined and can be ascribed to the implementation of improved surveillance measures, in addition to strict

zoning measures and the vaccination of horses (Bosman *et al.*, 1995; Mellor and Hamblin, 2004; Robin *et al.*, 2016).

Much of the pioneering research on AHSV was performed by Sir Arnold Theiler during the early 20th century (reviewed in Coetzer and Guthrie, 2004), and several studies were undertaken in the 1960s and 1970s to characterize the morphology and structure of AHSV (Oellerman *et al.*, 1970; Verwoerd and Huismans, 1972; Bremer, 1976). Consequently, AHSV has been classified as a member of the *Orbivirus* genus in the family *Sedoreoviridae* (formerly known as *Reoviridae*). This virus family consists of several viruses that all have segmented double-stranded (ds) RNA genomes located inside a virus particle comprising an inner and an outer protein capsid (Mertens, 2004). The development of gene cloning, genetic engineering and protein expression technologies has greatly facilitated studies aimed at characterizing the structure-function relationships of different AHSV genes and their cognate gene products (Uitenweerde *et al.*, 1995; Maree and Huismans, 1997; de Waal and Huismans, 2005; Stassen *et al.*, 2011; Bekker *et al.*, 2014; Boughan *et al.*, 2020). Despite the progress that has been made, much still remains to be understood concerning the molecular-genetic events underlying the infection cycle of AHSV and the role that individual viral proteins may play in these processes. Of special interest in this regard is the non-structural protein NS2. The NS2 protein is the only viral-encoded phosphoprotein and assembles into cytoplasmic virus inclusion bodies (VIBs), which are believed to be the sites at which virus morphogenesis occurs. Consequently, NS2 is thought to be crucially important in the generation of appropriately formed progeny virions and is considered central to a productive virus infection cycle. However, the functional importance of AHSV NS2 protein phosphorylation is not known and merits further investigation.

In this review of the literature, aspects relating to AHS epidemiology will be summarized. This will be followed by a discussion of AHSV structure, encoded viral proteins and the infection cycle of the virus. The literature review will then be concluded by a discussion of the non-structural protein NS2 and its role in virus replication and morphogenesis, after which a description of the aims of this study will be provided.

2.2 AFRICAN HORSE SICKNESS (AHS)

2.2.1 Geographical distribution

AHS is endemic in tropical and subtropical areas of Africa south of the Sahara, occupying a broad band stretching from Senegal in the west to Ethiopia and Somalia in the east, and extending as far south as northern South Africa (Mellor and Hamblin, 2004). All nine serotypes of AHSV occur throughout sub-Saharan Africa, including eastern, central and southern Africa (Coetzer and Guthrie, 2004). Outbreaks of AHS caused by multiple serotypes occurred in Ethiopia from 2007 to 2010, and outbreaks caused by AHSV-2 and AHSV-7 occurred in West Africa where only serotype 9 had previously been detected (Diouf *et al.*, 2013; Aklilu *et al.*, 2014). Although AHS is believed to be confined largely to sub-Saharan Africa, there have been several outbreaks of the disease in the Persian Gulf, the Middle East, and southern European countries (Zientara *et al.*, 2015). Countries, where epizootics occurred outside the African continent, include Yemen (1930), the Middle East (AHSV-9, 1959–1961), Israel (1944), Spain (AHSV-9, 1966; AHSV-4, 1987–1990), Portugal (AHSV-4, 1989) and Thailand (AHSV-1, 2020). Notably, the latter was the first incidence of AHS occurring in Southeast Asia and of serotype 1 outside of Africa (King *et al.*, 2020).

The impact of AHS on the equine industry is best illustrated by two outbreaks that occurred in the 20th century. The outbreak of AHS, caused by serotype 9, between 1959-1961 in the Middle Eastern countries and the Persian Gulf (Iran, Saudi Arabia, Pakistan, Afghanistan, India, Turkey, Cyprus, Iraq, Syria, Lebanon, and Jordan) resulted in the death of more than 300 000 equids (Howell, 1960; Howell, 1963), and is still regarded as the most extensive epizootic to date. Moreover, the outbreak of AHS, caused by serotype 4, in Spain from 1987-1990 resulted from the importation of sub-clinically infected zebra from Namibia to a safari park outside Madrid, and subsequently spread to Morocco and Portugal (Rodriguez *et al.* 1992). Although the outbreak was eradicated by means of massive vaccination campaigns and the culling of horses, the equine industries of the affected countries suffered major economic losses that were estimated at $30 million (Mellor, 1993). Different factors such as an increase in the number of different serotypes observed within the northern limits of the virus' range (Dufour *et al.*, 2008), climate change that affects the distribution of vector insects (Purse *et al.*, 2008; Gale *et al.*, 2010; Assefa *et al.*, 2022), and increased international trade and movement of animals

(MacLachlan and Guthrie, 2010; Martínez-Lopez *et al*., 2011) have raised concerns that AHSV may be re-introduced in European countries with potentially devastating consequences.

2.2.2 Susceptible species and transmission

African horse sickness (AHS) affects primarily equine species (horses, donkeys and mules). Horses are the most susceptible to the disease and mortality rates ranging between 70 to 95% have been recorded in naïve horse populations (Coetzer and Guthrie, 2004; Mellor and Hamblin, 2004). Zebra, however, rarely exhibit any clinical signs of AHSV infection. As a result, different African zebra species (*Equus burchelli*, *E. quagga*, and *E. grevyi*) are believed to be the natural vertebrate host and reservoir of AHSV and consequently, are considered to play an important role in the persistence of the virus in Africa (Barnard *et al.*, 1994). Notably, donkeys in South Africa appear to be naturally resistant to AHSV and infected animals rarely display clinical symptoms of the disease. The mortality rate in African donkeys (*E. africanus*) is less than 10% and they may therefore also act as an additional reservoir host for AHSV in South Africa (Hamblin *et al.*, 1998). Antibodies to AHSV have been detected in dogs, cattle, sheep, goats, camels, buffalo, and elephants (Erasmus *et al*., 1978; van Rensberg *et al*., 1981; Awad *et al.*, 1981; Barnard, 1997; Fassi-Fihri *et al*., 1998; El Hasnaoui *et al*., 1998; van Sittert *et al.*, 2013). However, there is a lack of evidence to support a role for domestic ruminants and wildlife, aside from zebra, in AHS epidemiology.

AHS is not contagious, and the virus is primarily transmitted to susceptible equid hosts via biting haematophagous midges of the *Culicoides* genus (du Toit, 1944; Carpenter *et al.*, 2017). An adult *Culicoides* becomes infective eight days after feeding on a viraemic animal and stays infected until death. The virus replicates in the gut and salivary glands of the insect vector, without adversely affecting the insect, and is subsequently transmitted from the *Culicoides* vector to a susceptible equid host when the midge takes a blood meal (Meiswinkel *et al.*, 2000). Although approximately 30 of the more than 1 500 *Culicoides* species are capable of transmitting orbiviruses, *C. imicola* is believed to be the primary vector of AHSV in Europe, Africa, and Asia (Mellor, 1994; Leta *et al.*, 2019). *C. bolitinos*, which has a wide distribution in southern Africa and is common in cooler highland areas where *C. imicola* is rare, has also been identified as a potential vector of AHSV (Venter *et al.*, 2000). Moreover, in Spain, AHSV has been found in *C. obsoletus* and *C. pulicaris*, both of which are the most common *Culicoides* species in northern and central Europe (Mellor *et al.*, 1983; Mellor *et al.*, 1990). In Australia and some parts of Asia, *C. falvus* and *C. actoni* are the primary vectors of AHSV (Mellor,

1994). It has also been reported that *C. sonorensis* (formerly known as *C. variipennis*), which is dominant in North America, is a highly efficient vector for AHSV in the laboratory (Boorman *et al*., 1975; Wellby *et al*., 1996). This has raised concerns that should AHSV viraemic animals enter areas of North America where *C. sonorensis* occurs (most of the southern and western United States), the transmission of the virus is highly possible and may have severe consequences on the equine industry (Mellor and Hamblin, 2004).

2.2.3 Clinical syndromes

After transfer of AHSV by the bite of infected *Culicoides* spp. midges, the virus is transported to the lymph nodes of the animal where initial virus replication occurs. The progeny virions are then disseminated by the bloodstream throughout the body of the animal, resulting in infection of myocardial endothelial cells and a range of secondary organs such as the choroid plexus, lungs, lymphoid tissues, pharynx, and spleen (Coetzer and Guthrie, 2004). Pathogenesis and the severity of disease symptoms displayed by the infected host are influenced by various factors that include viral tropism, the virulence of the virus strain, and the immunological status of susceptible animals (Laegreid *et al.*, 1993).

Four distinct clinical syndromes have been described in horses with AHS, *i.e.*, the pulmonary (acute), cardiac (subacute), mixed pulmonary and cardiac (cardio-pulmonary), and fever forms (Coetzer and Guthrie, 2004). The fever form of the disease frequently occurs in horses with some degree of pre-existing immunity or following infection with less virulent AHSV strains. Symptoms of the fever form develop after an incubation period of 5-14 days and the affected horses display mild to moderate fever, oedema of the supraorbital fossae, and mild depression. The animals make a complete recovery and there is no mortality associated with this form of the disease. The cardiac form has an incubation period of 7-14 days and results in mild fever, as well as pericardial effusion, and oedema of the subcutaneous and intermuscular tissue of the head, neck, and chest. Approximately 35% of horses affected with this form of the disease recover, but mortality rates exceeding 50% have been reported. The mixed pulmonary and cardiac form of AHS has symptoms of both forms of the disease. The mortality rate is approximately 70%, with death occurring within 3-6 days after the onset of fever. The pulmonary form of AHS, which occurs commonly in horses with no pre-existing immunity, develops rapidly (within 4 to 5 days), and is characterized by respiratory distress, dyspnea, coughing spasms, and a frothy, gelatinous exudate from the horse's nostrils that may be tainted with blood. The mortality rate exceeds 95%, with terminal hypothermia and death occurring

24-48 h after the occurrence of the first clinical signs (Coetzer and Guthrie, 2004; Thompson *et al.*, 2012).

2.2.4 Prevention and control of AHS

Although there is currently no specific treatment for animals suffering from AHS, the virus is non-contagious and can only be spread through the bites of infected *Culicoides* spp. Consequently, control of AHS is effected through the use of insecticides and repellents to control the vector insect population, as well as restriction of animal movement to prevent infected animals from initiating new foci of infection, and slaughtering of viraemic animals to prevent them from serving as sources of virus for vector insects (Mellor and Hamblin, 2004; Robin *et al.*, 2016; Shults *et al.*, 2021). Another control measure is aimed at minimizing host-vector interaction by stabling horses in insect-free facilities during times of maximum vector activity, thereby reducing the incidence of AHS (Meiswinkel *et al*., 2000).

In addition to the above, control of AHS in endemic areas may be effected by the vaccination of susceptible equines, which is considered to be the most practical and effective control measure. In South Africa, AHS is controlled by vaccination with polyvalent, live-attenuated vaccines that are administered twice in the first and second year of life of susceptible animals, and annually thereafter (MacLachlan *et al.*, 2007). The vaccine consists of two cocktails of different AHSV serotypes, namely a trivalent (serotypes 1, 3 and 4) and a quadrivalent (serotypes 2, 6, 7 and 8) combination. Serotypes 5 and 9 are excluded in the current vaccine formulation due to difficulties experienced in the attenuation of serotype 5, and serotype 9 historically rarely caused disease in South Africa. However, serotypes 8 and 6, respectively, afford a degree of cross-protection in vaccinated animals (von Teichman *et al.*, 2010). Although the polyvalent live-attenuated vaccine has reduced the impact of AHS in South Africa, its use is associated with several concerns. These include the possible exchange of genome segments with field strains that could result in new uncharacterized viruses, a high risk of introducing new virus serotypes into non-endemic countries since the vaccine cocktails are produced with viruses prevalent in South Africa, and the inability to distinguish (naturally) infected and vaccinated animals (DIVA principle) (MacLachlan *et al.*, 2007; Oura *et al.*, 2012; Weyer *et al.*, 2016). These drawbacks make live-attenuated vaccines unsuitable for use in the naïve horse populations of non-endemic geographic regions such as Europe.

To address the above concerns, various attempts have been made to develop safe and efficacious AHSV vaccines. Subunit vaccines, based on the use of the virus outer capsid protein VP2 and expressed by means of recombinant baculoviruses, have been investigated (Martínez-Torrecuadrada and Casal, 1995; Scanlen *et al.*, 2002; Kanai *et al.*, 2014). Although the VP2 subunit vaccines induced protection in horses, further development of these subunit vaccines has been hampered by the low yield of soluble baculovirus-expressed VP2 protein (du Plessis *et al.*, 1998) and the need for potent adjuvants to enhance immunogenicity (Scanlen *et al.*, 2002). Consequently, the use of recombinant virus vectors as a means of vaccine delivery has been investigated more extensively. A recombinant Venezuelan equine encephalitis virus-derived vector, expressing the AHSV-4 outer capsid proteins VP2 and VP5, has been developed but failed to induce neutralizing antibodies in horses (MacLachlan *et al.*, 2007). In contrast, immunization with recombinant canarypox virus-vectored vaccines, co-expressing VP2 and VP5, was reported to induce complete protection in horses (Guthrie *et al.*, 2009; El Garch *et al.*, 2012). Furthermore, a modified vaccinia Ankara (MVA) strain, which is replication-deficient, was used for the expression of different AHSV antigens (VP2, VP7 and NS3 of AHSV-4) and presented in ponies (Chiam *et al.*, 2009). Analysis of the antibody responses indicated that only the VP2 vaccine was capable of inducing a neutralizing antibody response. In a study to investigate a polyvalent vaccination approach, horses were immunized simultaneously with an MVA vector expressing VP2 of either AHSV-4 or AHSV-9 (Manning *et al.*, 2017). Immunization of horses with these virus vector vaccines induced neutralizing antibodies against both AHSV-4 and AHSV-9, as well as a cross-protective response to AHSV-6 in horses that received the MVA virus vector vaccine expressing VP2 of AHSV-9. More recently, virus-like particles (VLPs) have been synthesized through co-expression of the four AHSV capsid proteins (VP2, VP3, VP5 and VP7) in plants and evaluated as vaccines (Dennis *et al.*, 2018a; Rutkowska *et al.*, 2019; O'Kennedy *et al.*, 2022). These plant-produced AHSV VLPs were shown to elicit a strong neutralizing immune response in guinea pigs (Dennis *et al.*, 2018b) and a weak neutralizing humoral immune response in 6-month-old foals (Rutkowska *et al.*, 2019). A promising strategy to generate a new generation of AHS vaccines relies on the use of a reverse genetics approach. Despite variations in their molecular design and methodology, the various reverse genetics systems all share a common feature, which is the availability of cloned cDNA encoding viral genomes that can be genetically modified and manipulated to generate live viruses containing engineered changes in their genomic nucleic acids (Conradie *et al.*, 2016; Calvo-Pinilla *et al.*, 2020). This approach has been used to generate serotyped and replication-deficient AHS vaccine strains (van de Water *et al.*, 2015;

Lulla *et al*., 2016). Protective efficacy studies with the replication-deficient virus strains in mice showed that vaccinated mice were protected against homologous virulent virus challenge (Lulla *et al.*, 2016) and it was subsequently demonstrated that the virus strains also provided protection in ponies (Lulla *et al.*, 2017; Sullivan *et al.*, 2021).

2.3 AFRICAN HORSE SICKNESS VIRUS (AHSV)

2.3.1 Taxonomic classification

AHSV, of which nine different AHSV serotypes have been distinguished serologically (McIntosh, 1958), is a member of the *Orbivirus* genus within the family *Sedoreoviridae* (order *Reovirales*). Viruses within this family possess segmented double-stranded (ds) RNA genomes (10-12 segments) that are encapsidated within non-enveloped virus particles. The virus particles exhibit icosahedral symmetry and typically have a diameter of 55-87 nm (Matthijnssens *et al.*, 2022a). The *Reovirales* includes fifteen genera and is subdivided into two families, based on the presence of a "turret" protein on the core particle (Matthijnssens *et al.*, 2022a; Matthijnssens *et al.*, 2022b). The *Sedoreovirinae* family contains six non-turreted virus genera, *i.e.*, *Cardoreovirus*, *Mimoreovirus*, *Orbivirus*, *Phytoreovirus*, *Rotavirus* and *Seadornavirus*. The *Spinareovirinae* family contains nine "turreted" virus genera, *i.e.*, *Aquareovirus*, *Coltivirus*, *Cypovirus*, *Dinovernavirus*, *Fijivirus*, *Idnoreovirus*, *Orthoreovirus*, *Oryzavirus* and *Mycoreovirus*. Orbiviruses differ from other members of the *Reovirales* by the presence of a double-layered protein capsid, their greater sensitivity to lipid solvents and detergents, loss of virus infectivity in mildly acidic conditions, and they are able to replicate in both insects and vertebrates (Gorman *et al.*, 1983).

2.3.2 Virion structure

The AHSV virion comprises two concentric protein shells, which are also referred to as the inner and outer capsids, that surround the genome of 10 linear segments of dsRNA (Oellerman *et al.*, 1970; Manole *et al.*, 2012). The outer capsid comprises two proteins, VP2 and VP5, which together form a continuous layer that covers the inner capsid or core. The core particle is composed of two major (VP3 and VP7) and three minor (VP1, VP4 and VP6) proteins, in addition to the dsRNA genome (Manole *et al.*, 2012).

The structure of the AHSV-4 virion has been determined by making use of cryo-electron microscopy and three-dimensional image reconstruction (Manole *et al.*, 2012). The structure of the AHSV particle was reported to be comparable to that of the Bluetongue virus (BTV), the prototype orbivirus, of which the structure of the single- and double-shelled virus particles has been determined by cryo-electron microscopy and X-ray crystallography (Stuart and Grimes, 2006). The AHSV core particle can be segregated into two distinct layers. The innermost layer is a T=1 lattice composed of 60 asymmetric dimers of the triangular-shaped VP3 protein that forms a complete shell while minimizing conformational distortion. The internal VP3 scaffold is stabilized by the outer layer of the core, which is composed of 780 VP7 monomers and arranged as 260 trimers on a T=13 lattice. The core contains the dsRNA genome and the transcription complexes consisting of VP1, VP4, and VP6, each of which plays an important role in genome RNA replication (Mertens and Diprose, 2004; Patel and Roy, 2014). The outer shell of AHSV is highly ordered and consists of globular VP5 proteins that are located upon each of the six-membered rings of the VP7 trimers. Manole *et al.* (2012) suggested that AHSV VP5 is likely to be similar to the VP5 of BTV both in shape and fold topology, but they were unable to make a reliable homology model of AHSV VP5 to confirm this. Furthermore, the 180 copies of VP2 are arranged as 60 triskelion-type motifs, which are centred directly on top of the VP7 trimers. Together, VP2 and VP5 form a continuous layer surrounding the core. A schematic diagram of the AHSV particle is presented in Fig. 2.1.

2.3.3 The viral dsRNA genome

The genome of AHSV comprises 10 linear dsRNA segments of varying sizes, which are grouped into large (S1-S3), medium (S4-S6) and small (S7-S10), according to their electrophoretic mobility through a polyacrylamide gel (Oellerman *et al.*, 1970; Bremer, 1976). Except for S10 and S9, each of the genome segments encodes for a single protein. The S9 genome segment of AHSV contains two overlapping open reading frames and, in addition to VP6, encodes the non-structural protein NS4 (Firth, 2008; Zwart *et al.*, 2015). The S10 genome segment of AHSV encodes for the two related non-structural proteins NS3 and NS3A via different in-frame translation initiation sites (van Staden and Huismans, 1991).

The total length of the AHSV genome is approximately 19.5 kilobase pairs (kb) (Potgieter *et al*., 2015). The 5' untranslated regions (UTRs) of the respective genome segments range in size between 11 and 35 base pairs (bp), whereas the 3' UTRs are 29 to 100 bp in length (Roy *et al.*, 1994; Potgieter *et al*., 2015). In contrast to BTV (Rao *et al.*, 1983), the terminal

hexanucleotide sequences of AHSV are not conserved throughout all of the genome segments and comprise of 5'-GUU$^{A}/_{U}$ A$^{A}/_{U}$… and …AC$^{A}/_{U}$UAC-3' sequences (Potgieter *et al.*, 2015).

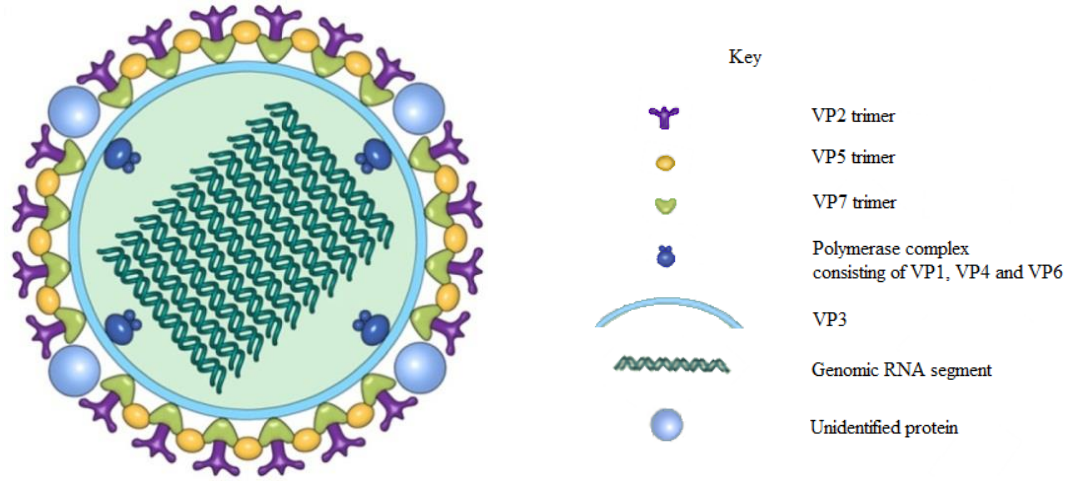

Figure 2.1: Schematic representation of the AHSV-4 virion. The structural arrangement of the AHSV virion was modelled based on data obtained from cryo-electron microscopy. The VP3 protein (light blue) encloses the dsRNA segments of the AHSV genome (forest green) and the proteins of the transcription complex, namely VP1, VP4 and VP6 (dark blue). Attached to the VP3 surface are the VP7 trimers (light green), upon which the VP2 protein (purple) is attached. The VP5 protein (yellow) is located in the spaces made by the VP2 lattice. The virion also has an additional density on the surface from an unidentified protein (pale blue circles). The figure was adapted from Manole *et al.* (2012).

However, similar to BTV (Roy, 1989), AHSV also contains short segment-specific sequences with partial inverted complementarity adjacent to the terminal hexanucleotide sequences (Roy *et al*., 1994). This feature is thought to play a role in determining the secondary (panhandle) structures in the corresponding viral mRNAs. The segment-specific secondary structures have been suggested to act as sorting signals for the incorporation of each positive-sense mRNA transcript into progeny viral capsids (Markotter *et al.*, 2004; Burkhardt *et al*., 2014). Alternatively, it has also been suggested that these structures may facilitate second-strand synthesis after packaging in the viral capsid by holding the ssRNA in a panhandle structure to guide the RNA-dependent RNA polymerase viral enzyme (Pritlove *et al.*, 1995; Mertens and Diprose, 2004). Moreover, these structural motifs have also been suggested to be involved in disparate functions such as protection of the viral mRNA against exonuclease degradation, transcriptional regulation, and/or facilitating translational termination (Roy, 2013).

2.3.4 AHSV proteins

The AHSV genome encodes seven structural proteins (VP1-VP7) and four non-structural proteins (NS1, NS2, NS3/3A and NS4). The 10 AHSV genome segments, together with their encoded proteins and likely functions, are summarized in Table 2.1. Based on the volume of research that has been undertaken on BTV, information on AHSV will be supplemented with that obtained from studies undertaken on BTV in the following sections.

2.3.4.1 Outer capsid proteins

The VP2 protein, one of the two major structural proteins that form the outer capsid, is the most variable of the viral proteins (Potgieter *et al.*, 2003). Based on its outermost location on the virion, VP2 is the major serotype-specific antigen (Huismans and Erasmus, 1981; Kanai *et al.*, 2014) and viral haemagglutinin (Cowley and Gorman, 1987). Neutralizing epitopes have been mapped on AHSV VP2 (Bentley *et al.*, 2000; Martínez-Torrecuadrada *et al.*, 2001) and VP2 is capable of eliciting neutralizing antibodies, as discussed previously (Section 2.2.4). Moreover, VP2 is involved in the attachment of the virus to cells and has been reported to bind to a sialoglycoprotein (Hassan and Roy, 1999; Zhang *et al.*, 2010), heparin sulfate (Mecham and McHolland, 2010), or sialic acid (Wu and Roy, 2022) prior to internalization of the virus particle. In addition to its role in attachment, VP2 is also an emerging player in the control of BTV assembly and egress from infected cells. The amino (N)-terminal of the protein interacts with vimentin intermediate filaments and this interaction was shown to contribute to virus

Table 2.1: AHSV-4 genome segments and encoded proteins

Genome segment (size in bp)	Protein(s) encoded (size in kDa)	Location	Protein functions
S1 (3 965)	VP1 (150)	Core	RNA-dependent RNA polymerase is responsible for RNA transcription/replication.
S2 (3 229)	VP2 (123)	Outer Capsid	Serotype-determining protein possesses viral haemagglutination and neutralization activity, cellular receptor binding protein that allows for the attachment of the virus to cells.
S3 (2 792)	VP3 (103)	Core	Subcore structural protein that controls the size and organization of the core structure, interacts with transcriptase complex proteins and recruits VP7 to VIBs in order to promote core assembly.
S4 (1 977)	VP4 (76)	Core	Methyl transferase protein that caps and methylates the viral mRNAs.
S5 (1 746)	NS1 (63)	Infected cell	Forms tubules during virus replication, which consist of helically coiled ribbons of dimers. Although the function of NS1 tubules in virus replication is unclear, it may be involved in viral morphogenesis, pathogenesis and/or regulation of viral gene expression.
S6 (1 564)	VP5 (57)	Outer Capsid	VP5 and VP2 form the outer capsid. VP5 induces low levels of neutralizing antibodies, and VP5 is involved in the permeabilization of the endosomal membrane in a pH-dependent manner to release the transcriptionally active core particle into the cell cytoplasm.
S7 (1 167)	VP7 (38)	Core	Forms the outer core surface and may mediate attachment of the core particle to insect cells.
S8 (1 166)	NS2 (41)	Infected cell	Forms viral inclusion bodies (VIBs), binds to ssRNA, and possesses NTPase activity that may play a role in providing energy for the assortment, movement, or packaging of viral mRNA.
S9 (1 160)	VP6 (38)	Core	Binds ssRNA and dsRNA, RNA-dependent ATPase and helicase activities that may function to unwind the dsRNA before replication or to dissociate newly synthesized viral mRNA from template strand after synthesis.
	NS4 (20)	Infected cell	Binds dsDNA may counteract the host anti-viral response (interferon antagonist) and is a virulence determinant.
S10 (822)	NS3 (23) / NS3A (22)	Infected cell	Disrupts the plasma membrane to enable virus release, affects virulence and down-regulates the interferon response.

transport and egress (Bhattacharya *et al*., 2007; Celma and Roy, 2009). It has also been reported that the extracellular treatment of mammalian cells with a combination of VP2 and VP5 proteins is sufficient to trigger apoptosis (Mortola *et al*., 2004; Vermaak and Theron, 2015). Recently, using a reverse genetics approach, van Gennip *et al.* (2017) reported that the expression of VP2 in mammalian cells is not essential for virus replication *in vitro*. In contrast, the lack of VP2 expression in insect cells severely hampered viral replication and abolished the release of virions.

Although present in the outer shell, the outer capsid protein VP5 is mostly unexposed on the surface of the virus and interacts with the core proteins (Manole *et al.*, 2012). Despite its location, the VP5 protein of AHSV may also play a role in neutralization. The AHSV VP5 protein, in contrast to that of BTV (Marshall and Roy, 1990), can induce neutralizing antibodies, albeit at lower levels than VP2 (Martínez-Torrecuadrada *et al.*, 1999). Consequently, AHSV VP5 may play a supportive role to VP2 in enhancing the immune response. With regards to a biological function, studies on VP5 of BTV (Hassan *et al.*, 2001; Xia *et al.*, 2021) and AHSV (Stassen *et al.*, 2011) have shown that the protein permeabilizes host cell membranes. This activity of VP5 is mediated by two N-terminal amphipathic helices (Forzan *et al*., 2007) and low pH-induced conformational changes in VP5 (Zhang *et al*., 2016; Xia *et al.*, 2021). The ability to permeabilize membranes is believed to play a major role in destabilizing the membrane of the endocytosized vesicle, thus allowing the release of the transcriptionally active core particle into the cytoplasm. BTV VP5 also interacts with membrane lipid rafts via a WHAL motif and is likely to play an important part in docking VP5 with plasma membranes for assembly and/or egress via membrane fusion (Bhattacharya and Roy, 2008).

2.3.4.2 Major core proteins

The major core proteins, VP7 and VP3, form the outer layer of the viral core particle. Co-expression of AHSV VP3 and VP7 in insect cells using baculovirus recombinants results in their spontaneous assembly into core-like particles (CLPs), which structurally resemble empty authentic AHSV cores (Maree *et al*., 1998; Maree *et al*., 2016). Of the two proteins, VP7 is the most abundant protein in the core particle and self-assembles into trimers, which form the outermost shell of the core (Basak *et al.*, 1992; Manole *et al*., 2012). For both BTV and AHSV, VP7 has been demonstrated to be a serogroup-specific antigen (Huismans and Erasmus, 1981; Chuma *et al*., 1992). The crystal structure of a single domain, namely the top domain, of AHSV

VP7 has been solved (Basak *et al.*, 1996) and was found to be structurally similar to that of BTV VP7 (Basak *et al.*, 1992). The top domain contains a conserved surface-exposed Arg-Gly-Asp (RGD) tripeptide, which in the case of BTV, has been demonstrated to mediate attachment of cores to cultured *Culicoides* cells in the absence of the outer capsid proteins (Xu *et al.*, 1997; Tan *et al.*, 2001). However, in contrast to BTV, AHSV VP7 forms flat hexagonal crystals in the cytoplasm of virus-infected cells (Burroughs *et al.*, 1994; Bekker *et al.*, 2014) and recombinant baculovirus-infected cells (Maree and Paweska, 2005; Bekker *et al.*, 2014). The functional significance of the VP7 crystalline structures is not yet understood fully. It has been proposed to represent a by-product rather than an essential component of AHSV replication (Burroughs *et al.*, 1994) and, more recently, it has been suggested that VP7 crystalline particles play a role in the release of AHSV from mammalian cells (Bekker *et al.*, 2022).

The VP3 protein is the most conserved major capsid protein among different AHSV serotypes (Iwata *et al.*, 1992). In addition to playing a crucial role in the structural integrity of the core particle by providing a scaffold for the VP7 trimers, the VP3 protein also contains group-specific antigenic determinants (Inumaru *et al.*, 1987), and it is capable of binding to RNA (Loudon and Roy, 1992), the non-structural protein NS2 (Kar *et al.*, 2004), and the structural protein VP6 (Matsuo *et al.*, 2018). The VP3 protein is the only viral protein that can self-assemble into particles in the absence of other viral proteins (Kar *et al.*, 2004). In addition to its structural role, a recent report suggested that VP3 of BTV interferes with the induction of the innate immune response by partially inhibiting the RIG-I-like Receptor (RLR)-dependent signalling pathway (Pourcelot *et al.*, 2021). Specially, VP3 was shown to interact with the mitochondrial antiviral-signalling protein (MAVS) and the IKKε kinase, which are two of the key components of the RLR-signalling pathway, thereby resulting in the inhibition of RIG-I-mediated interferon-β production.

2.3.4.3 Minor core proteins

The AHSV and BTV cores are transcriptionally active and have associated RNA-dependent RNA polymerase activity (van Dijk and Huismans, 1980; Vermaak *et al.*, 2015). The three minor structural proteins VP1, VP4, and VP6, which are collectively referred to as the "transcription complex", are candidates for the virus-directed RNA polymerase and associated enzymes that are solely responsible for the synthesis of capped and methylated transcripts of each dsRNA genome segment during the infection cycle (Mertens and Diprose, 2004).

The VP1 protein is the RNA-dependent RNA polymerase (RdRp) and exhibits detectable RNA-elongation activity in the presence of single-stranded poly(U) template and a poly(A) primer (Roy *et al*., 1988; Urakawa *et al*., 1989). More recently, it was reported that recombinant BTV VP1 also exhibits processive replicase activity, synthesizing complete complementary RNA strands of *in vitro*-synthesized BTV ssRNA templates (Boyce *et al.*, 2004). Crystallographic modelling of VP1 revealed the structure and organization of the protein to be typical of previously described RdRps and the protein comprises a polymerase domain (PD), N-terminal domain (NTD), and C-terminal domain (CTD) (Wehrfritz *et al.*, 2007; He *et al.*, 2019). Mutagenesis studies of a catalytic Gly-Asp-Asp (GDD) motif, located within the polymerase domain, concluded that this motif was essential to protein function (Wehrfritz *et al.*, 2007). Subsequent *in vitro* studies have indicated a degree of specificity in the replicase activity of VP1. The BTV VP1 protein was shown to synthesize dsRNA from BTV and rotavirus ssRNA transcripts, but not from non-virally derived sequences unless they were fused with BTV sequences at the 5' and 3' termini (Matsuo and Roy, 2011). This implies that common secondary structural elements present in the ssRNA transcripts of members of the *Sedoreoviridae* family may be required for RdRp replication.

The 5'-ends of the viral mRNA are capped and methylated during transcription, thus stabilizing the viral mRNA synthesized during virus infection and enabling efficient translation (Muthukrishnan *et al*., 1975; Matsuo and Roy, 2009). The BTV VP4 protein has been reported to possess guanylyltransferase and methyltransferase type 1 and type 2 activities, *i.e.*, guanine-N7-methyltransferase (N7MTase) and nucleoside-2'-O-methyltransferase (2' O MTase) activities (Ramadevi *et al.*, 1998; Martinez-Costas *et al.*, 1998; Stewart and Roy, 2015). BTV VP4 furthermore binds to GTP and displays nucleoside triphosphate phosphohydrolase (NTPase) activity, which may be important for transcription and RNA processing (Ramadevi and Roy, 1998). The atomic structure of BTV VP4 has been solved and reported to display an elongated architecture with various active sites (Sutton *et al*., 2007). The manner in which these active sites are organized suggests that it may allow the sequential catalytical activities required to produce the methylguanosine cap structures on nascent viral mRNA transcripts (Sutton *et al*., 2007). The 2' O MTase domain present in the VP4 protein of BTV has been characterized in order to identify the residues that are important for the catalytic activity of 2' O MTase and their influence on BTV replication was examined (Stewart and Roy, 2015). The results indicated that single substitution mutations in the catalytic tetrad Lys-Asp-Lys-Glu (K-

D-K-E) were sufficient to abolish 2' O MTase activity *in vitro* and completely inhibited BTV replication in mammalian cells. Although the AHSV VP4 protein has not yet been studied in any detail, the BTV and AHSV VP4 proteins share a high degree of homology (Noriko *et al*., 1993) and it can therefore be expected that the functions of the AHSV and BTV VP4 proteins may be conserved.

The third minor core protein, VP6, is a highly basic protein that is capable of binding to ATP, ssRNA and dsRNA, and displays ATPase and helicase activities (Roy *et al*., 1990; Hayama and Li, 1994; Stauber *et al*., 1997). AHSV VP6 contains a stretch of charged amino acids that is capable of binding to dsRNA (de Waal and Huismans, 2005). In the presence of a denaturing agent, the ssRNA and dsRNA binding activities are retained, suggesting that they occur independently of the VP6 tertiary structure and in close association with the viral genome in the core (Roy *et al*., 1990). Regions in VP6 of BTV (Hayama and Li, 1994) and AHSV (Turnbull *et al*., 1996) share homology with ATPase domains of known helicases. Similar to other helicases, BTV VP6 forms stable hexamers in the presence of nucleic acids (Kar and Roy, 2003). The RNA-dependent ATPase and helicase functions of VP6 may therefore mediate the unwinding of the dsRNA genome segments ahead of the VP1 RNA-dependent RNA polymerase and may also allow for separation of the parental and newly synthesized RNAs following transcription (Stauber *et al*., 1997). Mutagenesis studies indicated that deletion of amino acid residues 93-130 of the BTV VP6 protein, which contains an ATP-binding/ATPase motif, abrogated ATPase activity and precluded the recovery of viable BTV through a reverse genetics approach (Matsuo *et al.*, 2014). Likewise, targeted mutagenesis of a ssRNA binding motif (amino acid residues 246-258) in the VP6 protein of BTV also precluded virus recovery (Sung *et al.*, 2019). The results of these studies therefore not only indicate that VP6 is critical for virus replication, but also implicate VP6 in the packaging of viral genomic RNA. Indeed, studies on BTV and AHSV, utilizing reverse genetics, indicated that VP6-deficient viruses produced empty viral particles upon infection of BSR cells and are unable to replicate in these cells (Matsuo and Roy, 2009; Matsuo and Roy, 2013; Lulla *et al.*, 2016).

2.3.4.4 Non-structural proteins

The NS1 protein is synthesized abundantly and is readily assembled into tubular structures within the cytoplasm of AHSV- and BTV-infected cells. These tubules are biochemically and morphologically distinct from the microtubules and neurofilaments present in uninfected cells

(Huismans and Els, 1979). The tubular structures are formed by helically coiled ribbons of NS1 dimers (Kerviel *et al.*, 2019). The biophysical character of the tubules differs between BTV and AHSV. BTV tubules are 52.3 nm in diameter and 1 µm in length (Hewat *et al*., 1992a; Kerviel *et al*., 2019), whereas AHSV tubules are thinner and longer (23 nm in diameter; 4 µm in length), and they do not display the ladder-like structure characteristic of BTV NS1 tubules (Maree and Huismans, 1997). Several roles for NS1 have been proposed; however, its function in orbivirus infection still remains unclear. It was initially suggested that NS1 is involved in the trafficking of virus particles from the virus inclusion bodies (VIBs) to the cell membrane prior to virus release (Eaton *et al.*, 1990) or, alternatively, that tubules inhibit the formation of core particles before the incorporation of minor proteins and genome segments (Eaton *et al.*, 1990; Hewat *et al.*, 1992b). The NS1 protein has also been proposed to be a major determinant of BTV pathogenesis in the vertebrate host since it augments virus-cell association that ultimately leads to lysis of the infected cell and thereby, the release of progeny virions (Owens *et al*., 2004). More recently, it was shown that a luciferase reporter gene exhibited up-regulation of expression upon co-expression with NS1 and it appeared that NS1 enhanced BTV protein synthesis by specifically interacting with the hexanucleotides of the 3' UTRs of BTV ssRNA transcripts (Boyce *et al*., 2012). Based on these results, it was suggested that NS1 may play a crucial role in regulating viral gene expression by allowing preferential expression of BTV transcripts through interaction with the conserved sequence at their 3' terminus (Boyce *et al*., 2012).

The NS2 protein is a major component of the VIBs observed in the cytoplasm of cells infected with AHSV and BTV (Brookes *et al*., 1993; Uitenweerde *et al*., 1995). The VIBs are believed to be the sites at which assembly occurs since they contain ssRNA, virus structural proteins, and incomplete virus particles (Hyatt and Eaton, 1988; Eaton *et al*., 1990; Kar *et al.*, 2007). The NS2 protein has a strong affinity for ssRNA but not for dsRNA (Huismans *et al.*, 1987; Lymperopoulos *et al*., 2003), suggesting that it may play a role in the recruitment of viral mRNA prior to encapsidation. NS2 is the only virus-specific protein that binds to Ca^{2+} (Rahman et al., 2020) and is phosphorylated in infected cells (Huismans *et al*., 1987; Devaney *et al.*, 1988). In the case of BTV, phosphorylation of NS2 by Casein kinase 2 (CK2) is required for VIB formation (Modrof *et al.*, 2005). Furthermore, NS2 displays a nucleoside-triphosphatase (NTPase) activity and can bind and hydrolyze ATP and GTP to their corresponding nucleotide monophosphates (Horscroft and Roy, 2000; Taraporewala *et al*., 2001). However, the functional importance of these enzymatic activities is not yet understood

fully. The aforementioned properties of NS2 will be discussed in greater detail under Section 2.6 of the Literature Review, as they are related to the aims of this study.

The AHSV NS3 and NS3A proteins are encoded by the S10 genome segment from alternate in-phase translation initiation codons and differ only with respect to 10 amino acid residues present at the N-terminal end of NS3 (van Staden and Huismans, 1991). Interestingly, bioinformatics analysis of the S10 genome segment of different orbiviruses indicated the presence of an additional overlapping +1 open reading frame that encodes for a protein of 59 amino acids (Sealfon *et al.*, 2015). Although it has been established that this protein has a nucleolar localization, its function is not known and requires further investigation (Stewart e*t al.*, 2015). In contrast to NS1 and NS2, the NS3 and NS3A proteins are synthesized in low abundance in orbivirus-infected cells (Huismans, 1979; French *et al*., 1990; van Staden *et al*., 1995). The NS3 proteins are the only virus-encoded membrane-associated proteins (Wu *et al*., 1992; van Niekerk *et al.*, 2001) and transmission electron microscopy studies revealed that the NS3 proteins are localized to the sites of virus release in infected cells (Hyatt *et al.*, 1993; Stoltz *et al.*, 1996). NS3 has also been shown to interact specifically with VP2 in newly formed BTV virions (Beaton *et al.*, 2002; Celma and Roy, 2009). These findings suggest a role for NS3 during the final stages of viral morphogenesis by facilitating the release of progeny virus from infected cells. Despite its role in virus release, reports have also indicated that expression of NS3/NS3A is not required for virus replication in both mammalian and insect cells (Feenstra *et al.*, 2014; van Gennip *et al.*, 2014). Nevertheless, NS3 of BTV has been reported to interfere with the induction of the innate immune response in non-haematopoietic cells by down-regulating the production of type-I interferon via the RIG-I-like receptor (RLR)-dependent signalling pathway (Chauveau *et al.*, 2013), and more recently it was reported that both NS3 and NS4 of BTV interfere with interferon-I signalling in the JAK/STAT pathway by targeting the SH2 domain of STAT1 (Li *et al.*, 2021). Moreover, the NS3 protein has also been reported to activate the mitogen-activated protein kinase/extracellular signal-regulated kinase (MAPK/ERK) pathway through its interaction with the serine/threonine protein kinase B-Raf, thereby leading to increased viral replication in virus-infected cells (Kundlacz *et al.*, 2019).

The NS4 protein was described after bioinformatics analysis of the S9 genome segment of BTV detected an open reading frame overlapping the VP6 gene, as well as in the VP6 cistron of other orbiviruses such as AHSV (Firth, 2008). Characterization of the BTV NS4 protein indicated that it rapidly accumulates in both mammalian and *Culicoides* insect cells and, at 4 h

post-infection, NS4 aggregates are present throughout the cytoplasm as well as in the nucleoli of infected cells (Belhouchet *et al.*, 2011; Ratinier *et al.*, 2011). Although NS4 was shown to be dispensable for BTV replication, both in mammalian and insect cells, it nevertheless conferred a replication advantage to BTV-8, but not to BTV-1, in cells in an interferon-induced antiviral state (Ratinier *et al.*, 2011). It was suggested that NS4 may play an important role in virus-host interaction and that it may be a possible mechanism, at least by BTV-8, to counteract the antiviral response of the host. In addition to its role as a potential interferon antagonist, NS4 was more recently reported to be a key determinant of viral virulence (Ratinier *et al*., 2016). The NS4 protein of AHSV has only been characterized recently (Zwart *et al.*, 2015). In contrast to BTV and other orbiviruses, the AHSV NS4 protein occurs as one of two major types, depending on the virus serotype, and is designated as NS4-I or NS4-II. These iso-proteins differ in their amino acid lengths (145 for NS4-I and 154 for NS4-II) and are less conserved than the NS4 protein of different BTV serotypes. Although AHSV NS4 is capable of binding to dsDNA, the protein neither localizes to the nucleolus nor does it associate with cytoplasmic lipid droplets (Zwart *et al*., 2015). Interestingly, Boughan *et al.* (2020) suggested that the NS4 protein of AHSV might play a role in interfering with cellular factors involved in signalling related to the innate immune response. The NS4 protein was shown to co-localize with promyelocytic leukaemia nuclear bodies (PML-NBs), which are nuclear bodies involved in antiviral responses against a variety of DNA and RNA viruses (Boughan *et al.*, 2020). It was subsequently shown that NS4 of AHSV disrupts JAK/STAT signalling by interfering with the phosphorylation and/or translocation of STAT1 and pSTAT1 into the cell nucleus (Wall *et al.*, 2021). Such a role for AHSV NS4 would be in agreement with reports indicating that the NS4 protein of BTV acts as a type I interferon antagonist (Rojas *et al.*, 2021; Li *et al.*, 2021).

2.5 ORBIVIRUS INFECTION CYCLE

Although there are considerable differences in several of the replicative processes of members of the *Sedoreoviridae* family, the overall strategy appears to be the same. Using BTV as a model for orbivirus replication and morphogenesis (Fig. 2.2), four major events in the replication cycle of orbiviruses have been identified and are discussed below in greater detail. These events are: adsorption and penetration, uncoating and formation of replicative complexes, formation of virus tubules and virus inclusion bodies, and movement of the virus to, and release from, the cell surface (Mertens, 2004; Patel and Roy, 2014).

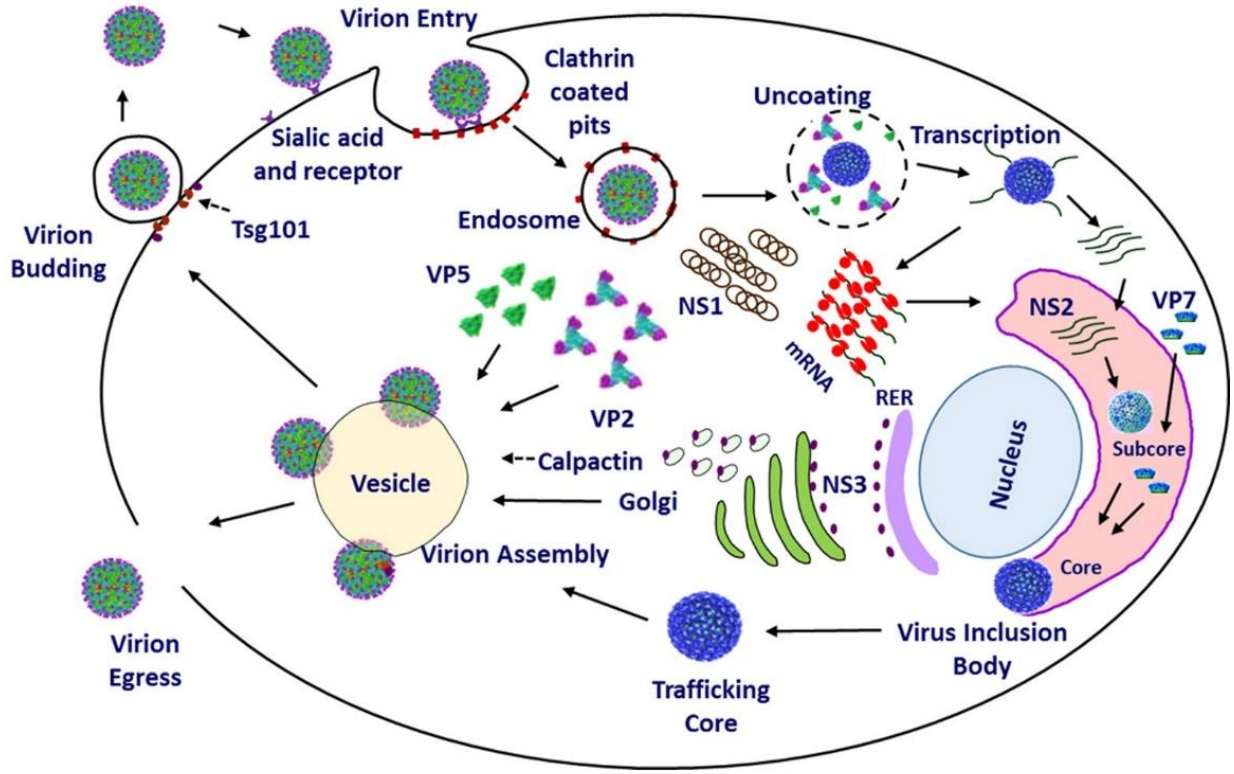

Figure 2.2: Schematic diagram representing the orbivirus replication cycle. The adsorption of the virus involves sialic acid and/or other receptors in the cell membrane of susceptible host cells. Following attachment, the virus particle enters the cell via clathrin-mediated endocytosis or macropinocytosis and is incorporated within an early endosome. The acidic pH in the endosome causes the loss of VP2 and mediates VP5 membrane permeabilization, which results in the uncoating of the virion and release of the transcriptionally active core particle into the host cell cytoplasm. Transcription and translation of viral proteins occur by making use of the host cell machinery. NS1 forms tubules and NS2 assembles the viral inclusion body (VIB) where components for core assembly are concentrated. Assembled core particles are then trafficked from the VIB on exocytotic vesicles by NS3 interaction with cellular calpactin. During this process, the outer capsid proteins VP5 and VP2 are acquired to produce mature virions. The virions are subsequently released via lysis or budding for the cells. The figure was adapted from Patel and Roy (2014).

In mammalian cells, the binding and internalization of BTV is mediated by the outer capsid VP2 protein (Huismans and van Dijk, 1990; Hassan and Roy, 1999). It has been reported previously that VP2 attaches to sialoglycoproteins (Hassan and Roy, 1999; Zhang *et al.*, 2010) or heparin sulfate (Mecham and McHolland, 2010) of mammalian cells prior to internalization. However, more recently, VP2 was shown to bind to α2,3-linked and α2,6-linked sialic acids and a putative binding site in VP2 was mapped to amino acid residues 185 to 194 (Wu and Roy, 2022). The virus then enters the cell through AP2-dependent clathrin-mediated endocytosis (Forzan *et al.*, 2007) or via a macropinocytosis-like entry route that is dependent on actin and dynamin (Gold *et al.*, 2010; Vermaak *et al.*, 2016; Stevens *et al.*, 2019). In both instances, the virus is incorporated in early endosomes. The low pH (6.0-6.5) within early endosomes has been proposed to disturb the interactions between VP2 and VP5, thereby facilitating the detachment of the VP2 (Zhang *et al.*, 2016; Wu *et al.*, 2019). Together with a further lowering of the pH (5.5) in the late endosome, the subsequent removal of VP2 causes VP5 to refold and results in the outward protrusion of barb-like structures, which are referred to as stalks, from the particle surface with the VP5 protein trimers remaining tethered to the particle by anchoring domains (Zhang *et al.*, 2016). Insertion of the stalk tip into the endosomal membrane causes membrane-disruptive interactions that ultimately lead to the formation of a pore in the endosomal membrane through which the uncoated core particle is released into the cytoplasm (Zhang *et al.*, 2016; Xia *et al.*, 2021). The replication of BTV is subsequently initiated by the synthesis and extrusion of capped and methylated mRNA from transcriptionally active cores within the cytoplasm and requires the enzyme activities encoded by VP1 (RNA-dependant RNA polymerase), VP4 (capping-enzyme) and VP6 (helicase) (Mertens and Diprose, 2004). The first viral proteins can be detected in the cell between 2-4 h post-infection, after which the rate of viral protein synthesis increases until 11-13 h post-infection (Huismans, 1979; Huismans and van Dijk, 1990). The mRNA transcripts function not only to encode proteins but are also used as templates for the production of negative sense strands to form the dsRNA genome segments encapsidated in the progeny virions (Mertens and Diprose, 2004).

For BTV, it has been suggested that the mechanism whereby viral mRNAs are selected and encapsidated prior to replication relies on a packaging order of the respective BTV ssRNA segments. Specifically, it was demonstrated that among all of the BTV genome segments, S10, the smallest genome segment with the longest UTRs, initiates RNA packaging. By making use of an *in vitro* RNA-RNA interaction assay system, it was shown that S10 plays a crucial role in first recruiting the other smaller RNA segments, probably by forming a complex or

complexes that then interact with larger segments (Sung and Roy, 2014). It was subsequently reported that nuclease-resistant oligoribonucleotides (ORNs) complementary to the 3' UTR of BTV mRNAs significantly inhibited virus replication without affecting protein synthesis (Fajardo *et al*., 2015). Notably, the exchange of 3' UTRs between segments demonstrated that RNA recognition was segment-specific, most likely acting as part of the secondary structure of the entire genomic segment (Burkhardt *et al*., 2014; Fajardo *et al*., 2015). These data suggest that genome packaging occurs via the formation of supramolecular complexes that form by the interaction of specific sequences located in the 3' UTRs of individual RNAs, after which the RNA complex is packaged into the assembling core particle through protein-RNA interactions. Although NS2 has long been believed to play a role in the selection and packaging of viral RNA, recent reports have implicated the minor core protein VP6 as being essential for genome packaging (Matsuo and Roy 2013; Matsuo *et al.*, 2018; Sung *et al.*, 2019). These reports have indicated that VP6 binds to ssRNA, in addition to dsRNA, and interacts with VP3. It was therefore suggested that VP6 may act to bridge the captured RNA with the assembling core particle and thereby result in the packaging of the viral genome into the virus particle (Sung *et al.*, 2019).

Soon after the initiation of the translation of BTV mRNAs, granular matrix structures accumulate near the core particles. These VIBs increase both in size and number as the viral infection progresses (Eaton *et al.*, 1990). In addition to VIBs, NS1-rich tubules form part of the "insoluble" phase in the cell and become a characteristic structure of cells in the early stages of infection (Huismans and Els, 1979; Eaton *et al.*, 1988). Newly synthesized viral transcripts, major and minor core proteins, as well as assembled cores and subcores have been identified in the VIBs and they are therefore recognized as the sites of orbivirus replication and early virus assembly (Hyatt and Eaton, 1988; Kar *et al.*, 2007). The assembly of the BTV VP3 subcore has been reported (Kar *et al.*, 2004). VP3 was reported to have three distinct domains, *i.e.*, an apical, a carapace, and a dimerization domain. The dimerization domain mediates the formation of VP3 dimers, which pack together in decamers to form the icosahedral structure of the VP3 layer. Although it has been reported that BTV VP3 can bind to ssRNA (Loudon and Roy, 1992), it was more recently reported that BTV RNAs failed to associate with VP3 decamers (Kar *et al.*, 2004). Consequently, it was suggested that assembly of the BTV core may begin with a complex formed by minor core proteins and the VP3 decamers and that these assembly intermediates recruit the viral RNA prior to completion of VP3 subcore assembly (Kar *et al.*, 2004; Matsuo *et al.*, 2018; Sung *et al.*, 2019). Although co-expression of the BTV

structural proteins with NS2 indicated that VP7 requires co-expression of VP3 to be recruited to the VIBs (Kar *et al.*, 2007), little is known regarding the exact mechanism whereby VP2 and VP5 are added to the developing virus particle. Initial reports indicated that neither of these outer capsid proteins has an affinity for the VIBs (Modrof *et al.*, 2005; Kar *et al.*, 2007). It was therefore suggested that the VP5 and VP2 proteins are added to the core particles at the periphery of the VIBs (Kar *et al.*, 2007), while a subsequent report indicated that VP5 of BTV associates with lipid rafts in the plasma membrane and that the core particles are transported to these sites for the final assembly of the outer capsid proteins (Bhattacharya and Roy, 2008). More recently, however, it was reported that VP5 is indeed associated with VIBs and that NS3 can also be observed in VIBs during the early stages of replication before being re-localized to the periphery of the VIBs during later stages of replication (Mohl *et al.*, 2020). In this case, it was suggested that the addition of VP5 may stabilize the core particles and prevent transcription from the newly assembled core particles, whereas NS3 could function as a bridge between the immature particles and VP2 and transport the newly formed particles to the plasma membrane. The localization of VP2 was not addressed in the study and it, therefore, remains unclear where, and how VP2 is added to the particles to generate mature virus particles.

Investigations regarding virus release from mammalian cells have demonstrated a strong correlation between the presence of NS3 and NS3A, and virus release (Hyatt *et al.*, 1989; Stoltz *et al.*, 1996). The virions may leave infected cells in one of two ways. Early after infection, when the host cell metabolism is not completely inhibited and the integrity of the host plasma membrane is maintained, progeny virions have been observed to bud through the plasma membrane surface and acquire a transient envelope. Alternatively, during the later stages of infection, when the integrity of the plasma membrane is not maintained, non-enveloped virions can be released by extrusion through the locally disrupted plasma membrane surface (Hyatt *et al.*, 1989; Han and Harty, 2004). The NS3 protein of BTV has also been shown to interact with the cellular proteins p11 and Tsg101, and these interactions were furthermore shown to assist in the egress of virus particles from infected cells in a non-lytic manner (Beaton *et al.*, 2002; Wirblich *et al.*, 2006; Celma and Roy, 2009; Celma and Roy, 2011). More recently, it has been reported that in some cell types, the majority of BTV particles are released in extracellular vesicles and it was subsequently shown that inhibition of multivesicular bodies (MVBs) or autophagous lysosomes decreased the release of infectious extracellular vesicles (Labadie and Roy, 2020). Based on the data, it was suggested that nascent BTV particles transit through the

MVBs towards the lysosomes, after which lysosomes carrying the virus are trafficked to the cell membrane and then released as extracellular vesicles.

2.6 THE NON-STRUCTURAL PROTEIN NS2

Since NS2 is the focus of this study, the following sections will discuss in greater detail the structure, properties and possible roles of the NS2 protein in virus replication and morphogenesis. The information on AHSV NS2 will be supplemented, where applicable, with information obtained from studies on NS2 of BTV.

2.6.1 Structure of NS2

A combination of sedimentation analyses and non-reducing SDS-polyacrylamide gel electrophoresis has indicated that the NS2 protein of both BTV and AHSV is a 7S homo-multimer with inter- and intra-molecular disulfide bonds and consists of approximately six to eight NS2 molecules (Uitenweerde *et al.*, 1995; Taraporewala *et al.*, 2001). The tendency of NS2 to form higher oligomers of variable size has prohibited structural analysis of the full-length NS2 protein. Nonetheless, structural analyses of the N-terminal and C-terminal domains of the BTV NS2 protein have been undertaken. Butan *et al.* (2004) reported a high-resolution structure of the N-terminal domain (amino acid residues 1-182) of NS2 from BTV. The crystal is composed of infinite chains of the N-terminal domain that form a spiral. The structure is a β-sandwich, and two extensive interfaces were described. One of these involves the extension of the β-sheet and the second involves an arm that links one protein molecule to the next, thereby generating oligomers that span the crystal. Mumtsidu *et al.* (2007) reported a low-resolution envelope, obtained from small-angle X-ray scattering measurements (SAXS), of the C-terminal domain (amino acid residues 178-354) of NS2. The C-terminal domain was modelled to likely be positioned on the inside of the spiral configuration of the N-terminal domain, which would prevent the spiral from closing. This configuration would prevent the NS2 protein from forming oligomers that consist of more than 10 to 12 monomers (Mumtsidu *et al.*, 2007).

2.6.2 Properties of NS2

2.6.2.1 NTPase enzymatic activity of NS2

As mentioned previously, BTV NS2 displays phosphohydrolase activity and can bind and hydrolyze both ATP and GTP to their corresponding nucleotide monophosphates (Horscroft and Roy, 2000). It was furthermore reported that the hydrolysis of these substrates by NS2 is dependent on divalent ions (such as Ca^{2+}, Mg^{2+} and Mn^{2+}) and that ouabain, an inhibitor of cellular ATPases, did not abolish the ATPase activity of NS2 (Horscroft and Roy, 2000). In a subsequent study, purified *Escherichia coli*-expressed BTV NS2 was shown to non-specifically hydrolyze the α-, β- and γ-phosphodiester bonds of all four nucleotide triphosphates to their corresponding nucleotide monophosphates (Taraporewala *et al.*, 2001). The recombinant NS2 displayed higher efficiency for the hydrolysis of ATP as compared with the other nucleotides for which NS2 has a preference in the order GTP > UTP/CTP. The regions of NS2 responsible for this enzymatic activity have not yet been mapped, but a truncated BTV NS2 protein that lacked the first 177 amino acids at the N terminus was still able to hydrolyze NTPs (Mumtsidu *et al.*, 2007). Although the functional importance of the NTPase activity of NS2 is not yet known, it has been suggested that the enzyme activity may play a role in providing energy for the assortment, transportation, packaging, or condensation of bound ssRNA (Horscroft and Roy, 2000).

2.6.2.2 RNA binding activity of NS2

Various early studies regarding the ssRNA binding ability of NS2 have indicated that the protein has a non-specific affinity for ssRNA. NS2 purified from cells infected with BTV (Huismans *et al.*, 1987), as well as NS2 of AHSV, BTV, and Epizootic haemorrhagic disease virus (EHDV) expressed by recombinant baculoviruses (Uitenweerde *et al.*, 1995), binds to poly(U)-Sepharose. Moreover, BTV NS2 is also capable of binding to *in vitro*-synthesized transcripts derived from plasmid DNA (Thomas *et al.*, 1990) and rotavirus gene 8 ssRNA (Taraporewala *et al.*, 2001). Subsequent studies have, however, indicated a degree of specificity in the NS2-ssRNA interaction. In this regard, competition UV cross-linking studies using radiolabelled BTV ssRNA and NS2 produced during virus replication in mammalian cells (Theron and Nel, 1997), as well as similar assays performed *in vitro* using purified baculovirus-expressed NS2 protein (Lymperopoulos *et al.*, 2003) concluded that NS2 bound preferentially to BTV ssRNA. The specificity of interactions between NS2 and ssRNA transcripts derived from genome segments S6, S8, S9 and S10 was also investigated in greater

detail. Different stem-loop structures in the respective BTV ssRNA transcripts were shown to be recognized by NS2, suggesting that NS2-ssRNA interaction is dependent on the ssRNA structure and that the structural interactions between NS2 and the different BTV ssRNA segments are likely to be independent events (Lymperopoulos *et al.*, 2006).

Studies aimed at identifying the ssRNA binding domains within NS2 have also been undertaken and these have indicated that the N terminus appears to be important for ssRNA binding. Truncated BTV NS2 with N-terminal deletions (up to amino acid residue 92) lost their ability to bind ssRNA (Zhao *et al.*, 1994). In addition, a short nine-amino-acid sequence, found within the NS2 of various orbiviruses and that resides within the N-terminal 92-amino-acid region, was shown through deletion and site-directed mutagenesis to be important for NS2 interaction with ssRNA (Theron *et al.*, 1996). Furthermore, three regions within the BTV NS2 amino acid sequence, of which two are located in the N-terminal region (amino acid residues 2-11 and 153-166, respectively) and one in the C-terminal region (amino acid residues 274-286), were identified by deletion mutagenesis as being important for the binding of ssRNA (Fillmore *et al.*, 2002). Deletion of singular domains reduced the affinity of NS2 toward ssRNA, and deletion of all three domains completely eliminated the ability of NS2 to bind to ssRNA. This data, therefore, suggests that sequential domains of NS2 may bind ssRNA in a cooperative manner, rather than ssRNA binding being mediated by a single domain (Fillmore *et al.*, 2002). In accordance with the apparent importance of the N-terminal region of NS2 for ssRNA binding activity, a recent report identified two consecutive arginine residues (Arg-6 and Arg-7) in the N terminus of BTV NS2 that was shown to be required for specific binding of NS2 to ssRNA derived from viral genome segment 10 (Rahman *et al.*, 2022). Whether these two arginine residues are also important for the binding of NS2 to other viral ssRNAs was, however, not investigated. Nevertheless, the study did report that non-specific ssRNA-binding occurs to lysine residues at positions 160/162 and 281/283, which corresponds to the ssRNA binding domains mapped previously by Fillmore *et al.* (2002).

Due to its ssRNA binding activity, NS2 has long been thought to be involved in the sorting, recruiting, or packaging of viral mRNA. However, recent evidence has indicated that BTV structural proteins and RNA segments alone can assemble to form infectious particles in the absence of the NS2, and the structural protein VP6 has been implicated as playing an essential role in the packaging of viral mRNA (Matsuo and Roy, 2009; Matsuo and Roy, 2013; Sung *et al.*, 2019). Consequently, it would appear that NS2 could serve to recruit virus ssRNAs

selectively from other RNA species within the cytoplasm of infected cells during virus replication and therefore may play a role *in vivo* as a condenser of the necessary components (viral mRNA and proteins) required for virion assembly in the host cytoplasm.

2.6.2.3 Virus inclusion body (VIB) formation

In AHSV- and BTV-infected cells, VIBs are observed as large, electron-dense perinuclear structures in the cell cytoplasm (Breese *et al.*, 1969; Eaton *et al.*, 1990; Brookes *et al.*, 1993). VIBs can be detected as early as 4 h post-infection and increase both in size and number as the infection progresses, with the most significant increase occurring between 12-20 h post-infection (Eaton *et al.*, 1990; Brookes *et al.*, 1993). The NS2 protein is the predominant component of VIBs and expression of NS2, in the absence of other viral proteins in both insect and mammalian cells, results in the formation of inclusion bodies (IBs) that are indistinguishable from VIBs found in virus-infected cells (Thomas *et al.*, 1990; Brookes *et al.*, 1993; Uitenweerde *et al.*, 1995; Modrof *et al.*, 2005). These results, therefore, indicate that the NS2 proteins are the minimal components required to form VIBs. In addition to NS2, the four subcore viral proteins (VP1, VP3, VP4 and VP6), core protein VP7, outer capsid protein VP5, BTV mRNA transcripts, as well as assembled subcores and cores have been identified in the VIBs (Hyatt and Eaton, 1988; Kar *et al.*, 2007; Mohl *et al.*, 2020). Consequently, VIBs are considered the sites where viral assembly occurs. It has also been shown that truncated NS2 proteins lacking N-terminal (amino acid residues 1-115 or 1-237) and C-terminal (amino acid residues 116-357 or 238-357) fragments were impaired in their ability to form IBs. Interestingly, expression of the N-terminal (1-115) and C-terminal (116-357) deletion NS2 mutants in mammalian cells, which had been infected with BTV, was shown to result in a marked reduction in overall virus yield and therefore indicates that virus replication was adversely affected (Kar *et al.*, 2007).

2.6.2.4 NS2 protein phosphorylation

The NS2 protein is the only orbivirus protein that undergoes phosphorylation during virus replication (Huismans *et al.*, 1987), and subsequent studies have indicated that NS2 expressed in insect cells by recombinant baculoviruses is also phosphorylated (Thomas *et al.*, 1990; Theron *et al.*, 1994). Notably, NS2 expressed in orbivirus-infected cells and NS2 expressed in insect cells shared the same phosphorylated peptides, indicating that phosphorylation of the same residues occurs in both cell types. Serine residues were identified as the phosphorylated amino acids in both BTV and AHSV NS2 hydrolysates (Devaney *et al.*, 1988), and the sites of

BTV NS2 phosphorylation have been identified as Ser-249 and Ser-259, located within the C-terminal segment of the protein (Modrof *et al.*, 2005; Mumtsidu *et al.*, 2007).

The NS2 protein lacks autokinase activity since an unphosphorylated form of EHDV NS2, obtained by expressing the NS2 gene in *E. coli*, could only be phosphorylated *in vitro* by a protein kinase associated with the cytoplasm of insect cells (Theron *et al.*, 1994). Likewise, unphosphorylated BTV NS2 also expressed in *E. coli*, could be phosphorylated by cellular kinases when mixed with a cytoplasmic extract from uninfected mammalian cells (Taraporewala *et al.*, 2001). These results, therefore, ruled out the phosphorylation of NS2 by another orbivirus protein but suggested that the NS2 protein is phosphorylated by a ubiquitous cellular protein kinase. The protein kinase responsible for BTV NS2 phosphorylation has since been identified as casein kinase 2 (CK2), as evidenced by the use of CK2-specific inhibitors that significantly reduced NS2 phosphorylation (Modrof *et al.*, 2005; Mohl and Roy, 2016).

In contrast to EHDV, where phosphorylation of the NS2 protein appears to down-regulate its ssRNA binding ability (Theron *et al.*, 1994), the phosphorylation of BTV NS2 does not affect its ability to bind to ssRNA (Thomas *et al.*, 1990; Modrof *et al.*, 2005). However, phosphorylation of the BTV NS2 protein appears to be essential for the ability of the protein to form VIBs. In contrast to phosphorylated NS2 that exhibited VIB formation, an unphosphorylated version of the protein failed to assemble as VIBs and partially phosphorylated NS2 produced irregular VIB-like structures (Modrof *et al.*, 2005). In a subsequent study, it was reported that protein phosphatase 2A (PP2A) is involved in BTV NS2 dephosphorylation and, together with CK2, regulates VIB morphology (Mohl and Roy, 2016). It was postulated that whereas phosphorylation of BTV NS2 is required for VIB formation, dephosphorylation of the protein may allow for the disassembly of the VIBs with subsequent release of the assembled viral cores and incomplete virus particles (Mohl and Roy, 2016).

Recently, Rahman *et al.* (2020) reported that the NS2 protein of BTV, which had been expressed in *E. coli*, is capable of binding Ca^{2+} efficiently by means of an atypical EF-hand-like Ca^{2+} binding motif that is located in the C-terminal region of the protein (amino acid residues 200-300). A DDDE amino acid sequence (residues 250-253) that is in juxtaposition of a serine residue known to be phosphorylated (Ser-249) was implicated in the Ca^{2+} binding activity of NS2 since substitution of the consecutive Asp residues and the Glu residue with four alanine residues affected the Ca^{2+} binding activity significantly (Rahman *et al.*, 2020).

Although it was also shown that binding of Ca^{2+} increases the phosphorylation level of the purified *E. coli*-expressed NS2 protein by CK2 in an *in vitro* phosphorylation assay, recombinant BTV obtained through a reverse genetics approach displayed a reduced level of NS2 phosphorylation and VIB assembly. Based on the results, it was proposed that Ca^{2+} binding affects the phosphorylation level of NS2 and therefore has a role in regulating VIB assembly (Rahman *et al.*, 2020).

2.7 AIMS OF THE STUDY

Although orbiviruses and especially AHSV are important pathogens of domestic and native animals (Coetzer and Guthrie, 2004; Clemmons *et al.*, 2021), much still remains to be elucidated regarding the molecular mechanisms that underlie virus replication and assembly in infected cells. The non-structural proteins are thought to play an important role in the replication cycle of these viruses, and information obtained for BTV suggests that the NS2 protein may be of particular relevance in these processes. In contrast, limited information is available regarding the functional importance and relevance of the NS2 protein of AHSV. In the past, studies were aimed at characterizing the properties of the AHSV NS2 protein and the results from these studies have indicated that the protein is phosphorylated at serine residues in the C terminus, is capable of binding ssRNA, and is the principal component of cytoplasmic VIBs in virus-infected cells (Devaney *et al.*, 1988; Theron *et al.*, 1994; Uitenweerde *et al.*, 1995). The current study therefore aimed to cross the divide between the known properties of the AHSV NS2 protein and determine the functional importance of these properties. As a first step, the functional significance of NS2 protein phosphorylation on the formation of VIBs, which are believed to be the sites in which virus replication and morphogenesis occur (Hyatt and Eaton, 1988; Kar *et al.*, 2007), was investigated. Notably, recombinant NS2, expressed by the baculovirus expression system, has been reported to form intracellular inclusion bodies (IBs) in insect cells that are identical to VIBs of AHSV-infected cells (Uitenweerde *et al.*, 1995) and NS2 is phosphorylated at the same residues in both mammalian and insect cells (Devaney *et al.*, 1988; Theron *et al.*, 1994). It can therefore be envisaged that a combination of mutagenesis and re-expression of phosphorylation-deficient AHSV NS2 protein by baculovirus recombinants would allow for a focused understanding of the functional importance of NS2 phosphorylation on the formation of VIBs. Consequently, towards the long-term goal of mapping the role of NS2 in the AHSV replication cycle, the primary aim of this study was to generate and evaluate NS2 mutants lacking phosphorylated amino acids with

respect to their ability to form intracellular inclusion bodies. The aim was addressed by the following specific objectives:

- Identification of the kinase responsible for NS2 phosphorylation
- Identification of putatively phosphorylated serine residues
- Construction and characterization of mutant NS2 genes with serine-to-alanine and serine-to-aspartate mutations
- Construction and characterization of recombinant baculoviruses expressing wild-type and mutant NS2 proteins
- Evaluation of the phosphorylation status of wild-type and mutant NS2 proteins
- Evaluation of the ability of wild-type and mutant NS2 proteins to form inclusion bodies

CHAPTER THREE

MATERIALS AND METHODS

3.1 Bacterial strains and plasmids

The bacterial strains and plasmids used in this study are listed in Table 3.1. The *Escherichia coli* strains were routinely cultured at 37°C with shaking at 200 rpm in Lysogeny Broth (LB: 1% [w/v] tryptone; 1% [w/v] NaCl; 0.5% [w/v] yeast extract; pH 7.4). Bacterial colonies were maintained at 4°C on LB agar (LB containing 1.2% [w/v] bacteriological agar) or at -80°C as glycerol cultures. For plasmid DNA selection and maintenance in *E. coli*, the medium was supplemented with ampicillin, kanamycin, gentamycin, or tetracycline as indicated in the text. All antibiotics were obtained from Sigma-Aldrich.

Recombinant plasmid pJET-S8 was obtained from Prof. J. Theron (Department of Biochemistry, Genetics and Microbiology, University of Pretoria). This recombinant plasmid comprises a pJET1.2/blunt cloning vector backbone that harbours a cloned copy of the full-length NS2 open reading frame (ORF) encoded by genome segment S8 of AHSV-4. The cloned NS2 gene is flanked by *Eco*RI and *Xho*I restriction endonuclease recognition sequences. The pJET1.2/blunt cloning vector was obtained from Thermo Scientific, whereas the pET-26b(+) bacterial expression vector and the pFastBac HTa bacmid donor vector were obtained from Novagen and Invitrogen, respectively.

3.2 Construction of a tailored AHSV-4 NS2 gene for expression *in E. coli*

Although the NS2 gene of AHSV-4 had been cloned previously into the pJET1.2/blunt cloning vector, the restriction enzyme recognition sequences flanking the insert DNA are not compatible with those required for cloning of the NS2 gene into the pET-26b(+) bacterial expression vector used in this study. Moreover, to enable purification of the NS2 protein, the stop codon had to be deleted in order for the NS2 coding sequence to be cloned in-frame with the C-terminal hexahistidine tag present in the pET-26b(+) bacterial expression vector. The strategy used for the construction and characterization of the tailored NS2 gene lacking the stop codon is detailed below.

3.2.1 Primers

Primers used to amplify a tailored version of the NS2 gene were designed based on the nucleotide sequence of the AHSV-4 NS2 gene (GenBank Accession no. KM820856; van de Water *et al.*, 2015). The primers were designed with DNAMAN v.4.0 software (Lynnon Biosoft). To facilitate cloning procedures, either a *Xho*I or *Nde*I restriction endonuclease recognition sequence was included at the 5' terminus of the respective primers. The primers

Table 3.1 Bacterial strains and plasmids used in this study

Strains or Plasmids	Characteristics	Reference
Strains:		
E. coli DH5α	**Cloning host:** F⁻ φ80*lac*ZΔM15 Δ(*lac*ZYA-*arg*F)U169 *rec*A1 *end*A1 *hsd*R17(r_K^-, m_K^+) *pho*A *sup*E44 λ⁻ *thi*-1 *gyr*A96 *rel*A1	Invitrogen
E. coli BL21(DE3)	**Expression host**: F⁻*omp*T *hsd*S_B (r_B^-, m_B^-) *gal dcm* (DE3)	Novagen
E. coli DH10Bac	**Production of recombinant bacmids**: F⁻*mcr*A Δ(*mrr*-hsdRMS-*mcr*BC) Φ80*lac*ZΔM15 Δ*lac*X74 *rec*A1 *end*A1 *ara*D139 Δ(*ara*, *leu*)7697 *gal*U *gal*K λ⁻*rps*L *nup*G/pMON7124	Invitrogen
Plasmids:		
pET-26b(+)	***E. coli* expression vector**: f1 *ori*, pBR322 *ori*, *lacI*, Kan^r, C-terminal 6 × His tag, T7 RNA polymerase promoter	Novagen
pFastBac HTa	**Bacmid donor vector:** f1 *ori*, pUC *ori*, Amp^r, $Gent^r$, N-terminal 6 × His tag, Tn7R and Tn7L borders, SV40 polyadenylation signal, polyhedrin promoter	Invitrogen
pJET1.2/blunt	**Blunt end cloning vector for PCR amplicons**: pMB1 replicon, Amp^r, *eco47IR* lethal gene for positive selection	Thermo Scientific
pJET-S8	pJET1.2 harbouring the full-length NS2 open reading frame (ORF), flanked by a *Eco*RI and *Xho*I restriction enzyme recognition sequences	Prof J Theron (unpublished)
pJET-NS2	AHSV-4 NS2 ORF lacking the stop codon and flanked by *Nde*I and *Xho*I restriction enzyme recognition sequences blunt-end cloned into pJET1.2	This study
pET-NS2	pET-26b(+) harbouring the truncated NS2 ORF from pJET-NS2 cloned into the *Nde*I and *Xho*I sites in frame with the C-terminal His tag sequence	This study
pJET-NS2 S-A256	pJET-S8 harbouring Ser-to-Ala mutation at residue 256 in NS2 ORF	This study
pJET-NS2 S-A258	pJET-S8 harbouring Ser-to-Ala mutation at residue 258 in NS2 ORF	This study
pJET-NS2 S-A262	pJET-S8 harbouring Ser-to-Ala mutation at residue 262 in NS2 ORF	This study
pJET-NS2 S-A270	pJET-S8 harbouring Ser-to-Ala mutation at residue 270 in NS2 ORF	This study
pJET-NS2 S-A256,258	pJET-S8 harbouring Ser-to-Ala mutations at residues 256 and 258 in NS2 ORF	This study
pJET-NS2 S-D256	pJET-S8 harbouring Ser-to-Asp mutation at residue 256 in NS2 ORF	This study
pJET-NS2 S-D258	pJET-S8 harbouring Ser-to-Asp mutation at residue 258 in NS2 ORF	This study
pJET-NS2 S-D256,258	pJET-S8 harbouring Ser-to-Asp mutation at residues 256 and 258 in NS2 ORF	This study
pFB-NS2 S-A256	pFastBac HTa harbouring mutant NS2 gene from pJET-NS2 S-A256 cloned into the *Eco*RI and *Xho*I sites in frame with the N-terminal His tag sequence	This study
pFB-NS2 S-A258	pFastBac HTa harbouring mutant NS2 gene from pJET-NS2 S-A258 cloned into the *Eco*RI and *Xho*I sites in frame with the N-terminal His tag sequence	This study
pFBNS2 S-A262	pFastBac HTa harbouring mutant NS2 gene from pJET-NS2 S-A262 cloned into the *Eco*RI and *Xho*I sites in frame with the N-terminal His tag sequence	This study
pFB-NS2 S-A270	pFastBac HTa harbouring mutant NS2 gene from pJET-NS2 S-A270 cloned into the *Eco*RI and *Xho*I sites in frame with the N-terminal His tag sequence	This study
pFB-NS2 S-A256,258	pFastBac HTa harbouring mutant NS2 gene from pJET-NS2 S-A256,258 cloned into the *Eco*RI and *Xho*I sites in frame with the N-terminal His tag sequence	This study
pFB-NS2 S-D256	pFastBac HTa harbouring mutant NS2 gene from pJET-NS2 S-D256 cloned into the *Eco*RI and *Xho*I sites in frame with the N-terminal His tag sequence	This study
pFB-NS2 S-D258	pFastBac HTa harbouring mutant NS2 gene from pJET-NS2 S-D258 cloned into the *Eco*RI and *Xho*I sites in frame with the N-terminal His tag sequence	This study
pFB-NS2 S-D256,258	pFastBac HTa harbouring mutant NS2 gene from pJET-NS2 S-D256,258 cloned into the *Eco*RI and *Xho*I sites in frame with the N-terminal His tag sequence	This study
pFB-NS2	pFastBac HTa harbouring wild-type NS2 gene from pJET-S8 cloned into the *Eco*RI and *Xho*I sites in frame with N-terminal His tag sequence	This study

are indicated in Table 3.2 and were synthesized by Inqaba Biotechnical Industries.

3.2.2 Polymerase chain reaction (PCR)

The PCR reaction mixture (50 µl) contained 4 ng of pJET-S8 plasmid DNA as template, 10 µM of each primer, TailorNS2-F and TailorNS2-R (Table 3.2), 10 µl of 5 × Phusion HF Reaction Buffer, each deoxynucleoside triphosphate (dNTP) at a concentration of 200 µM, and 1 U of high-fidelity Phusion DNA polymerase (2 U/µl; Thermo Scientific). The tubes were placed in a BioRad T100 thermal cycler. Following initial denaturation at 98°C for 30 s, the reactions were subjected to 30 cycles of denaturation at 98°C for 10 s, primer annealing at 55°C for 30 s and primer extension at 72°C for 4 min. After the last cycle, the reaction was kept at 72°C for 10 min to ensure complete synthesis of all DNA strands. As a negative control, an identical reaction was included except that the template DNA was omitted.

3.2.3 Agarose gel electrophoresis

The PCR reaction mixtures were analyzed by agarose gel electrophoresis (Sambrook and Russell, 2001). A horizontal 1% (w/v) agarose gel (Agarose LM; Lasec) was cast and electrophoresed at 100 V in 1 × TAE buffer (40 mM Tris-HCl; 20 mM NaOAc; 1 mM EDTA; pH 8.5). The agarose gel was supplemented with ethidium bromide (0.5 µg/ml) to allow for visualization of the DNA, and gel images were captured with the Gel DOC EZ Imager system (BioRad). The PCR amplicon was sized according to its migration in the agarose gel as compared to that of a standard DNA molecular marker, namely 1 kb DNA Ladder (New England Biolabs).

3.2.4 Purification of amplicon from the agarose gel

The GeneJET Gel Extraction Kit (Thermo Scientific) was used to purify the PCR amplicon from an agarose gel, according to the manufacturer's instructions. Briefly, the amplicon was excised from the agarose gel using a scalpel blade and the gel slice was placed into a 1.5-ml Eppendorf tube. For each 100 mg of agarose gel, one volume of Binding Buffer was added, and the tube was incubated at 60°C for 10 min. The melted agarose solution was centrifuged through a GeneJET Purification column at 14 000 rpm for 1 min. The column was washed twice with 700 µl each of the supplied Wash buffer and the DNA was then eluted in 15 µl of nuclease-free water. The DNA concentration was determined with the Nanodrop ND-2000 spectrophotometer (NanoDrop Technologies, Inc.).

Table 3.2: Oligonucleotide primers used in this study

Primer	Sequence (5' – 3')	Comments
Amplification primers		
TailorNS2-F	ACTCGA**catatg**ATGGCAGAGGTCAGAAAG	Tailoring of NS2 gene to delete the 3' stop codon (TGA) and to introduce a *Nde*I (bold) and *Xho*I (bold underlined) restriction enzyme recognition sequence
TailorNS2-R	ATTATA**ctcgag**ACCGCTCCCCC	
pHed-F	AAATGATAACCATCTCGC	Primers used for screening of recombinant bacmid DNA to verify transposition of wild-type and mutant NS2 genes
pUC/M13-R	CAGGAAACAGCTATGAC	
Mutagenesis primers		
iPCR-S-A 256F	CAA**GCC**GATAGTGATGATCA	Inverse PCR primers used to introduce either Ser (S) to Ala (A) or Ser (S) to Asp (D) site-specific mutations into the NS2 coding sequence; numbers denote mutated serine residue; site-specific mutations are indicated in bold underlined capital letters
iPCR-S-A 256R*	ACACCACATACTCTCTGTACGTA	
iPCR-S-A 258-F	AGTGAT**GCC**GATGATCAATCT	
iPCR-S-A 258-R	TTGACACCACATACTCTCTGTAC	
iPCR-S-A 262-F	GATCAA**GCC**GATGAGGATCA	
iPCR-S-A 262-R	ATCACTATCACTTTGACACCACATACT	
iPCR-S-A 270-F	TTGGG**GCC**ACAGAGCCAGAA	
iPCR-S-A 270-R	CCTCGTGATCCTCATCAGATTG	
iPCR-S-A 256,258-F	CAA**GCC**GAT**GCC**GATGATCAATCTGAT	
iPCR-S-D 256-F	CAA**GAC**GATAGTGATGATCAATCTGAT	
iPCR-S-D 258-F	CAAAGTGAT**GAC**GATGATCAATCTGAT	
iPCR-S-D 256,258-F	CAA**GAC**GAT**GAC**GATGATCAATCTGAT	
Sequencing primers		
pJET-F	CGACTCACTATAGGGAGAGCGGC	
pJET R	AAGAACATCGATTTTCCATGGCAG	
S8-F	ACAACTTTGGATGTTGGAG	
S8-R	TCTCACGCACATCATTTC	
S8 Internal-F	ACAACTTTGGATGTTGGAG	
S8 Internal-R	TCTCACGCACATCATTTC	

* Primer iPCR-S-A 256R was used as the reverse primer in inverse PCR reactions to introduce a Ser-to-Ala mutation at position 256 and a Ser-to-Ala double mutation at positions 256 and 258, as well as to introduce single and double Ser-to-Asp mutations into the NS2 coding sequence.

3.2.5 Construction of the intermediate plasmid pJET-NS2

3.2.5.1 Ligation reaction

For cloning of the PCR amplicon, the pJET1.2/blunt cloning vector, together with the CloneJET PCR cloning kit (Thermo Scientific), was used according to the manufacturer's instructions. The ligation reaction contained 1 µl of T4 DNA ligase (5 U/µl), 10 µl of 2 × Reaction Buffer, 2 µl of 40% (w/v) PEG-4000, 50 ng of the pJET1.2/blunt vector, 750 ng of purified amplicon and nuclease-free water to a final volume of 20 µl. The ligation reaction was incubated at 22°C for 1 h and then transformed into competent *Escherichia coli* DH5α cells.

3.2.5.2 Preparation of competent *E. coli* DH5α cells

Competent *E. coli* DH5α cells were prepared by the $CaCl_2$ method, as described by Bergmans *et al*. (1981). A single colony of a freshly streaked culture of *E. coli* DH5α was inoculated into 5 ml of LB broth and cultured overnight at 37°C with shaking at 250 rpm. Following incubation, 1 ml of the culture was inoculated into 100 ml of LB broth (pre-warmed to 37°C) in a 250-ml Erlenmeyer flask. The culture was incubated at 37°C with shaking and the optical density at 600 nm (OD_{600}) was measured at regular intervals with an Eppendorf BioPhotometer Plus spectrophotometer. Once an OD_{600} of 0.4 was reached, the flask was incubated on ice for 15 min to inhibit further bacterial growth. The cells from 50 ml of the culture were harvested by centrifugation at 2 000 rpm for 10 min at 4°C in an Eppendorf 5804 R centrifuge. The bacterial cell pellet was suspended gently in 25 ml of ice-cold 50 mM $CaCl_2$ and incubated on ice for 30 min. The cells were harvested as described above and suspended in 5 ml of the 50 mM $CaCl_2$ solution. The competent cells were incubated on ice for at least 1 h prior to transformation or, alternatively, the competent cells were snap-frozen in 15% (v/v) sterile glycerol and stored as 100-µl aliquots at -80°C until further use.

3.2.5.3 Transformation of competent cells

To transform the prepared competent *E. coli* DH5α cells, 100 µl of the competent cells were mixed in a pre-chilled Eppendorf tube with the ligation reaction mixture (20 µl). After incubation on ice for 30 min, the tube was subjected to a heat shock by incubating the tube at 42°C for 90 s and then immediately incubated on ice for 2 min. Subsequently, 900 µl of pre-warmed (37°C) LB broth was added and the tube was incubated at 37°C for 1 h. As controls, competent cells were transformed with plasmid DNA (pUC19) of a known concentration to

determine the transformation efficiency, and untransformed cells were used to test for contamination. Aliquots (200 µl) of the transformation mixtures were plated onto LB agar supplemented with ampicillin (100 µg/ml) and the agar plates were incubated overnight at 37°C.

3.2.6 Screening and characterization of recombinant plasmid pJET-NS2

3.2.6.1 Plasmid DNA extraction

Single bacterial colonies were inoculated into 5 ml of LB broth supplemented with ampicillin (100 µg/ml) and incubated overnight at 37°C. Plasmid DNA was subsequently extracted with the GeneJET Plasmid Miniprep kit (Thermo Scientific) according to the manufacturer's instructions. Briefly, cells from 2 ml of the overnight cultures were harvested by centrifugation at 14 000 rpm for 1 min. Following the sequential addition of 250 µl each of the Resuspension solution and the Lysis solution, 350 µl of Neutralization solution was added to the cell pellet. The cell lysate was centrifuged at 14 000 rpm for 5 min and the cleared lysate (supernatant) was then centrifuged through a GeneJET DNA-binding column at 14 000 rpm for 1 min. The column was washed twice with 500 µl of the supplied Wash solution and the plasmid DNA was subsequently eluted in 30 µl of nuclease-free water. The plasmid DNA was analyzed on a 1% (w/v) agarose gel to assess its purity and the concentration was determined with a NanoDrop ND-2000 spectrophotometer (NanoDrop Technologies, Inc.).

3.2.6.2 Restriction enzyme digestion

Approximately 200-750 ng of plasmid DNA was digested with 1 U each of the restriction enzymes *Nde*I and *Xho*I, using the 10× FastDigest Green Buffer supplied by the manufacturer (Thermo Scientific). The final reaction volume was 20 µl and incubation was at 37°C for 1 h, after which the enzymes were inactivated by heating to 80°C for 5 min. The digestion products were analyzed on a 1% (w/v) agarose gel in the presence of a DNA molecular weight marker.

3.2.6.3 DNA sequencing and sequence analysis

Nucleotide sequencing of the cloned insert DNA was performed with the ABI-PRISM BigDye Terminator v.3.1 Cycle Sequencing Ready Reaction kit (Perkin-Elmer Applied Biosystems) according to the manufacturer's instructions. Each sequencing reaction comprised 150 ng of purified plasmid DNA, 3.2 µM of the sequencing primer pJET-F or pJET-R (Table 3.2), 2 µl of BigDye Reaction mix, 1 µl of 5 × BigDye Sequencing buffer and nuclease-free water to a

final volume of 10 µl. Cycle sequencing reactions were performed in a BioRad T100 thermal cycler and consisted of an initial denaturation at 96°C for 1 min, followed by 30 cycles of denaturation at 96°C for 10 s, primer annealing at 50°C for 15 s and primer extension at 60°C for 4 min. The extension products were precipitated by the addition of 250 µl of ice-cold isopropanol and incubation at room temperature for 2 min, followed by centrifugation at 14 000 rpm for 15 min. The supernatant was carefully aspirated, and the pellet was washed twice with 70% ethanol before being allowed to air dry. The samples were submitted to the University of Pretoria's Sequencing Facility for sequencing on an ABI PRISM 3130XL DNA sequencer. The nucleotide sequence and deduced amino acid sequence were analyzed with MEGA-X software (https://www.megasoftware.net/).

3.3 Construction and characterization of the recombinant bacterial expression plasmid pET-NS2

All molecular techniques used in the construction of the recombinant bacterial expression vector were performed according to the procedures described in the sections above. To enable cloning of the tailored NS2 gene into the bacterial expression vector pET-26b(+), both the recombinant pJET-NS2 plasmid DNA and pET-26b(+) vector DNA were digested with *Nde*I and *Xho*I. The excised NS2 gene and digested pET-26b(+) vector DNA were purified from a 1% (w/v) agarose gel with the GeneJET Gel Extraction kit (Thermo Scientific) prior to their use in a ligation reaction. The prepared vector DNA (50 ng) and insert DNA (50 ng) were ligated overnight at 22°C in a final volume of 20 µl, which also contained 2 µl of 10 × DNA ligase buffer and 5 U of T4 DNA ligase (5 U/µl; Thermo Scientific). Following the transformation of competent *E. coli* DH5α cells, the transformation mixture was plated onto LB agar plates supplemented with kanamycin (30 µg/ml) and the agar plates were incubated overnight at 37°C. Plasmid DNA was subsequently extracted from randomly selected kanamycin-resistant transformants and characterized by restriction enzyme digestion with both *Nde*I and *Xho*I. One of the recombinant clones, designated pET-NS2, was selected and used in all subsequent experiments. The absence of the C-terminal stop codon and in-frame cloning of the NS2 gene with the hexahistidine tag of the expression vector was verified by DNA sequencing with the ABI-PRISM BigDye Terminator v.3.1 Cycle Sequencing Ready Reaction kit (Perkin-Elmer Applied Biosystems) and by making use of S8 Internal-F or S8 Internal-R as the sequencing primer (Table 3.2).

3.4 Expression of recombinant NS2 in *E. coli* BL21(DE3)

For expression of the AHSV-4 NS2 protein in *E. coli*, the recombinant plasmid pET-NS2 was transformed into *E. coli* BL21(DE3) which carries the gene for T7 RNA polymerase under control of the lacUV5 promoter. The competent cells were prepared and then transformed with either recombinant pET-NS2 or parental pET-26b(+) plasmid DNA, as described previously (Sections 3.2.5.2 and 3.2.5.3), except that the transformation mixtures were plated onto LB agar supplemented with kanamycin (30 µg/ml). Single colonies were inoculated into 5 ml of LB broth supplemented with kanamycin (30 µg/ml) and incubated overnight at 37°C with shaking. Expression of the recombinant NS2 protein was induced with IPTG (Sigma-Aldrich). For this purpose, 100 µl of the overnight cultures were inoculated into 10 ml of pre-warmed (37°C) sterile LB broth supplemented with kanamycin (30 µg/ml) and incubated at 37°C until an OD_{600} of 0.4 was reached. To each culture, IPTG was added to a final concentration of 0.1 mM and the cultures were incubated at 37°C with shaking at 200 rpm for an additional 3-6 h. The bacterial cells were subsequently harvested by centrifugation at 14 000 rpm for 10 min at 4°C and each cell pellet was suspended in 1 ml of 1 × Phosphate-buffered saline (PBS: 137 mM NaCl; 2.7 mM KCl; 4.3 mM $Na_2HPO_4.2H_2O$; 1.4 mM KH_2PO_4; pH 7.5). Aliquots (20 µl) of the whole-cell lysates were analyzed by electrophoresis on a SDS-polyacrylamide gel and Western blot analysis, as described below in Section 3.6.

3.5 Purification of the recombinant histidine-tagged NS2 protein

3.5.1 Large-scale expression of recombinant NS2 in *E. coli* BL21(DE3)

To facilitate the purification of the recombinant hexahistidine-tagged NS2 protein, the recombinant protein was expressed on a large scale as follows. Single colonies of *E. coli* BL21(DE3) containing pET-NS2 were inoculated into 5 ml of LB broth supplemented with kanamycin (30 µg/ml) and incubated overnight at 37°C with shaking. A 1 ml volume of the overnight culture was inoculated into 100 ml of LB broth supplemented with 30 µg/ml of kanamycin in a 250-ml Erlenmeyer flask. The cultures were incubated at 37°C with shaking until an OD_{600} of 0.4 was reached and IPTG was then added to a final concentration of 0.1 mM. The cultures were incubated overnight at 25°C with shaking at 150 rpm. Following incubation, the cultures were incubated on ice for 5 min and the bacterial cells were collected by centrifugation at 11 000 rpm for 5 min at 4°C. The bacterial cell pellets were washed once with 25 ml of 20 mM Tris-HCl (pH 8), the supernatant was aspirated, and the cells were suspended in 8 ml of ice-cold Tris buffer (50 mM Tris-HCl; pH 7.4). The bacterial cells were

lysed by sonication on ice for 5 min using a Branson Sonifier Cell Disruptor B-30 at a power output of 45% (30 s pulses, followed by 30 s rest for a total of 5 min). The cell lysate was clarified by centrifugation at 11 000 rpm for 5 min at 4°C and the supernatant, considered as the soluble cytoplasmic protein extract, was recovered for protein purification as described below.

3.5.2 Purification of the histidine-tagged NS2 protein by affinity chromatography

The recombinant hexahistidine-tagged NS2 protein was purified by immobilized metal affinity chromatography (IMAC) with the HisPur Cobalt Purification kit (Thermo Scientific) according to the manufacturer's instructions. Prior to their use, the HisPur Cobalt spin columns were centrifuged at 2 700 rpm for 2 min to remove the storage buffer and were then equilibrated with two resin-bed volumes (400 µl) of the supplied Equilibration/Wash buffer (50 mM Na_2PO_4; 300 mM NaCl; 10 mM imidazole; pH 7.4). The soluble protein extract (400 µl) was mixed with an equal volume of Equilibration/Wash buffer, pipetted into the spin column, and incubated at 4°C for 30 min with gentle agitation to allow maximal adsorption of the NS2 fusion protein to the resin. Following incubation, the columns were centrifuged at 2 700 rpm for 2 min and washed three times with 400 µl each of the Equilibration/Wash buffer to remove unbound proteins. The hexahistidine-tagged NS2 protein was subsequently eluted in 200 µl of the supplied Elution buffer (50 mM Na_2PO_4; 300 mM NaCl; 150 mM imidazole; pH 7.4). The elution step was repeated twice more to ensure maximal recovery of the recombinant NS2 protein. Samples (20 µl) of the eluted recombinant protein were analyzed by electrophoresis on a SDS-polyacrylamide gel.

3.6 Analysis of recombinant NS2 proteins

3.6.1 SDS-polyacrylamide gel electrophoresis (SDS-PAGE)

Prior to analysis, protein samples were mixed with an equal volume of 2 × Protein Solvent Buffer (PSB: 0.5 mM Tris-HCl [pH 6.8]; 4% [w/v] SDS; 20% [v/v] glycerol; 10% [v/v] 2-mercaptoethanol; 0.06% [w/v] Bromophenol blue) and then denatured by heating to 100°C for 5 min in a heating block. The proteins were resolved by electrophoresis in a discontinuous gel system, as described by Laemmli (1970). A 5% (w/v) acrylamide stacking gel (0.125 M Tris-HCl [pH 6.8]; 0.1% [w/v] SDS) and a 12% (w/v) acrylamide separating gel (0.375 M Tris-HCl [pH 8.8]; 0.1% [w/v] SDS), with an acrylamide:bisacrylamide ratio of 29:0.8, were polymerized by addition of 100 µl of 10% (w/v) ammonium persulphate and 10 µl of TEMED.

Electrophoresis was performed in a Hoefer miniVE vertical electrophoresis system at 200 V for 2 h in 1 × TGS electrophoresis buffer (25 mM Tris-HCl [pH 8.3]; 192 mM glycine; 0.1% [w/v] SDS). To visualize the proteins, the gels were stained for 15 min with 0.125% (w/v) Coomassie brilliant blue (prepared in 50% [v/v] methanol and 10% [v/v] acetic acid) and then counterstained by repeatedly soaking the gels in destaining solution (10% [v/v] methanol; 10% [v/v] acetic acid). The sizes of the resolved proteins were determined by comparison to reference molecular mass proteins (PageRuler Prestained Protein Ladder 10-180 kDa; Thermo Scientific).

3.6.2 Western blot analysis

For Western blot analysis (Sambrook and Russell, 2001), proteins from an unstained SDS-polyacrylamide gel were electroblotted onto a Hybond-C^+ nitrocellulose membrane (Amersham Pharmacia Biotech AB). Two sheets of filter paper and the nitrocellulose membrane cut to the same size as the gel, were equilibrated for 10 min in transfer buffer (25 mM Tris; 192 mM glycine). The proteins were electroblotted onto the membrane at 120 V for 90 min with a Mighty Small Transphor blotting apparatus (Hoefer). Following transfer, the membrane was washed in 1 × PBS for 5 min and non-specific binding sites were blocked by immersing the membrane for 30 min at room temperature in 100 ml of blocking solution (1% [w/v] fat-free milk powder in 1 × PBS). The membrane was then incubated overnight at 4°C with gentle agitation in the presence of a polyclonal anti-NS2 antibody (GenScript Corp.) that was diluted 1:250 in blocking buffer. Following incubation, the unbound primary antibody was removed by washing the membrane three times for 5 min each in wash buffer (0.05% [v/v] Tween-20 in 1 × PBS). The secondary antibody, Protein-A conjugated to horseradish peroxidase (Sigma-Aldrich) that had been diluted 1:10 000 in blocking buffer, was added to the membrane and then incubated for 2 h at room temperature with gentle agitation. The membrane was washed three times for 5 min each in wash buffer, and once in 1 × PBS for 5 min. Immune-reactive proteins were detected by immersing the membrane in freshly prepared enzyme substrate solution (60 mg of 4-chloro-1-naphtol in 20 ml of ice-cold methanol and 60 µl of H_2O_2 in 100 ml of 1 × PBS, mixed just before use), followed by incubation at room temperature in the dark until the protein bands became visible. Once the bands became visible, the membranes were rinsed with distilled water and air-dried.

3.7 Protein concentration determination

The concentration of purified recombinant NS2 proteins was determined by the method of Bradford (1976) with the Quick Start Protein Assay kit (BioRad), and with bovine serum albumin (BSA) as standard. Aliquots (5 µl) of each sample were mixed with 250 µl of Protein Assay reagent in the wells of a 96-well microplate (Sigma-Aldrich), incubated at room temperature for 10 min and the absorbance (A) at 595 nm was then determined with a Multiskan GO Microplate spectrophotometer (Thermo Scientific). Distilled water containing Protein Assay reagent was used to zero the absorbance readings, and the protein concentration was determined from a BSA standard curve that had been prepared by plotting the A_{595} values (y-axis) versus their concentration (0-2 000 µg/ml; x-axis).

3.8 Protein phosphorylation assays

3.8.1 *In vitro* phosphorylation of NS2

To provide a source of unphosphorylated NS2, a cell lysate was prepared from an IPTG-induced culture of *E. coli* BL21(DE3) containing pET-NS2, as described previously (Section 3.5.1). To provide a source of cellular kinase, a cell lysate was prepared from *Spodoptera frugiperda* clone 9 (Sf-9) insect cells. To this end, the cells from 5 ml of a Sf-9 suspension culture (2.5×10^6 cells/ml) were harvested by centrifugation at 5 000 rpm for 5 min. The cell pellet was washed with 1 ml of 1 × PBS and suspended in 500 µl of 1 × PBS before lysis of the cells by passing the cell suspension through a 22G needle multiple times. For the *in vitro* phosphorylation reaction, equal volumes (250 µl) of the cell lysates were mixed together and incubated at 37ºC for 1 h in the presence of 0.5 mM ATP (New England Biolabs). An additional reaction was prepared as above, except that the Casein kinase 2 (CK2)-specific inhibitor TBB (4, 5, 6, 7–tetrabromobenzotriazole; Sigma-Aldrich) was added to the reaction mixture at 100 µM. Following incubation, NS2 was purified from the reaction mixtures by affinity chromatography using the HisPur Cobalt Purification kit (Section 3.5.2). The samples were analyzed by SDS-PAGE to assess the successful recovery of the NS2 protein, and a duplicate SDS-polyacrylamide gel was stained with Pro-Q Diamond Phosphoprotein Gel Stain (Invitrogen) to visualize phosphoproteins.

3.8.2 *In vitro* phosphorylation of NS2 by Casein kinase 2 (CK2)

Purified NS2 protein, expressed in *E. coli* BL21(DE3), was phosphorylated *in vitro* with CK2 (Millipore Corp.). The purified NS2 protein (5 µg) and 5 µl of CK2 (10 µg/ml stock solution)

were incubated in 1 × MTD buffer (50 mM Tris-HCl [pH 8]; 50 mM $MgCl_2$; 50 mM DTT) supplemented with 0.5 mM ATP. In a control reaction, TBB was added at 100 µM. The reactions were incubated at 37ºC for 1 h. Phosphoproteins were subsequently visualized by SDS-PAGE and staining of the SDS-polyacrylamide gel with Pro-Q Diamond Phosphoprotein Gel Stain (Invitrogen).

3.9 Phosphoprotein staining of SDS-polyacrylamide gels

To visualize phosphorylated proteins in SDS-polyacrylamide gels, the gel was stained with Pro-Q Diamond Phosphoprotein Gel Stain (Invitrogen) according to the manufacturer's instructions. Briefly, the gels were fixed by immersion in 100 ml of fixing solution (50% [v/v] methanol; 10% [v/v] acetic acid) for 30 min at room temperature with gentle agitation. This step was repeated once more to ensure that all the SDS was washed out of the gel. Subsequently, the gel was washed three times, for 10 min each wash, in 100 ml of ultrapure water and then stained in the dark for 90 min with gentle agitation in 60 ml of the Pro-Q Diamond phosphoprotein gel stain. The gel was destained for 30 min at room temperature with gentle agitation in 100 ml of Pro-Q destaining solution (20% [v/v] acetonitrile; 50 mM sodium acetate [pH 4]). This step was repeated twice more, after which the gel was washed twice with 100 ml of ultrapure water for 5 min per wash. The stained SDS-polyacrylamide gel was then imaged on a 302-nm UV transilluminator, and the image was captured with the Gel DOC EZ Imager system (BioRad).

3.10 Bioinformatics analyses

The NS2 protein of different orbiviruses, including AHSV, has been reported previously to be phosphorylated at C-terminal serine residues only (Devaney *et al.*, 1988). To identify putative phospho-acceptor serine residues, the amino acid sequence of the AHSV-4 NS2 protein (GenBank Accession no. KM820856; van de Water *et al.*, 2015) was subjected to bioinformatics analyses using different computer prediction programmes, *i.e.*, NetPhos-3.1 (http://www.cbs.dtu.dk/services/NetPhos/), Group-based prediction system (GPS) v.5 (http://gps.biocuckoo.cn/) and Scansite 4.0 (https://scansite4.mit.edu/#home).

3.11 Construction of mutated NS2 genes

For the construction of NS2 genes containing targeted mutations of potential phospho-acceptor serine residues in the C terminus of the protein, an inverse PCR-based method of mutagenesis was used. In this approach, plasmid pJET-S8 which contains a cloned copy of the NS2 gene

from AHSV-4 was used as a template, together with appropriately designed back-to-back mutagenic primers (Table 3.2). The primers were designed with DNAMAN v.4.0 software (Lynnon Biosoft) and synthesized by Inqaba Biotechnical Industries. The inverse PCR approach has the advantage of amplifying the recombinant plasmid, whilst introducing the desired mutations into the cloned NS2 gene. The sections below provide information on the methodology that was used to introduce the mutations and to characterize the derived mutant pJET plasmid constructs.

3.11.1 Inverse PCR

Each inverse PCR reaction mixture (50 µl) contained 4 ng of pJET-S8 plasmid DNA as template, 10 µM of each the appropriate iPCR-F and iPCR-R primer (Table 3.2), 10 µl of 5 × Phusion HF Reaction Buffer, 200 µM of each dNTP, and 1 U of high-fidelity Phusion DNA polymerase (2 U/µl; Thermo Scientific). Negative controls were included, in which template DNA was omitted from the reaction mixtures. The PCR reactions were performed in a BioRad T100 thermal cycler with the following cycling parameters: initial denaturation at 98°C for 30 s, followed by 30 cycles of denaturation at 98°C for 10 s, primer annealing at 55°C for 30 s and primer extension at 72°C for 4 min. After a final extension at 72°C for 10 min, the reaction mixtures were analyzed by electrophoresis on a 1% (w/v) agarose gel in the presence of a DNA molecular weight marker, and the amplicons were purified from the gel with the GeneJET Gel Extraction kit (Thermo Scientific).

3.11.2 Self-ligation of amplicon DNA

The primers used in the above inverse amplification reactions were not phosphorylated at their 5'-end. Consequently, for ligation to occur, the respective amplicons were phosphorylated at their 5'-ends with T4 Polynucleotide kinase. Each reaction mixture contained 100 ng of purified amplicon, 1 × Reaction Buffer A (50 mM Tris-HCl; 10 mM $MgCl_2$; 5 mM DTT; 0.1 mM spermidine), 10 mM ATP, 10 U of T4 Polynucleotide kinase (10 U/µl; Thermo Scientific) and nuclease-free water to a final volume of 20 µl. The reaction mixtures were incubated at 37°C for 30 min and then at 75°C for 10 min to inactivate the enzyme. The phosphorylated amplicons were purified from a 1% (w/v) agarose gel with the GeneJET Gel Extraction kit (Thermo Scientific) and then self-ligated at 22°C for 1 h in a final volume of 20 µl that comprised 80 ng of phosphorylated PCR product, 10 µl of 2 × DNA ligase buffer, 2 µl of 40% (w/v) PEG-4000 and 5 U of T4 DNA ligase (5 U/µl; Thermo Scientific). Following self-ligation, the reaction mixtures were used to transform competent *E. coli* DH5α cells, and the

transformation mixtures were then plated onto LB agar supplemented with ampicillin (100 µg/ml). The agar plates were incubated overnight at 37°C.

3.11.3 Characterization of mutant pJET-NS2 plasmid constructs

Single colonies resulting from the above transformations were inoculated into 5 ml of LB broth containing ampicillin (100 µg/ml), incubated overnight at 37°C and plasmid DNA was subsequently extracted with the GeneJet Plasmid Miniprep kit (Thermo Scientific). Prior to their use in subsequent experiments, each of the mutant pJET-NS2 plasmid constructs was characterized by DNA sequencing. The nucleotide sequence of the mutated NS2 genes was determined using the ABI-PRISM BigDye Terminator Cycle Sequencing Ready Reaction kit v.3.1 (Perkin-Elmer Applied Biosystems), together with pJET-F or pJET-R as the sequencing primer (Table 3.2), followed by resolution on an ABI-PRISM 3130XL DNA sequencer. Nucleotide and deduced amino sequences were analyzed with MEGA-X software (https://www.megasoftware.net/) to confirm the presence of the newly introduced mutations.

3.12 Construction and characterization of recombinant pFastBac HTa donor plasmids

To enable in-frame cloning of the wild-type and mutated NS2 genes with the N-terminal hexahistidine tag present in the pFastBac HTa donor vector, the insert DNA was excised from the various mutant pJET-NS2 plasmid constructs by digestion with both *Eco*RI and *Xho*I. The restriction enzyme digestion reactions were performed in Eppendorf tubes and consisted of 500 ng of plasmid DNA, 2 µl of 10 × FastDigest Green buffer, 1 U each of *Eco*RI and *Xho*I (Thermo Scientific) and nuclease-free water to a final volume of 20 µl. Accordingly, the pFastBac HTa bacmid donor vector was digested in an identical manner. The desired insert and vector DNA fragments were purified from the agarose gels with the GeneJET Gel Extraction kit (Thermo Scientific), and the DNA concentrations were determined with a Nanodrop ND-1000 spectrophotometer (NanoDrop Technologies, Inc.) prior to their use in ligation reactions. Each ligation reaction mixture (20 µl) contained 50 ng of pFastBac HTa vector DNA, 100 ng of insert DNA, 2 µl of 10 × DNA ligase buffer and 1 µl of T4 DNA ligase (5 U/µl; Thermo Scientific). The ligation reactions were incubated at 22°C for 1 h and then transformed into competent *E. coli* DH5α cells, as described previously (Section 3.2.5.3). Plasmid DNA extracted from the resultant ampicillin-resistant transformants were screened for the presence of cloned insert DNA by digestion with both *Eco*RI and *Xho*I, followed by analysis of the digestion products on a 1% (w/v) agarose gel in the presence of a DNA molecular weight

marker. The integrity of the cloned insert DNAs was also verified by DNA sequencing (Section 3.2.6.3) using S8-F or S8-R as the sequencing primer (Table 3.2). The recombinant plasmids were designated pFB-NS2, pFB-NS2 S-A256, pFB-NS2 S-A258, pFBNS2 S-A262, pFB-NS2 S-A270, pFB-NS2 S-A256,258, pFB-NS2 S-D256, pFB-NS2 S-D258, and pFB-NS2 S-D256,258 (Table 3.1).

3.13 Generation and characterization of recombinant bacmids

3.13.1 Transposition

An overnight culture of *E. coli* DH10Bac cells, containing the bacmid genome and a pMON7124 helper plasmid, was prepared by inoculating a single colony into LB broth supplemented with kanamycin (50 µg/ml) and tetracycline (10 µg/ml). Competent *E. coli* DH10Bac cells were prepared, as described previously (Section 3.2.5.2). For transformation, 1 ng of the recombinant pFastBac HTa donor plasmid DNA was mixed with 100 µl of the competent *E. coli* DH10Bac cells and then incubated on ice for 30 min. The cells were heat-shocked at 42°C for 45 s and incubated on ice for 2 min before 900 µl of pre-warmed (37°C) LB broth was added. The transformation mixtures were incubated at 37°C for 4 h with shaking to allow the cells to recover, to express the antibiotic resistance genes and to allow for transposition to occur. The transformation mixtures were plated in aliquots of 200 µl onto LB agar supplemented with 50 µg/ml of kanamycin, 7 µg/ml of gentamycin and 10 µg/ml of tetracycline in the presence of 50 µl of 2% (w/v) X-gal and 10 µl of 100 mM IPTG. The agar plates were incubated at 37°C for 48 h and transformants displaying a white-colony phenotype were selected. One colony displaying a blue-colony phenotype was selected as a non-recombinant bacmid control.

3.13.2 Extraction of recombinant bacmid DNA

Selected colonies were inoculated into 5 ml of LB broth supplemented with antibiotics (50 µg/ml kanamycin; 7 µg/ml gentamycin; 10 µg/ml tetracycline) and cultured overnight at 37°C with shaking. The recombinant and non-recombinant bacmid DNA was isolated by making use of the following protocol that had been developed for the isolation of large plasmid DNA and was subsequently adapted for the isolation of high-molecular-weight bacmid DNA (Fawcett, 1999). The bacterial cells from 2 ml of each overnight culture were harvested by centrifugation at 14 000 rpm for 1 min. The supernatant was decanted, and the bacterial cell pellet was suspended in 300 µl of ice-cold Solution I (15 mM Tris-HCl [pH 8.0]; 10 mM

EDTA; 100 µg/ml RNase A), followed by the addition of 300 µl of Solution II (0.2 N NaOH; 1% [w/v] SDS). After incubation at room temperature for 5 min, 300 µl of ice-cold Solution III (3 M KOAc; pH 5.5) was added and the tubes were incubated on ice for 10 min. The white precipitate consisting of proteins and *E. coli* genomic DNA was removed by centrifugation at 14 000 rpm for 10 min. The bacmid DNA was precipitated from the recovered supernatant by the addition of 800 µl isopropanol and incubation on ice for 10 min. The precipitated bacmid DNA was collected by centrifugation at 14 000 rpm for 15 min, washed twice with 70% ethanol, air-dried at room temperature, and then suspended in 50 µl of 1 × TE buffer (10 mM Tris-HCl; 1 mM EDTA; pH 8.0). An aliquot of each bacmid DNA extract was analyzed by electrophoresis on a 1% (w/v) agarose gel.

3.13.3 Analysis of recombinant bacmids

To confirm the successful transposition of the wild-type NS2 gene and the respective mutated NS2 genes into the bacmid DNA, PCR analysis of the extracted bacmid DNA was performed. The PCR reactions were performed with DreamTaq Green PCR Master Mix (Thermo Scientific). Each PCR reaction mixture contained 400 ng of bacmid DNA as template, 10 µM each of primers pHed-F and pUC/M13-R (Table 3.2), 10 µl of 2 × DreamTaq Green PCR Master Mix (inclusive of DreamTaq DNA polymerase; optimized DreamTaq Green Buffer; 4 mM $MgCl_2$; 0.4 mM of each dNTP) and nuclease-free water to a final volume of 20 µl. The tubes were placed in a BioRad T100 thermal cycler and the thermocycling conditions comprised an initial denaturation at 95°C for 3 min, followed by 25 cycles of denaturation at 95°C for 30 s, primer annealing at 55°C for 30 s, and primer extension at 72°C for 4 min. After the last cycle, the reactions were kept at 72°C for 10 min to complete the synthesis of all DNA strands. To test for contamination, a reaction mixture from which template DNA was omitted was also included. The PCR reaction mixtures were analyzed by electrophoresis on a 1% (w/v) agarose gel in the presence of a DNA molecular weight marker.

3.14 Generation of recombinant baculoviruses

3.14.1 Cell culture

Spodoptera frugiperda clone 9 (Sf-9) insect cells were maintained as adherent cultures in 25-cm^2 cell culture flasks (TPP®; Sigma-Aldrich) in TC-100 medium (Gibco) supplemented with 10% (v/v) foetal bovine serum (FBS; Gibco) and antibiotics (1.2% [v/v] Amphotericin B, 1% [v/v] of 20 000 U/ml penicillin-20 000 U/ml streptomycin mix; Lonza). Suspension cultures

of Sf-9 cells in 250-ml Erlenmeyer flasks (140 rpm) were maintained in the same medium, except that 1% (v/v) Pluronic-F68 (Sigma-Aldrich) was added to the medium. The cell monolayers and suspension cultures were incubated at 27°C. The cell density and viability were determined by staining 500 µl of the cells with an equal volume of Trypan blue (0.4% [w/v] Trypan blue in 1 × PBS) and then counting on a haemocytometer (Drews *et al.*, 1995). Suspension cultures were seeded at an initial density of 1-2 × 10^5 cells/ml and sub-cultured when they reached 2-5 × 10^6 cells/ml.

3.14.2 Transfection of Sf-9 cells

Recombinant and non-recombinant bacmid DNA was transfected into Sf-9 cells with Cellfectin II reagent (Gibco) according to the manufacturer's instructions. The cells were seeded into the wells of 6-well tissue culture plates (8 × 10^5 cells/well) and allowed to attach at 27°C for 1 h. For each transfection, two separate transfection solutions were prepared by diluting 8 µl of Cellfectin II reagent in 100 µl of incomplete TC-100 medium (medium lacking serum and antibiotics) and by diluting 1 µg of bacmid DNA in 100 µl of incomplete TC-100 medium. The two solutions were then combined, mixed gently, and incubated at room temperature for 30 min, after which 800 µl of incomplete TC-100 medium was added. The cell monolayers were prepared for transfection by aspirating the medium from the attached cells and the cells were rinsed with 2 ml of incomplete TC-100 medium. The transfection mixtures were then added dropwise onto the cells and the tissue culture plates were incubated at 27°C for 5 h in a humidified environment. Subsequently, the transfection mixtures were aspirated and replaced with 2 ml of complete TC-100 medium (medium supplemented with FBS and antibiotics), and incubation was continued at 27°C for 72 h in a humidified environment. Following incubation, the cells were harvested from the surface of tissue culture plates and collected by centrifugation at 2 000 rpm for 5 min. The cell-free supernatants, containing the recombinant baculovirus, were stored at 4°C. Mock-transfected cells were included as controls whereby infection of the cells could be monitored.

3.14.3 Preparation and titration of virus stocks

To prepare virus stocks, 500 µl of the supernatants obtained following transfection of Sf-9 cells were used to infect cell monolayers in 75-cm^2 tissue culture flasks (1 × 10^7 cells/flask) and the flasks were incubated at 27°C for 7 days in a humidified environment. The cells were subsequently harvested by centrifugation (2 000 rpm for 5 min) and 500 µl of the cell-free

supernatant was used to infect fresh Sf-9 cell monolayers in 75-cm^2 tissue culture flasks. This procedure was repeated three times to generate P3 virus stocks. To determine the virus titre, a plaque assay was performed according to Brown and Faulkner (1977), with the following modifications. Sf-9 cells were seeded into the wells of a 6-well tissue culture plate (1.7×10^6 cells/well) and after cell attachment at 27°C for 1 h, the medium was replaced with 900 µl of the virus dilutions (10^{-3} to 10^{-6}) that had been prepared in incomplete TC-100 medium. After incubation at 27°C for 1 h to allow virus particles to infect the cells, the virus dilutions were removed and replaced with 2 ml of pre-warmed (38°C) plaquing medium (2% [w/v] low melting agarose [Cleaver Scientific] in 1 × PBS, diluted 1:1 with complete TC-100 medium). Once the overlay had set, the tissue culture plates were incubated at 27°C for 6 days in a humidified environment. Following incubation, the cell monolayers were flooded with 500 µl of 0.1% (w/v) MTT [(3-(4,5-dimethylthiazol-2-yl)-2,5-diphenyltetrazolium bromide; Sigma-Aldrich]. The excess MTT solution was aspirated, and the tissue culture plates were incubated overnight at 27°C for plaques to appear. The plaques were counted, and the virus titres were determined.

3.15 Expression of recombinant wild-type and mutant NS2 proteins in Sf-9 insect cells

Sf-9 cells were seeded into the wells of a 6-well tissue culture plate (1.5×10^6 cells/well) and subsequently infected with parental or recombinant baculoviruses at a multiplicity of infection (MOI) of 1 pfu/cell. Mock-infected cells were included as a control in the analysis. The tissue culture plates were incubated at 27°C for 72 h in a humidified environment. Following incubation, the cells were harvested by centrifugation at 2 000 rpm for 5 min and washed once with 1 × PBS. The cell pellets were each suspended in 200 µl of 1 × PBS and aliquots (20 µl) of the whole-cell lysates were analyzed by Western blot analysis following electrophoresis on SDS-polyacrylamide gels.

3.16 Purification of baculovirus-expressed wild-type and mutant NS2 proteins and evaluation of their phosphorylation status

Recombinant baculoviruses were used to infect Sf-9 cell monolayers in 6-well tissue culture plates (1.5×10^6 cells/well) at a MOI of 2 pfu/cell. Following incubation at 27°C for 72 h, the baculovirus-infected Sf-9 cells were harvested from the surface of tissue culture plates, collected by centrifugation at 2 000 rpm for 5 min, and washed once with 1 × PBS. The cell pellets were each suspended in 1 ml of 1 × PBS and the cells were lysed by passing the cell suspension through a 22G needle multiple times. Following centrifugation at 3 000 rpm for 2

min, the supernatant (soluble protein extract) was collected. Since the wild-type and mutant NS2 proteins were expressed with a N-terminal hexahistidine tag, the recombinant NS2 proteins were purified with the HisPur Cobalt Purification kit (Thermo Scientific), as described previously (Section 3.5.2), and successful recovery of the purified wild-type and mutant NS2 proteins was confirmed by SDS-PAGE analysis.

To examine whether the serine residues selected for mutagenesis were indeed the phosphorylation sites of the NS2 protein, the concentration of the purified wild-type and mutant NS2 proteins was determined with the Quick Start Bradford Protein Assay kit (BioRad) and equal amounts of the purified NS2 proteins were then electrophoresed on a SDS-polyacrylamide gel. Following electrophoresis, the gel was stained with Pro-Q Diamond Phosphoprotein Gel Stain (Invitrogen), as described previously (Section 3.9), to visualize phosphorylated proteins. For the relative quantification of the phosphorylation signals, images of the stained SDS-polyacrylamide gels were analyzed with ImageJ software (https://imagej.nih.gov/ij/).

3.17 Immunofluorescence confocal microscopy

Sf-9 cells were grown on sterile glass coverslips placed in the wells of a 24-well tissue culture plate (3.8×10^5 cells/well). The cells were mock-infected or infected with parental and recombinant baculoviruses at a MOI of 5 pfu/cell. Following incubation of the tissue culture plates at 27°C for 48 h, the cell monolayers were washed once with 1 × PBS and then fixed in 400 µl of 4% (w/v) paraformaldehyde (prepared in 1 × PBS) for 30 min at room temperature. The fixing solution was aspirated, and the cells were permeabilized by incubation for 10 min at room temperature with 400 µl of TX-100 (0.2% (v/v) Triton X-100 in 1 × PBS). The cell monolayers were then incubated with 500 µl of blocking solution (1% [w/v] fat-free milk powder in 1 × PBS) for 30 min at room temperature, followed by incubation for 1 h at room temperature with 80 µl of the anti-NS2 antibody (diluted 1:250 in blocking solution). The cells were washed three times with wash buffer (0.05% [v/v] Tween-20 in 1 × PBS) and then incubated for 1 h at room temperature with 80 µl of goat anti-rabbit Alexa Fluor 488 antibody (Thermo Scientific), which was diluted 1:250 in blocking solution. Following incubation, the cell monolayers were washed three times with wash buffer and once with 1 × PBS. The coverslips were mounted onto glass slides using ProLong Gold Antifade mountant with DAPI (Life Technologies). The slides were viewed with a Zeiss LSM 880 confocal microscope with Airyscan at the Laboratory for Microscopy and Microanalytics, University of Pretoria. The

images were captured with a Zeiss AxioObserver digital camera and analyzed with ZEN (blue edition) v.2.3 software.

CHAPTER FOUR

RESULTS

4.1 Construction of the *Escherichia coli* expression vector pET-NS2

To facilitate studies aimed at identifying the kinase responsible for AHSV-4 NS2 protein phosphorylation and to aid in the identification of phosphorylated residues within NS2, an unphosphorylated version of the NS2 protein was required for use in subsequent phosphorylation assays. Considering that heterologous proteins expressed in *E. coli* do not undergo post-translational modifications, such as phosphorylation, the NS2 protein was therefore expressed in *E. coli* BL21(DE3) using the pET-26b(+) expression vector. The pET26b(+) vector allows for the selective and active expression of heterologous proteins that may comprise more than 50% of the total cellular protein content a few hours after induction. Moreover, the expression vector also contains a C-terminal hexahistidine tag that serves as a fusion partner for the purification of the heterologous protein (Fig. 4.1A).

To enable in-frame cloning of the NS2 gene with the C-terminal hexahistidine tag present in the pET-26b(+) expression vector, the NS2 gene was PCR-amplified using a 3'-specific primer designed to amplify a truncated version of AHSV-4 NS2 gene that lacked the TGA stop codon. Furthermore, this primer and the 5'-specific primer were designed to introduce a unique *Xho*I and *Nde*I restriction endonuclease recognition site at the 3'- and 5'-end, respectively, of the PCR-amplified NS2 gene in order to facilitate directional cloning.

Using plasmid pJET-S8 as template DNA, PCR amplification was performed using the appropriate primers. An aliquot of the reaction mixture was analyzed by agarose gel electrophoresis and a single amplicon of the expected size (1.095 kb) was observed (Fig. 4.1B, lane 2). The amplicon was purified from the agarose gel, blunt-end cloned into pJET 1.2/blunt vector DNA to yield the intermediate plasmid pJET-NS2 and then characterized by restriction enzyme digestion (Fig. 4.1C) and nucleotide sequencing. Having confirmed that the stop codon was deleted, the truncated NS2 gene was recovered and cloned into the *Nde*I and *Xho*I sites of pET-26b(+), thereby generating pET-NS2. The recombinant plasmid DNA was characterized by agarose gel electrophoresis, following restriction endonuclease digestion. *Nde*I and *Xho*I digestion yielded two DNA fragments corresponding to the size of the pET-26b(+) vector DNA (5.360 kb) and the cloned truncated NS2 gene (1.095 kb) (Fig. 4.1D, lane 3).

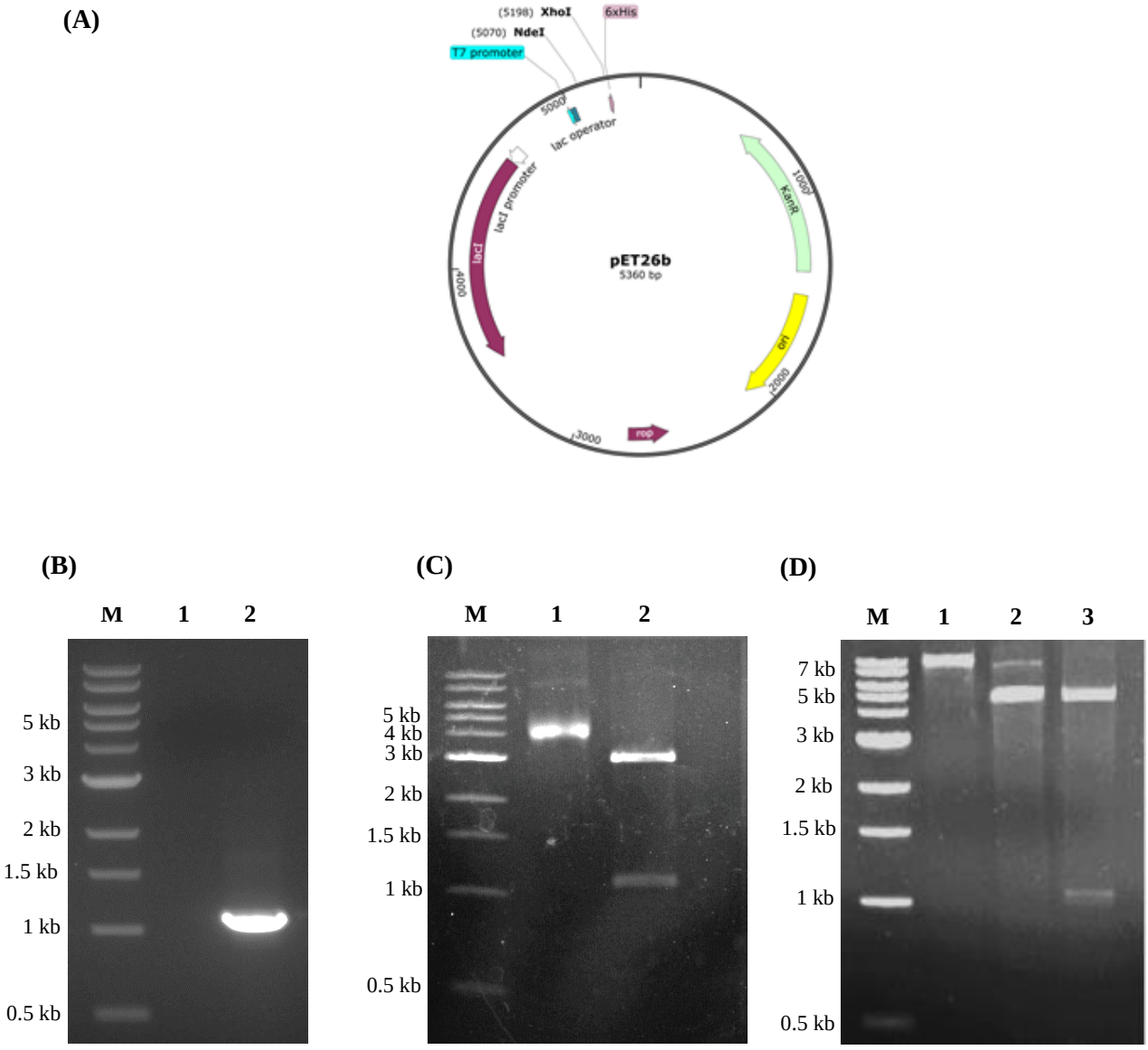

Figure 4.1: Agarose gel electrophoretic analysis of recombinant pET-NS2 and the intermediate plasmid pJET-NS2 used in its construction. (A) Plasmid map of the pET-26b(+) bacterial expression vector, indicating the cloning sites used for insertion of the AHSV-4 NS2 gene and the location of the T7 RNA polymerase promoter and hexahistidine tag sequence. (B) PCR amplification of a tailored NS2 gene. Lane M, DNA molecular weight marker; lane 1, negative control PCR reaction mixture lacking template DNA; lane 2, amplicon obtained by PCR amplification using pJET-S8 plasmid DNA as template and primers TailorNS2-F and TailorNS2-R. (C) Analysis of recombinant plasmid pJET-NS2. Lane M, DNA molecular weight marker; lane 1, uncut recombinant plasmid pJET-NS2; lane 2, pJET-NS2 plasmid DNA digested with both *Nde*I and *Xho*I. (D) Analysis of recombinant plasmid pET-NS2. Lane M, DNA molecular weight marker; lane 1, uncut parental pET-26b(+) vector DNA; lane 2, pET-26b(+) vector DNA digested with both *Nde*I and *Xho*I; lane 3, pET-NS2 plasmid DNA digested with both *Nde*I and *Xho*I. The sizes of the DNA molecular weight marker (1 kb DNA Ladder; New England Biolabs) are indicated to the left of the figures.

The integrity of the cloned insert DNA was verified by nucleotide sequencing, the result of which confirmed that nucleotides specifying the C-terminal stop codon of the NS2 were successfully deleted. In addition, analysis of the deduced amino acid sequence confirmed that the NS2 gene was cloned in frame with the hexahistidine tag sequence. The complete nucleotide and deduced amino sequence of the cloned NS2 gene is provided in the Appendix to this dissertation.

4.2 Analysis of recombinant NS2 protein expression in *E. coli* BL21(DE3)

4.2.1 SDS-PAGE and Western blot analyses

To determine whether the AHSV-4 NS2 protein could be expressed in *E. coli*, the non-recombinant pET-26b(+) vector and recombinant pET-NS2 expression plasmid were transformed into *E. coli* BL21(DE3) cells. For bacterial expression, overnight cultures of the respective bacterial strains were inoculated into LB broth and grown in the presence of IPTG to induce high-level protein expression. Following incubation, the cells of each culture were harvested and whole-cell lysates were prepared. These samples were analyzed, together with uninduced samples of the recombinant bacterial cultures, by SDS-PAGE and Western blot analyses.

Analysis of the Coomassie blue-stained gel indicated the presence of an over-expressed protein (45 kDa) in the sample prepared from induced *E. coli* BL21(DE3) cells transformed with pET-NS2. A similarly over-expressed protein was not observed in the protein samples prepared from *E. coli* BL21(DE3) cells transformed with the non-recombinant pET-26b(+) vector or in the control uninduced bacterial cultures (Fig. 4.2A). To confirm the identity of the over-expressed protein, an unstained SDS-polyacrylamide gel was subjected to Western blot analysis. The results indicated that the over-expressed protein reacted specifically with the anti-NS2 antibody, and no cross-reaction was observed with a similarly sized protein in the control cell lysates (Fig. 4.2B). Thus, it was concluded that the AHSV-4 NS2 protein was successfully expressed by the constructed recombinant bacterial expression vector.

4.2.2 Purification and characterization of the recombinant NS2 protein

Considering that the recombinant NS2 protein was expressed in *E. coli* BL21(DE3) with a hexahistidine affinity tag at the C terminus and based on the requirement for pure NS2 protein to be used in phosphorylation assays, it was next determined if the recombinant proteins could

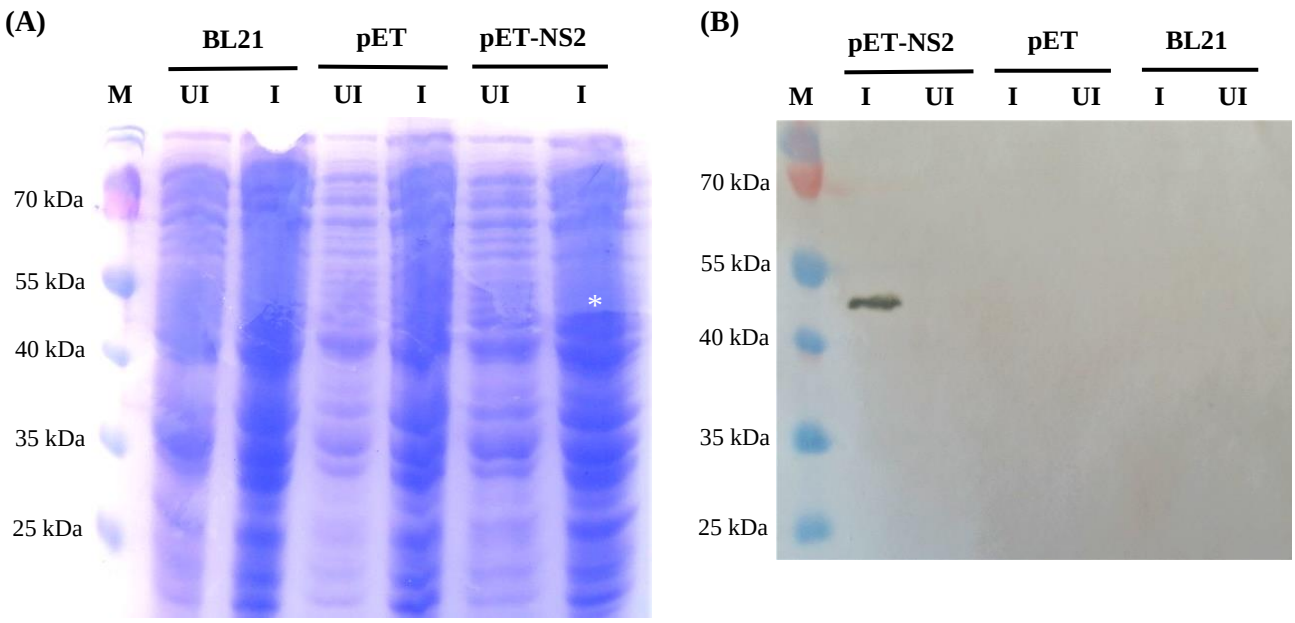

Figure 4.2: Expression of recombinant NS2 protein in *E. coli* BL21(DE3). Uninduced (UI) and IPTG-induced (I) cultures of *E. coli* BL21(DE3) cells transformed with the non-recombinant pET26b(+) vector (pET) or with the recombinant pET-NS2 plasmid (pET-NS2) were harvested at 4 h post-induction. Uninduced and IPTG-induced *E. coli* BL21(DE3) cells (BL21) were included as controls. The bacterial whole-cell lysates were resolved by SDS-PAGE (A) and proteins from an unstained gel were electroblotted onto a nitrocellulose membrane and subjected to Western blot analysis with an anti-NS2 antibody (B). The position of the NS2 protein expressed with a histidine tag in the Coomassie blue-stained gel is indicated by an asterisk. The sizes of the PageRuler Prestained Protein Ladder (Thermo Scientific) are indicated in kDa to the left of the figures.

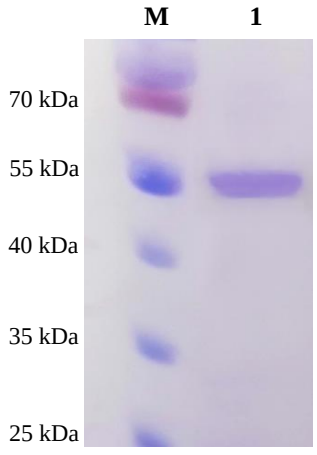

Figure 4.3: Purification of the recombinant NS2 protein expressed in *E. coli* BL21(DE3). Following expression of the NS2 protein in IPTG-induced *E. coli* BL21(DE3) cultures, cytoplasmic protein fractions was prepared and the hexahistidine-tagged NS2 protein was purified by IMAC. The purified NS2 protein (lane 1) was analyzed by SDS-PAGE and visualized by staining the gel with Coomassie brilliant blue. The sizes of the PageRuler Prestained Protein Ladder (Thermo Scientific) are indicated in kDa to the left of the figure.

be purified by immobilized metal affinity chromatography (IMAC). This procedure is based on the interactions between a transition metal ion (*e.g.*, Co^{2+}, Ni^{2+}, Cu^{2+} or Zn^{2+}) immobilized on a matrix and specific amino acid side chains. Among the different amino acids, histidine exhibits the strongest interaction with immobilized metal ion matrices, as electron donor groups on the histidine imidazole ring readily form coordination bonds with the immobilized transition metal. Following the washing of the matrix, proteins containing a polyhistidine affinity tag can be eluted by adding free imidazole to the elution buffer (Porath, 1992; Bornhorst and Falke, 2000).

The HisPur Cobalt Protein Purification kit (Thermo Scientific) was used to purify the recombinant NS2 protein from IPTG-induced *E. coli* BL21(DE3) cultures. The NS2 protein was purified from soluble protein fractions under non-denaturing (native) conditions and the purity of the protein was assessed by SDS-PAGE. The result, presented in Fig. 4.3, indicated that the NS2 protein was purified to near homogeneity and there was no apparent evidence of degradation of the protein.

4.3 Identification of the kinase responsible for AHSV-4 NS2 protein phosphorylation

It has been reported previously that NS2 of EHDV and BTV can be phosphorylated by a cellular kinase present in the cytoplasm of *S. frugiperda*-9 (Sf-9) insect cells (Theron *et al.*, 1994; Taraporewala *et al.*, 2001), and it was subsequently reported that Casein kinase 2 (CK2) mediates phosphorylation of the BTV NS2 protein (Modrof *et al.*, 2005). To investigate whether AHSV-4 NS2 could likewise be phosphorylated, the *E. coli*-expressed AHSV-4 NS2 protein was mixed with a Sf-9 cell lysate and incubated in the presence of ATP. An additional reaction was also included in which 4, 5, 6, 7-tetrabromobenzotriazole (TBB), a specific inhibitor of CK2, was added to the phosphorylation reaction mixture. Following incubation, the NS2 protein was purified by IMAC and analyzed by SDS-PAGE to verify the successful recovery of the recombinant NS2 protein. To determine whether the NS2 protein was phosphorylated, a duplicate SDS-polyacrylamide gel was stained with Pro-Q Diamond Phosphoprotein Gel Stain. This gel stain is a proprietary fluorescent stain that allows for the selective staining of phosphoproteins in polyacrylamide gels, without the need for antibodies or radioisotopes (Steinberg *et al*, 2003; Schulenberg *et al*, 2004).

As shown in Fig. 4.4, a cellular kinase present in the Sf-9 cell lysate was capable of phosphorylating an unphosphorylated version of the *E. coli*-expressed NS2 protein (Fig. 4.4B,

lane 3) and TBB was able to inhibit phosphorylation of NS2 (Fig. 4.4B, lane 4). These results thus suggested that CK2 could be responsible for NS2 protein phosphorylation. To confirm that CK2 is indeed responsible for the phosphorylation of NS2, equal amounts of the purified unphosphorylated *E. coli*-expressed NS2 protein were incubated in the presence of CK2 and in the absence or presence of TBB. Subsequent analysis of the SDS-polyacrylamide gel stained with Pro-Q Phosphoprotein Gel Stain indicated that CK2 was able to phosphorylate the NS2 protein, whereas TBB inhibited phosphorylation of NS2 by CK2 (Fig. 4.5). Taken together, the results of these experiments thus provide evidence that AHSV-4 NS2 is phosphorylated by CK2.

4.4 Identification of serine residues representing targets for Casein Kinase 2

The NS2 protein of orbiviruses is the only virus-specified protein that is phosphorylated (Huismans *et al.*, 1987), and for both BTV (Modrof *et al.*, 2005; Mohl and Roy, 2016) and AHSV (this study) the NS2 protein is phosphorylated by Casein kinase 2 (CK2). Phosphoamino acid analyses have revealed that serine residues located in the C terminus of the BTV and AHSV NS2 proteins are the only phosphate acceptor sites (Devaney *et al.*, 1988). Thus, to identify serine residues that may represent potential targets for phosphorylation by CK2, the amino acid sequence of AHSV-4 NS2 was analyzed with three different computer prediction programmes.

A total of six serine residues present in the C terminus of the AHSV-4 NS2 protein were predicted as potential phosphorylation sites of CK2. Of these, serine residues located at positions 221 and 223 were identified with only one of the prediction programmes (GPS v.5) and were therefore disregarded. Consequently, based on these analyses, four serine residues of AHSV-4 NS2 were selected as potential phosphorylation sites, *i.e.*, residues 256, 258, 262 and 270. In each of the analyses, the serine residue located at position 262 within the NS2 protein sequence demonstrated the highest likelihood of being phosphorylated, while the serine residues located at positions 256, 258 and 270 were also likely candidates albeit with comparatively lower scores (Table 4.1).

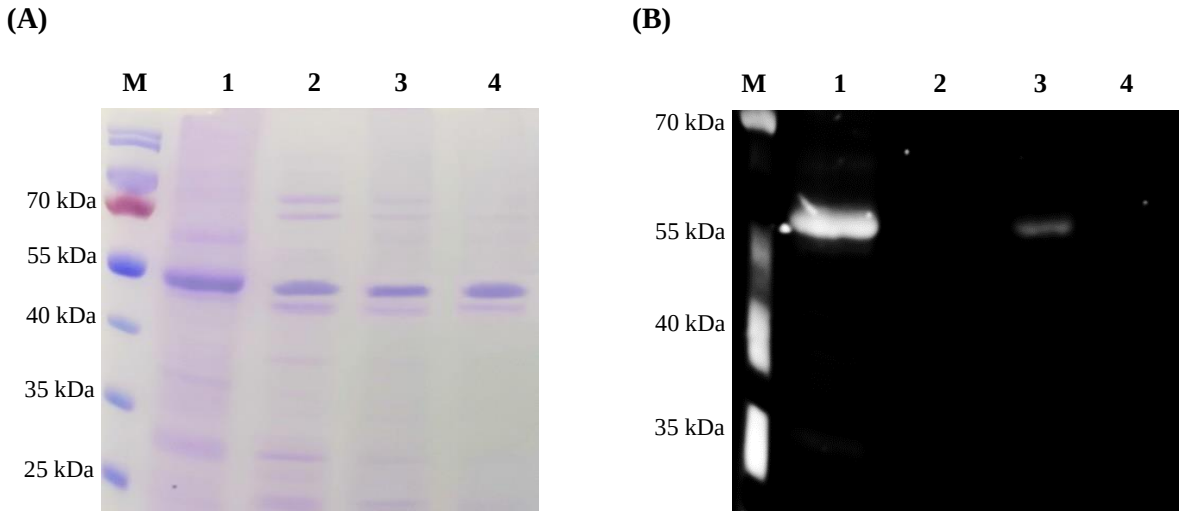

Figure 4.4: *In vitro* phosphorylation of the *E. coli*-expressed NS2 protein. The *E. coli*-expressed NS2 protein was mixed with a Sf-9 cell lysate and incubated in the presence of ATP. The hexahistidine-tagged NS2 protein was then purified by IMAC and analyzed by SDS-PAGE (A), and a duplicate gel was stained with Pro-Q Diamond Phosphoprotein Gel Stain to visualize phosphorylated proteins (B). Lanes M, Protein molecular mass marker; lanes 1, Purified NS2 expressed in Sf-9 cells by a baculovirus recombinant; lanes 2, Purified NS2 expressed in *E. coli* BL21(DE3); lanes 3, NS2 purified from the phosphorylation mixture; lanes 4, NS2 purified from a phosphorylation reaction mixture containing 100 µM TBB to inhibit CK2 activity. The sizes of the PageRuler Prestained Protein Ladder (Thermo Scientific) are indicated in kDa to the left of the figures.

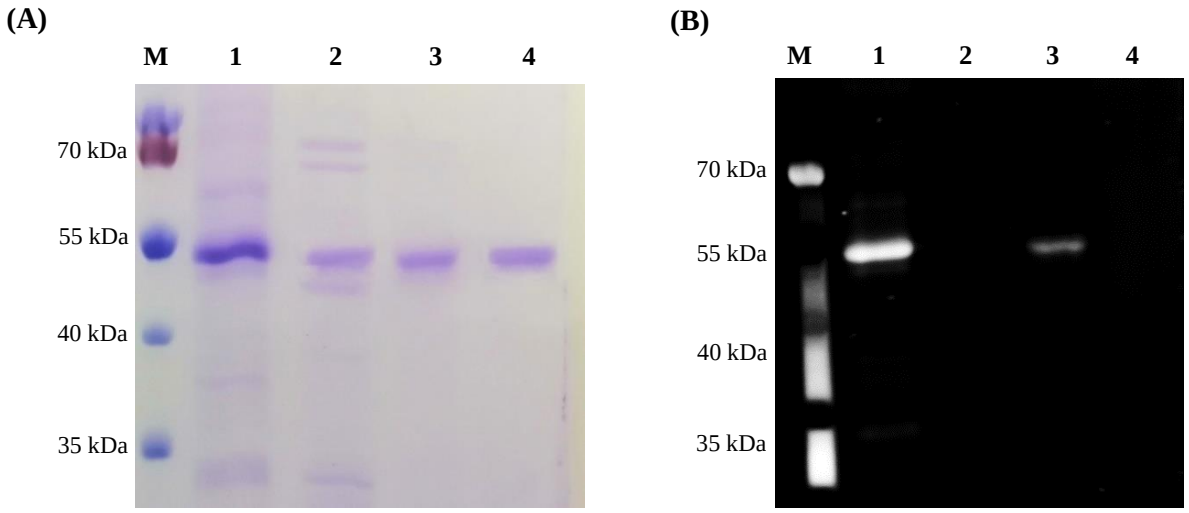

Figure 4.5: Phosphorylation of NS2 by protein kinase CK2. Equal amounts (0.3 µg) of purified hexahistidine-tagged NS2 expressed in *E. coli* were mixed with CK2 and ATP. Following incubation, the samples were electrophoresed on a SDS-polyacrylamide gel (A), and a duplicate gel was stained with Pro-Q Diamond Phosphoprotein Gel Stain to visualize phosphorylated proteins (B). Lanes M, Protein molecular mass marker; lanes 1, Purified NS2 expressed in Sf-9 cells by a baculovirus recombinant; lanes 2, Purified NS2 expressed in *E. coli* BL21(DE3); lanes 3, NS2 incubated with CK2; lanes 4, NS2 incubated with CK2 in the presence of 100 µM TBB to inhibit CK2 activity. The sizes of the PageRuler Prestained Protein Ladder (Thermo Scientific) are indicated in kDa to the left of the figures.

Table 4.1 Putative CK2-phosphorylated serine residues (bold, underlined) within the C terminus of the AHSV-4 NS2 protein, as predicted with different computer prediction programmes

Scansite 4.0[a]		
Position	**Amino acid sequence**	**Score**
256	TESMWCQ**S**DSDDQSD	0.567
258	SMWCQSD**S**DDQSDED	0.536
262	QSDSDDQ**S**DEDHEVG	0.391
270	DEDHEVG**S**TEPENYI	0.584
Group-based Prediction System (GPS) v.5[b]		
Position	**Amino acid sequence**	**Score**
221	LSVQSNE**S**RSDDVAR	11.693
223	VQSNESR**S**DDVARRH	8.124
256	TESMWCQ**S**DSDDQSD	12.217
258	SMWCQSD**S**DDQSDED	14.578
262	QSDSDDQ**S**DEDHEVG	18.145
270	DEDHEVG**S**TEPENYI	5.358
NetPhos-3.1[c]		
Position	**Amino acid sequence**	**Score**
256	MWCQ**S**DSDD	0.523
258	CQSD**S**DDQS	0.657
262	SDDQ**S**DEDH	0.707
270	HEVG**S**TEPE	0.262

a ScanSite 4.0 predicts potential phosphorylation sites based on sequence comparisons between the protein of interest and the optimal motif sequence of a given kinase. A score of 0.00 is considered to be a perfect match between the optimal motif sequence and the protein of interest.

b Group-based Prediction System (GPS) v.5 predicts locations for serine phosphorylation by CK2 according to a hierarchical model by comparison of the protein sequence of interest to experimentally verified eukaryotic phosphorylation sites found in the Phospho.ELM database. The evolutionary likelihood of a specific amino acid mutating into a different residue is calculated, allowing for a score to be awarded based on the hypothesis that closely related sequences would likely have similar three-dimensional structures and biochemical properties. The scores are calculated as an average of the substitution scores of the sequence of interest compared with the known target sequences. The higher the final score, the more similar the sequence is to other known sequences (Xue *et al.*, 2008).

c NetPhos-3.1 predicts the likelihood of phosphorylation of serine residues by various cellular kinases using an artificial neural network approach. A score is assigned to the candidate site that reflects the likelihood of it being phosphorylated, with 0.000 being the most unlikely and 1.000 being the most likely (Blom *et al.*, 2004).

4.5 Construction of site-directed mutants of the AHSV-4 NS2 gene

To determine whether the identified serine residues are indeed phosphorylation sites of the AHSV-4 NS2 protein, NS2 mutants were generated by substituting the respective serine residues with alanine residues singularly (residues 256, 258, 262 and 270) and in combination (residues 256 and 258). To characterize further the phosphorylation of NS2, additional NS2 mutants were generated in which selected serine residues were substituted with aspartate residues (residues 256 and 258 singularly and in combination). An aspartate residue is considered to mimic a phosphoserine residue due to its negative charge (Reddy *et al.*, 2004; Lewellyn and Loeb, 2011).

To generate the desired mutant NS2 genes, inverse PCR reactions were performed using recombinant plasmid pJET-S8 as template DNA and appropriately designed primer pairs for each mutant. The amplicons of approximately 4.1 kb, comprising the pJET1.2/blunt vector (2.974 kb) and mutated NS2 gene (1.098 kb), were purified from an agarose gel, phosphorylated in the presence of T4 Polynucleotide kinase and then self-ligated. Following the transformation of competent *E. coli* DH5α cells, plasmid DNA was extracted from randomly selected transformants and subjected to DNA sequencing. The results, presented in Fig. 4.6, confirmed the presence of the newly introduced site-specific mutations. These plasmid constructs were designated pJET-NS2 S-A256, pJET-NS2 S-A258, pJET-NS2 S-A262, pJET-NS2 S-A270, pJET-NS2 S-A256,258, pJET-NS2 S-D256, pJET-NS2 S-D258 and pJET-NS2 S-D256,258, respectively.

The full-length nucleotide and deduced amino acid sequences of these mutated NS2 genes are provided in the Appendix to this dissertation and furthermore confirm the absence of any nucleotide differences other than the newly introduced site-specific mutations.

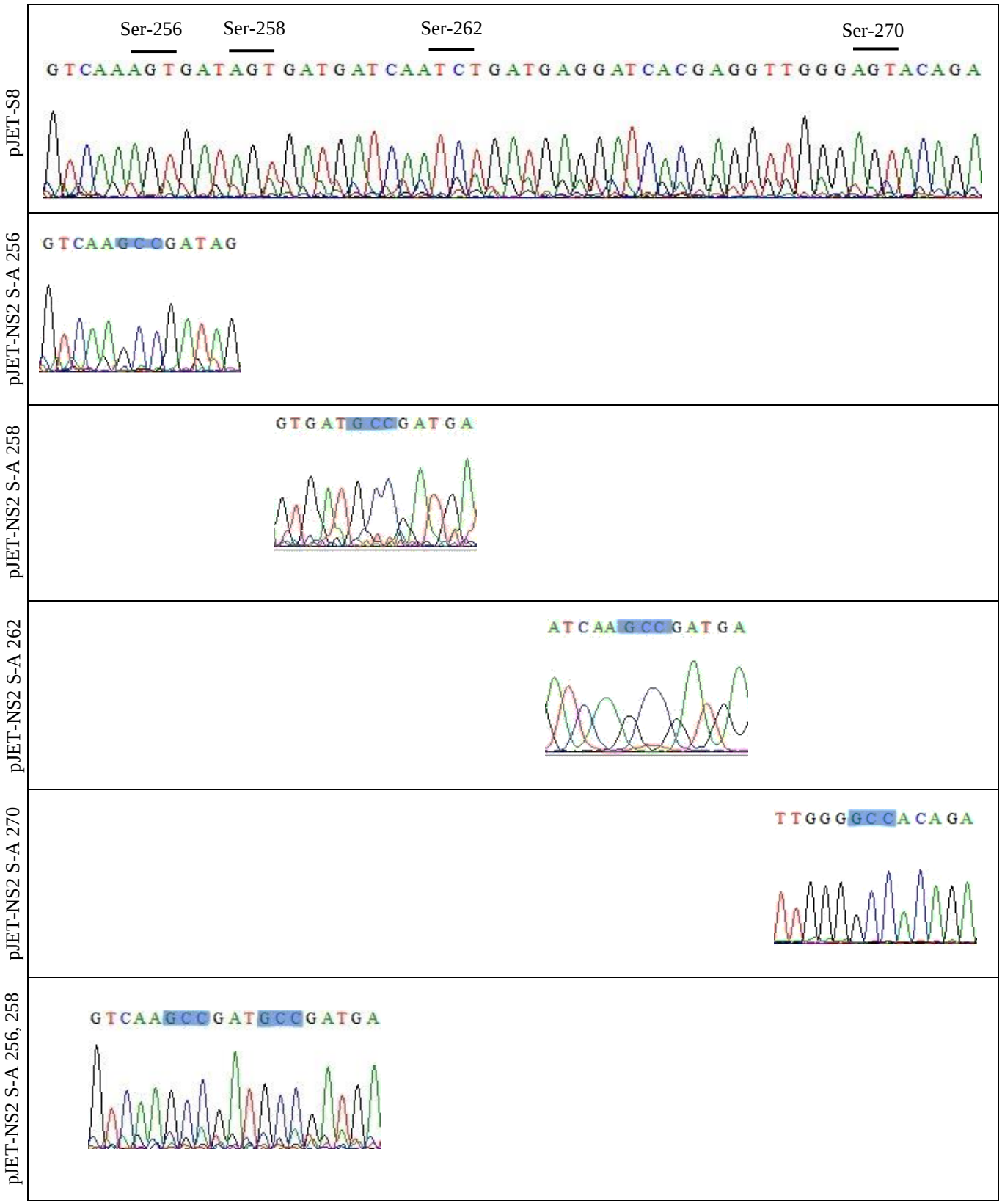
pJET-S8
Ser-256
Ser-258
Ser-262
Ser-270
GTCAAAGTGATAGTGATGATCAATCTGATGAGGATCACGAGGTTGGGGAGTACAGA
pJET-NS2 S-A 256
GTCAAGCCGATAG
pJET-NS2 S-A 258
GTGATGCCGATGA
pJET-NS2 S-A 262
ATCAAGCCGATGA
pJET-NS2 S-A 270
TTGGGGCCACAGA
pJET-NS2 S-A 256, 258
GTCAAGCCGATGCCGATGA

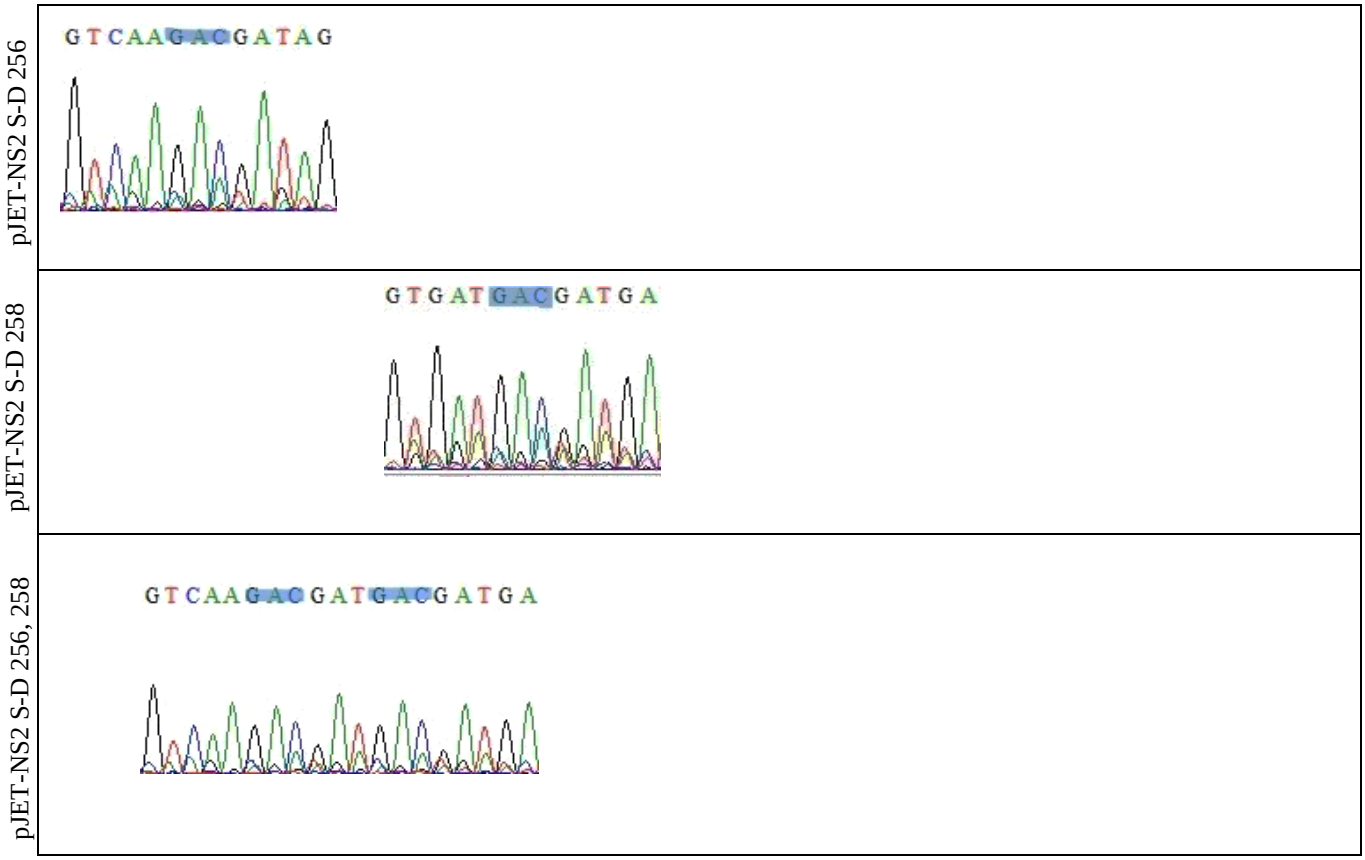

Figure 4.6: Sequence chromatograms indicating the presence of site-specific mutations introduced into the NS2 gene. An inverse PCR strategy was used to mutate serine residues (AGT / TCT), representing potential target sites for Casein kinase 2 in the C terminus of the NS2 protein, to either alanine residues (GCC) or aspartate residues (GAC). The derived mutant plasmids were sequenced and shown is relevant sequences compared to that of the wild-type NS2 gene sequence.

4.6 Construction of recombinant bacmid donor plasmids harbouring wild-type and mutated NS2 genes

It had been established earlier that Casein kinase 2 present in *S. frugiperda*-9 (Sf-9) insect cells is capable of phosphorylating the NS2 protein of AHSV-4 (Fig. 4.4). Therefore, to facilitate studies aimed at identifying phosphorylated serine residues in the C terminus of the AHSV-4 NS2 protein and to evaluate the relevance of NS2 protein phosphorylation on the ability of the protein to form inclusion bodies (IBs), the Bac-to-Bac baculovirus expression system was used for the synthesis of the wild-type and mutant versions of the NS2 protein in Sf-9 cells. The pFastBac HTa donor vector (Fig. 4.7A) was selected to ensure cloning of the wild-type and mutated NS2 genes in frame with the N-terminal hexahistidine tag present in the vector. Expression of the respective wild-type and mutant NS2 proteins with a hexahistidine tag would facilitate purification of the recombinant proteins from Sf-9 cells and thus allow for evaluation of NS2 protein phosphorylation with minimal to no interference from other cellular phosphoproteins.

To enable cloning of the wild-type and mutated versions of the NS2 gene into the bacmid donor vector pFastBac HTa, the recombinant pJET-S8 plasmid, harbouring the wild-type NS2 gene, the various pJET-NS2 mutant plasmid constructs and pFastBac HTa donor vector DNA were digested with both *Eco*RI and *Xho*I. The excised wild-type and mutated NS2 genes, as well as digested donor vector DNA were purified from an agarose gel and ligated. Following the transformation of competent *E. coli* DH5α cells with the ligation reaction mixtures, plasmid DNA isolated from randomly selected ampicillin-resistant transformants was analyzed by agarose gel electrophoresis. Plasmid DNA migrating slower than the parental pFastBac HTa vector DNA on an agarose gel was selected and characterized further by restriction enzyme digestion. Digestion of the recombinant bacmid donor plasmids with both *Eco*RI and *Xho*I resulted in the excision of a 1.098-kb DNA fragment, indicating that the wild-type NS2 gene and mutated versions of the NS2 gene had been cloned successfully (Fig. 4.7B). These recombinant donor plasmids were subsequently used to generate recombinant bacmids, as described in the following section.

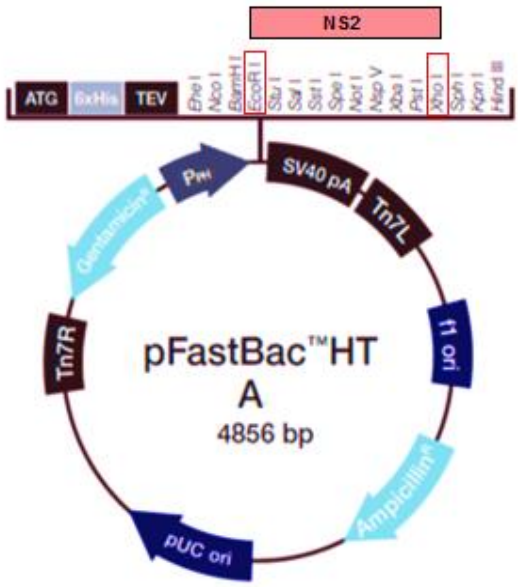

Figure 4.7A: Plasmid map of the pFastBac HTa donor vector. The cloning sites used for the insertion of the wild-type and mutated AHSV-4 NS2 genes are indicated in red boxes.

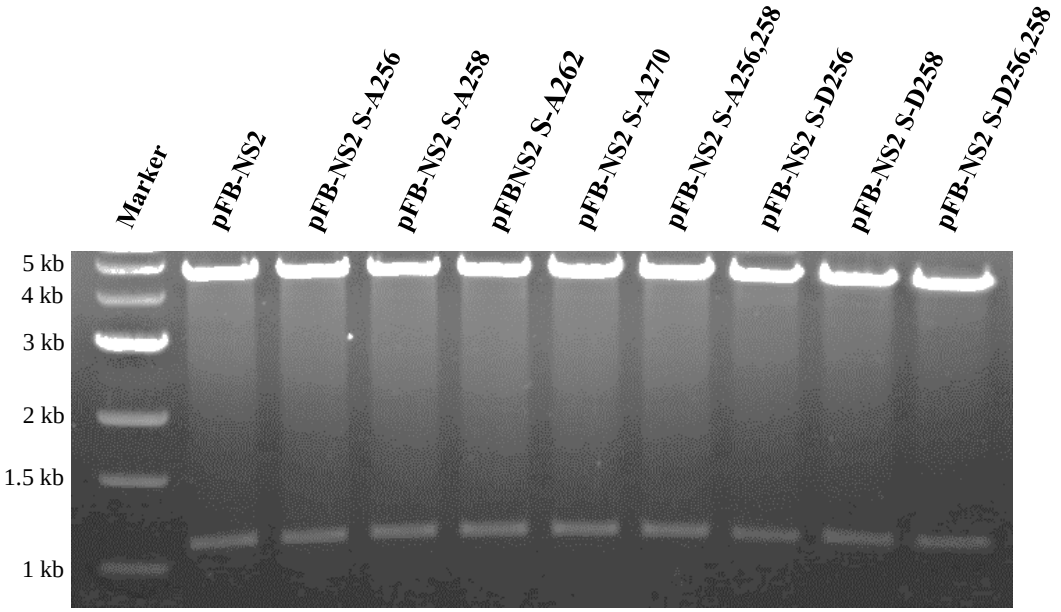

Figure 4.7B: Agarose gel electrophoretic analysis of recombinant pFastBac HTa plasmids harbouring wild-type and mutated NS2 genes. The recombinant bacmid donor plasmids, as indicated in the figure, were digested with both *Eco*RI and *Xho*I to excise the NS2-specific insert DNA. The sizes of the DNA molecular weight marker (1 kb DNA Ladder; New England Biolabs) are indicated to the left of the figure.

4.7 Engineering and characterization of recombinant bacmids

Bacmid DNA replicates as a large plasmid (135 kb) in *E. coli* DH10Bac cells and confers resistance to kanamycin, as well as complements a *lacZ*-deletion present on the *E. coli* genome to form colonies that are blue in the presence of X-gal. During the site-specific transposition of the recombinant donor plasmid, a mini-Tn7 cassette is inserted from the donor plasmid into the mini-*att*Tn7 attachment site on the bacmid DNA, thereby disrupting expression of the LacZα peptide. Consequently, colonies containing the recombinant bacmid display a white phenotype and can be easily distinguished from blue colonies that harbour the unaltered bacmid when plated in the presence of X-gal and IPTG. The transposition functions are provided *in trans* by a helper plasmid (pMON7124) that encodes the transposase and confers resistance to tetracycline (Luckow *et al*., 1993).

Recombinant bacmid DNA was engineered by transforming competent *E. coli* DH10Bac cells with the respective recombinant pFastBac HTa donor plasmids and selecting recombinant bacmids by plating the transformed cells onto a selective medium. The high-molecular-weight recombinant DNA was subsequently extracted from transformants with a white-colony phenotype and used as template DNA in PCR assays to confirm the successful transposition of the respective wild-type and mutated NS2 genes into the bacmid DNA. For this purpose, the pHed-F forward primer and universal pUC/M13-R reverse primer were used. The pHed-F primer anneals to the polyhedrin promoter of the transposed vector DNA, whereas the pUC/M13-R oligonucleotide anneals to the 3'-end of the mini-*att*Tn7 site within the *lacZ*α gene of the bacmid DNA (Fig. 4.8A).

By making use of recombinant bacmid DNA transposed with either the wild-type or various mutant NS2 donor plasmids as template DNA for PCR, together with the pHed-F and universal pUC/M13-R primers, bands of approximately 1.7 kb were observed (Fig. 4.8B). The size of the observed amplicons corresponded with the size of the NS2 (1.098 kb) gene, together with the size of the mini-Tn7 cassette (458 bp) and bacmid DNA flanking the mini-*att*Tn7 site (145 bp). By contrast, no amplification products were observed when wild-type bacmid DNA was used as a template in the PCR reactions. Recombinant bacmids were selected and designated Bac-NS2 S-A256, Bac-NS2 S-A258, Bac-NS2 S-A262, Bac-NS2 S-A270, Bac-NS2 S-A256,258, Bac-NS2 S-D256, Bac-NS2 S-D258 and Bac-NS2 S-D256,258, respectively. These recombinant bacmids were used in all subsequent experiments.

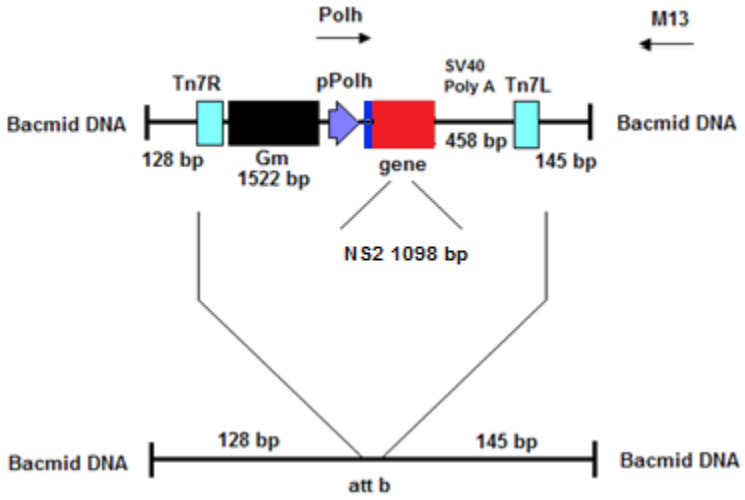

Figure 4.8A: Schematic representation of transposed bacmid DNA. The annealing positions of the polyhedrin forward primer (Polh) and the pUC/M13 revere primer (M13) is indicated, as well as the size of the mini-*att*Tn7 cassette DNA and the bacmid DNA flanking the cassette. The position of the transposed AHSV-4 wild-type or mutated NS2 gene (red), along with the N-terminal hexahistidine tag (blue), within the bacmid DNA is also indicated.

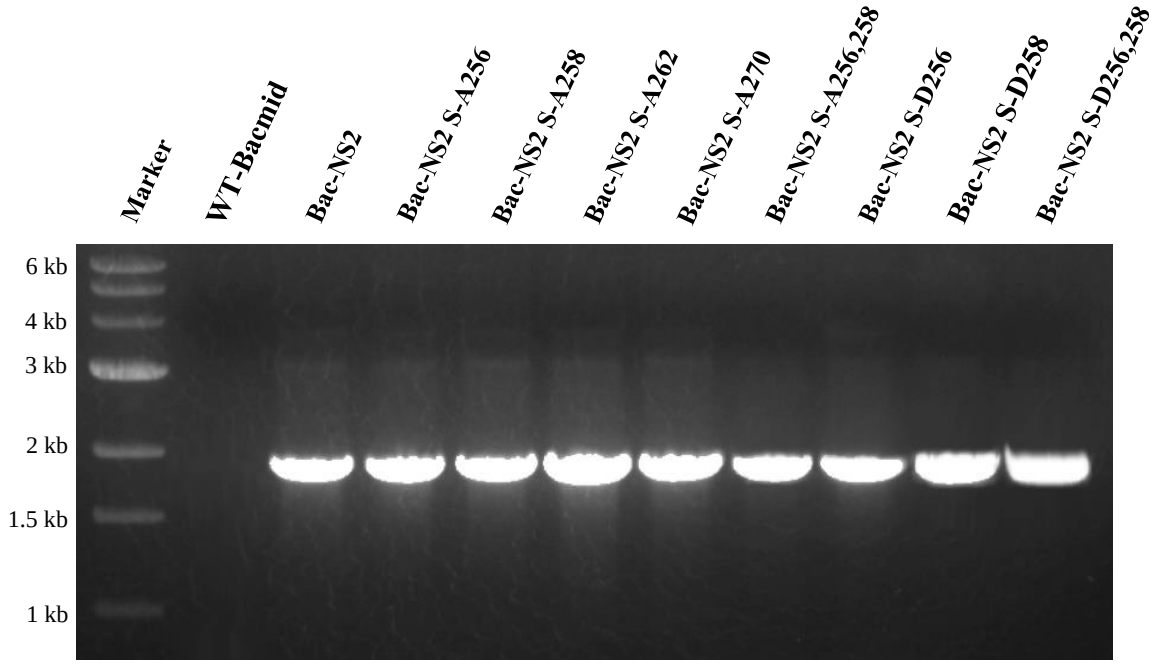

Figure 4.8B: Agarose gel electrophoretic analysis of amplicons derived from recombinant bacmid DNA following PCR analysis. Wild-type bacmid DNA and recombinant bacmid DNA, as indicated in the figure, were used as templates in PCR analysis together with polyhedrin forward and the pUC/M13 reverse primers. The sizes of the DNA molecular weight marker (1 kb DNA Ladder; New England Biolabs) are indicated to the left of the figures.

4.8 Recombinant NS2 protein expression in Sf-9 cells

Wild-type and recombinant bacmid DNA were isolated from *E. coli* DH10Bac cultures and transfected into Sf-9 cells. The progeny virus, resulting from each transfection, was collected at 72 h post-transfection, and propagated in monolayer cultures and the titre of the recombinant virus stocks was determined by plaque assays. The titre of each baculovirus stock ranged between 7.8×10^7 and 2.3×10^8 pfu/ml. To determine whether the respective AHSV-4 wild-type and mutant NS2 proteins were synthesized in recombinant baculovirus-infected cells, monolayers of Sf-9 cells were mock-infected and infected with either the wild-type or recombinant baculoviruses. Following incubation for 72 h, whole-cell lysates were analyzed by Western blot analysis.

Analysis of the Western blot indicated that the anti-NS2 antibody reacted specifically with a single protein present in the whole-cell lysates prepared from Sf-9 cells infected with recombinant baculoviruses expressing the wild-type and mutant NS2 proteins. However, the molecular mass of the proteins differed and appeared to be dependent on the nature and position of the introduced mutations. In the case of mutant NS2 proteins in which Ser-256, Ser-258 or Ser-262 as well as both Ser-256 and Ser-258 were substituted with alanine, the primary antibody reacted with proteins of an approximate molecular mass of 36 kDa. In contrast, the primary antibody reacted with a protein of an approximate molecular mass of 38 kDa in the case of mutant NS2 in which Ser-270 was substituted with alanine (Fig. 4.9). For mutant NS2 proteins in which the targeted serine residues were substituted with aspartate, the primary antibody reacted with a single protein with a molecular mass of 48 kDa and is in agreement with the result obtained for the wild-type NS2 protein (Fig. 4.9). Notably, in the case of the wild-type NS2 protein, the anti-NS2 antibody also occasionally reacted with an additional protein present in the whole-cell lysate prepared from Sf-9 cells infected with the baculovirus recombinant. The molecular mass of this immune-reactive NS2 protein was 35 kDa. It is tempting to speculate that this protein may represent an unphosphorylated version of the NS2 protein, as it could not be detected in subsequent phosphorylation assays (Figs. 4.10 and 4.11).

From the results, it could be concluded that the wild-type NS2 protein and the different mutant NS2 proteins were expressed successfully in Sf-9 cells by means of the engineered baculovirus recombinants, albeit the electrophoretic mobility of the mutant NS2 proteins was affected by the nature and position of the introduced mutations.

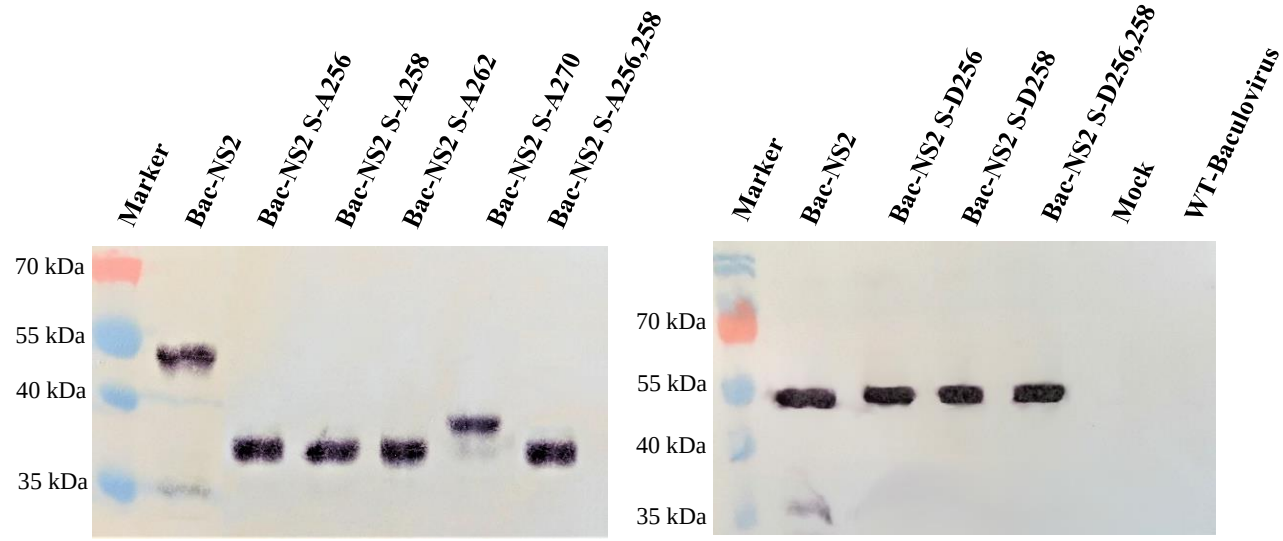

Figure 4.9: Western blot analyses of whole-cell lysates prepared from *S. frugiperda* cells infected with recombinant baculoviruses. *S. frugiperda* cells were mock-infected and infected with the non-recombinant (WT) baculovirus or recombinant baculoviruses, as indicated in the figure, and analyzed for protein expression at 72 h post-infection. Whole-cell lysate proteins were resolved by SDS-PAGE, electroblotted onto nitrocellulose membranes and then subjected to Western blot analysis with an anti-NS2 antibody. The sizes of the PageRuler Prestained Protein Ladder (Thermo Scientific) are indicated in kDa to the left of the figures.

4.9 Mapping of phosphorylated serine residues in NS2

To determine whether the serine residues identified and selected during bioinformatics analysis of the AHSV-4 NS2 protein were the phosphorylation sites of the protein, the wild-type NS2 and NS2 mutants were expressed in Sf-9 cells by making use of the engineered baculovirus recombinants. Following incubation for 72 h, the NS2 and NS2 mutant proteins were purified from the infected cell lysates with IMAC and analyzed by SDS-PAGE to confirm the expression and purification of the respective proteins. Subsequently, a duplicate gel was stained with Pro-Q Diamond Phosphoprotein Gel Stain in order to determine the phosphorylation state of the wild-type and mutant NS2 proteins.

As observed previously (Figs. 4.4B and 4.5B, lanes 1), the wild-type NS2 protein was strongly phosphorylated. However, the substitution of Ser-256 (NS2 S-A256) or Ser-258 (NS2 S-A258) with alanine resulted in reduced levels of phosphorylation. Notably, when both these residues were mutated to alanine, the NS2 mutant (NS2 S-A256,258) showed a complete loss of a phosphorylation signal. In contrast, the substitution of Ser-262 (NS2 S-A262) or Ser-270 (NS2 S-A270) with alanine appeared to have a lesser effect on NS2 phosphorylation (Fig. 4.10).

For relative quantification of the phosphorylation state of the serine-to-alanine NS2 mutant proteins, the phosphorylation signal was quantified from the acquired image with ImageJ software and compared to wild-type NS2, which was considered to be 100% phosphorylated. The NS2 S-A256 and NS2 S-A258 mutant proteins were phosphorylated to 27% and 25%, respectively, compared to the wild-type NS2 protein, whereas the NS2 S-A256,258 dual mutant protein was phosphorylated to 15% compared to the wild-type NS2 protein. In contrast, a smaller difference was noted for the NS2 S-A262 (63%) and NS2 S-A270 (67%) mutant proteins compared to the wild-type NS2 protein (Fig. 4.10C).

To further characterize the phosphorylation of NS2, Sf-9 cells were infected with recombinant baculoviruses expressing NS2 mutants in which Ser-256 (NS2 S-D256) or Ser-258 (NS2 S-D258) and both of these residues were substituted with aspartate residues (NS2 S-D256,258). Using the same approach described above, the wild-type NS2 protein was highly phosphorylated and, as expected, the mutant proteins NS2 S-D256 and NS2 S-D258 showed lower levels of phosphorylation and NS2 S-D256,258 gave no detectable signal on the phosphoprotein-stained gel (Fig. 4.11). Relative quantification of the phosphorylation state of

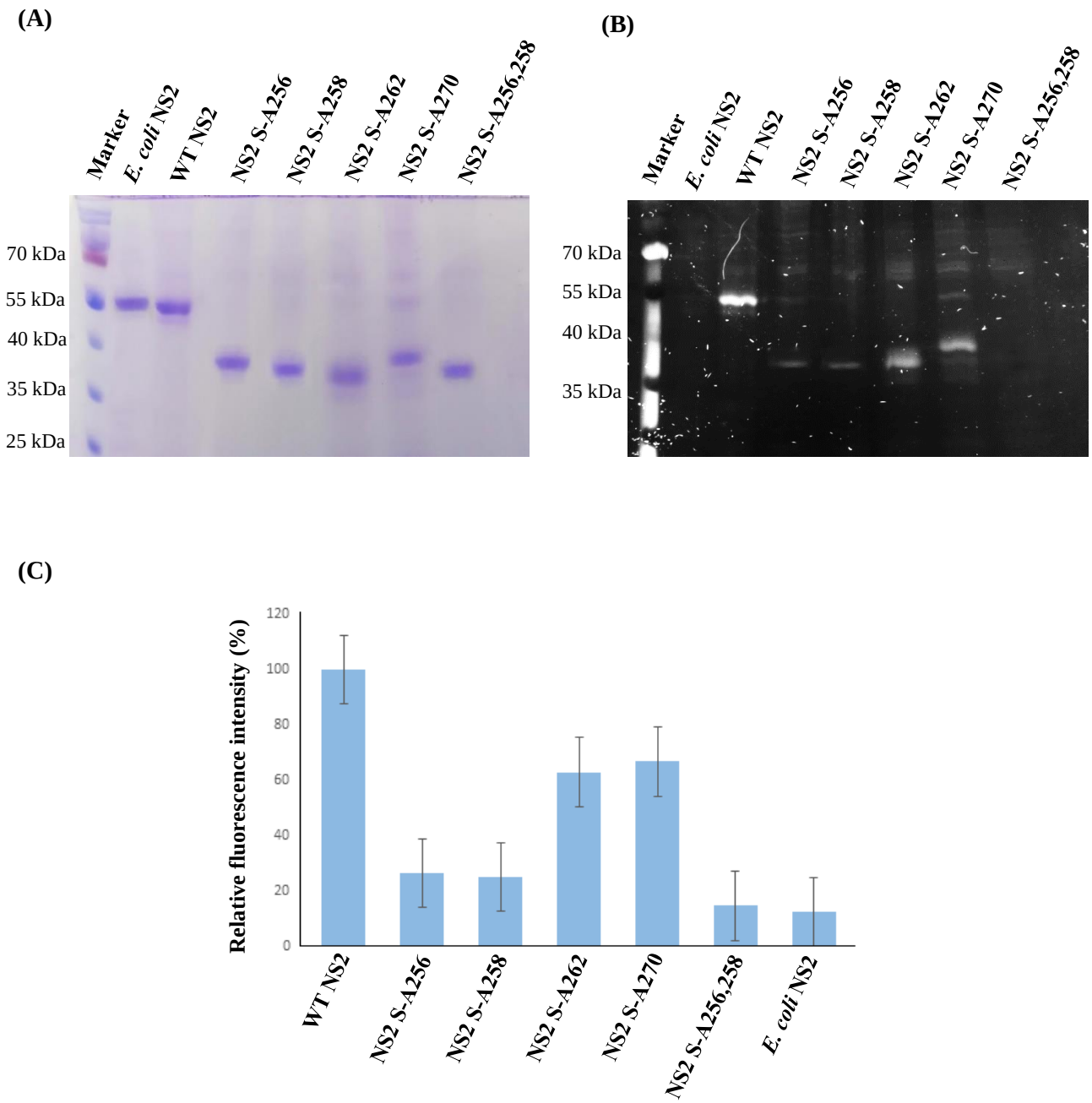

Figure 4.10: Phosphorylation state analysis of NS2 and serine-to-alanine NS2 mutant proteins expressed in *S. frugiperda* cells. The hexahistidine-tagged wild-type and mutant NS2 proteins were purified at 72 h post-infection by IMAC from cytoplasmic protein fractions prepared from cells infected with the recombinant baculoviruses. Equal amounts (0.3 µg) of the purified protein samples, as indicated in the figures, were analyzed by SDS-PAGE (A), and a duplicate SDS-polyacrylamide gel was stained with Pro-Q Diamond Phosphoprotein Gel Stain to visualize phosphorylated proteins (B). NS2 expressed in *E. coli* BL21(DE3) was included in the assay as an unphosphorylated NS2 control. The sizes of the PageRuler Prestained Protein Ladder (Thermo Scientific) are indicated in kDa to the left of the figures. (C) Relative quantification of the phosphorylation state of NS2 mutant proteins. The fluorescence signals of wild-type NS2 and NS2 mutants from the acquired image presented in (B) were quantified using ImageJ software and compared to the wild-type NS2 phosphorylation level (set as 100%). Error bars represent the standard deviation values from three independent measurements.

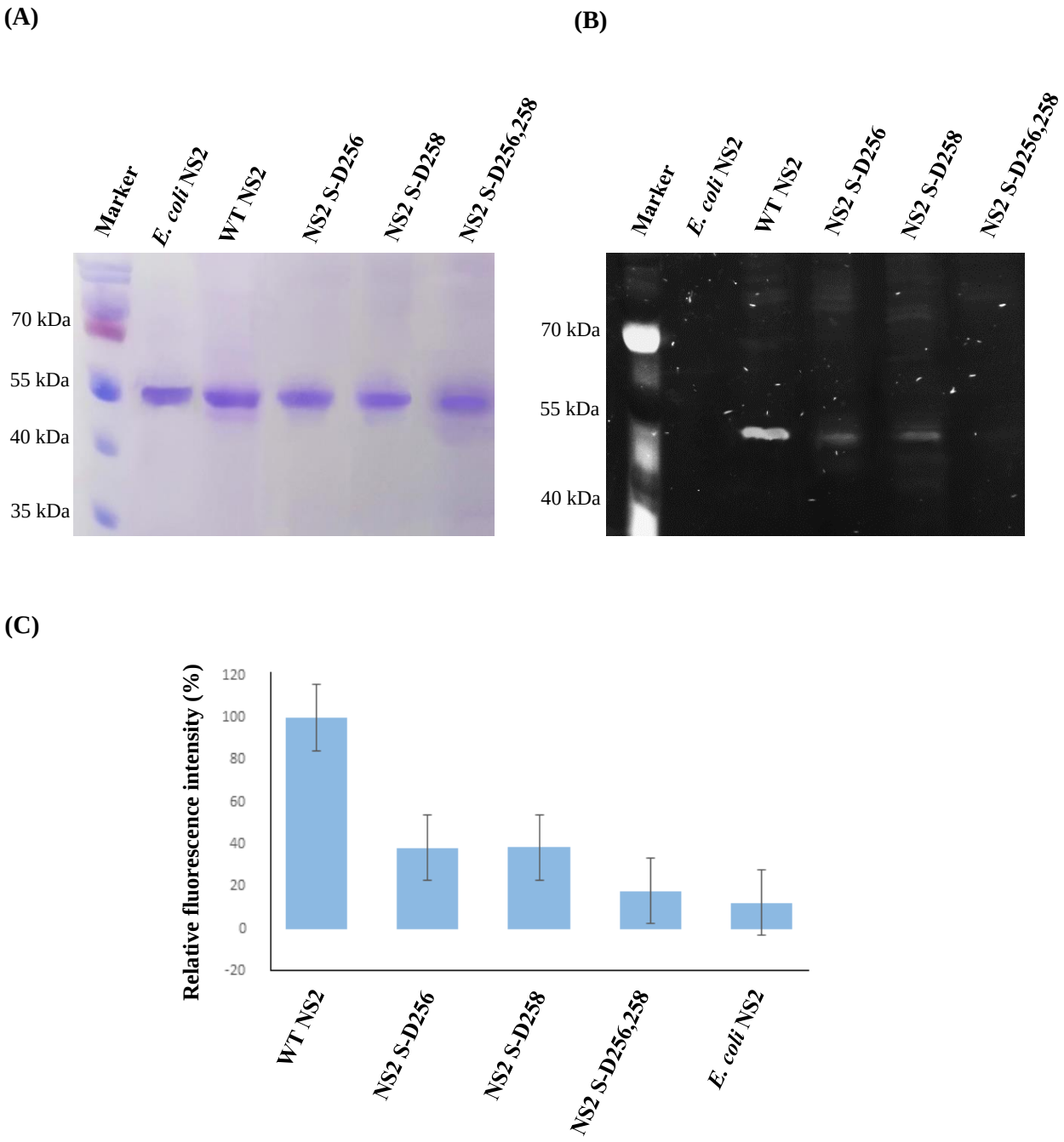

Figure 4.11: Phosphorylation state analysis of NS2 and serine-to-aspartate NS2 mutant proteins expressed in *S. frugiperda* cells. The hexahistidine-tagged wild-type and mutant NS2 proteins were prepared, as described in the legend to Fig. 4.10. Equal amounts (0.3 µg) of the purified protein samples, as indicated in the figures, were analyzed by SDS-PAGE (A), and a duplicate SDS polyacrylamide gel was stained with Pro-Q Diamond Phosphoprotein Gel Stain to visualize phosphorylated proteins (B). NS2 expressed in *E. coli* BL21(DE3) was included in the assay as an unphosphorylated NS2 control. The sizes of the PageRuler Prestained Protein Ladder (Thermo Scientific) are indicated in kDa to the left of the figures. (C) Relative quantification of the phosphorylation state of NS2 mutant proteins. The fluorescence signals of wild-type NS2 and NS2 mutants from the acquired image presented in (B) were quantified using ImageJ software and compared to the wild-type NS2 phosphorylation level (set as 100%). Error bars represent the standard deviation values from three independent measurements.

these serine-to-aspartate NS2 mutant proteins indicated that both the NS2 S-D256 and NS2 S-D258 mutant proteins were phosphorylated to 28%, compared to the wild-type NS2 protein, whilst the NS2 S-D256,258 dual mutant protein was phosphorylated to 18% compared to the wild-type NS2 protein (Fig. 4.11C).

The data, together with that presented earlier (Section 4.3), provides evidence that NS2 is predominantly phosphorylated at serine residues, specifically serine residues 256 and 258, and that both these residues are recognized as substrates by cellular protein kinase CK2.

4.10 Influence of phosphorylation of NS2 on the formation of AHSV inclusion bodies

The NS2 protein is the main component of virus inclusion bodies (VIBs) that appear in the cytoplasm of orbivirus-infected cells (Kar *et al.*, 2007), and it has been reported that recombinant baculovirus-expressed NS2 of BTV and AHSV can form similar inclusion bodies (Brookes *et al.*, 1993; Uitenweerde *et al.*, 1995). To determine whether phosphorylation of NS2 is responsible for the formation of inclusion bodies (IBs), Sf-9 cell monolayers grown on cover slips were infected with recombinant baculoviruses expressing the mutant versions of the AHSV-4 NS2 protein and processed at 72 h post-infection for immunofluorescence analysis using confocal microscopy. As a control, the wild-type NS2 was similarly expressed and examined.

Throughout this study, a hexahistidine-tagged NS2 protein was used as the wild-type protein. Comparison of the IBs formed by this tagged NS2 protein and those formed by NS2 lacking a tag sequence and the VIBs formed in BSR mammalian cells infected with AHSV-4, indicated no discernible differences. This, therefore, indicated that the hexahistidine tag did not interfere with NS2 inclusion body formation and confirmed that the IBs formed by expression of NS2 in Sf-9 cells resemble the VIBs observed in virus-infected cells (Fig. 4.12, Top panel).

In contrast to the expression of wild-type NS2 in Sf-9 cells, which resulted in the formation of NS2 aggregates similar to VIBs, the expression of NS2 S-A256,258 did not show the distinct aggregation of the wild-type NS2 protein. Indeed, NS2 S-A256,258 was predominantly dispersed throughout the cytoplasm of infected cells. Analysis of NS2 mutants with substitution of either Ser-256 (NS2 S-A256) or Ser-258 (NS2 S-A258) indicated intermediate distribution patterns. When Ser-256 only was substituted, the NS2 S-A256 mutant protein formed aggregates that were larger and less defined, and the mutant protein was also partially

dispersed throughout the cytoplasm of infected cells. In contrast, when only Ser-258 was substituted, the NS2 S-A258 mutant protein was mainly distributed throughout the cytoplasm of infected cells. Investigation of the NS2 mutants with substitution of either Ser-262 (NS2 S-A262) or Ser-270 (NS2 S-A270) indicated aggregation of the mutant NS2 proteins into IBs that resembled those observed in cells infected with the baculovirus recombinant expressing wild-type NS2. Analysis of NS2 mutants in which selected serine residues were substituted with aspartate (NS2 S-D256, NS2 S-D258 and NS2 S-D256,258, respectively) indicated the formation of intracellular IBs that punctuated the cell cytoplasm of infected cells and was similar to that of the wild-type NS2 protein (Fig. 4.12).

Based on the results, it was concluded that phosphorylation of NS2 appears to be important for the formation of NS2 inclusion bodies and also that the negative charges on the phosphoserine residues rather than the serine residues themselves are crucial for the formation of IBs.

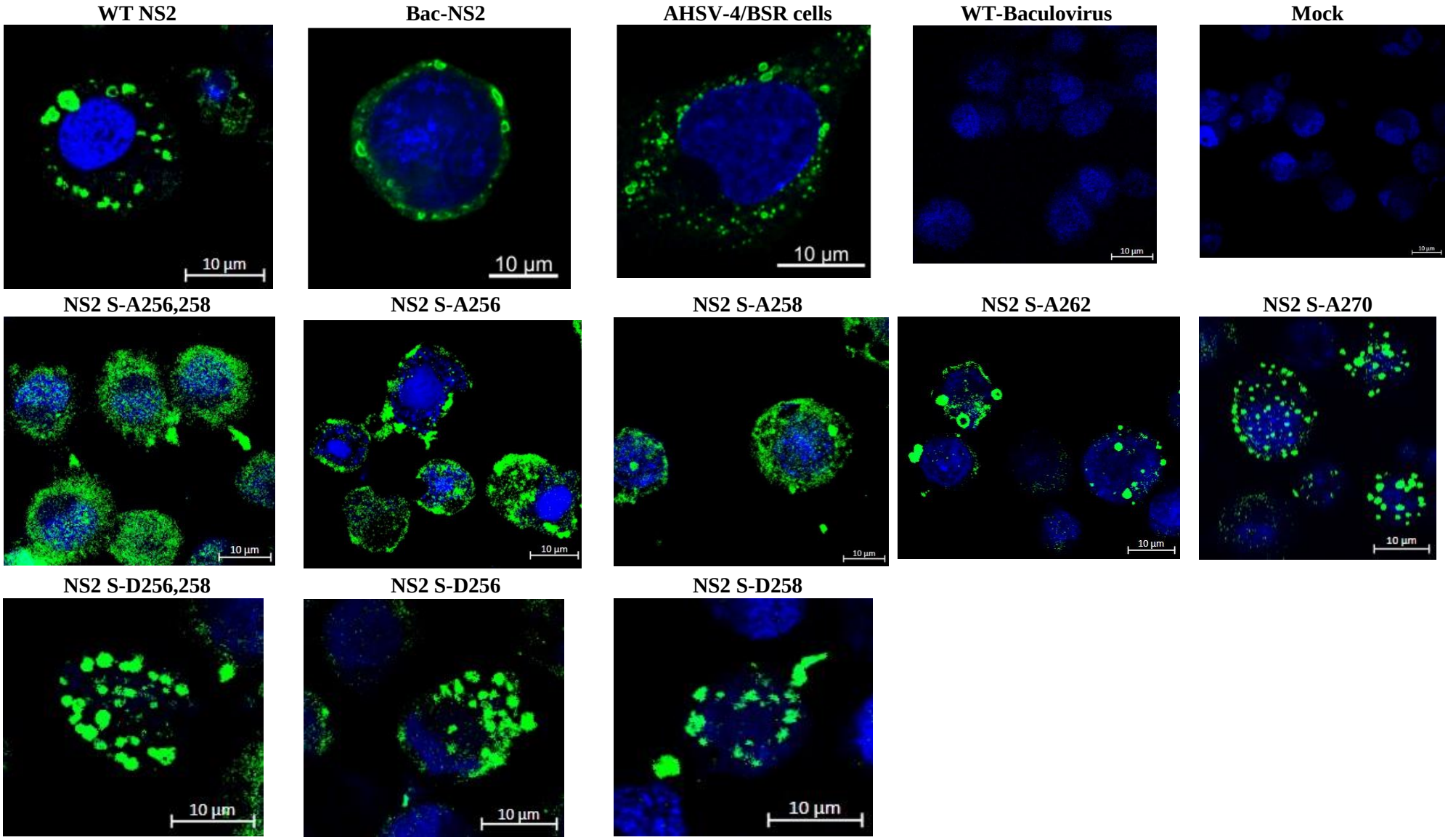

Figure 4.12: Confocal microscopy micrographs showing the inclusion bodies in *S. frugiperda* cells infected with baculovirus recombinants expressing NS2 and NS2 mutant proteins. *S. frugiperda* cells were infected with recombinant baculoviruses expressing wild-type (WT) NS2 or NS2 mutant proteins in which serine (S) residues were substituted with either alanine (A) or aspartate (D) residues, as indicated in the figure. The cells were fixed at 24 h post-infection, and the respective NS2 proteins were detected with an anti-NS2 primary antibody (rabbit) and Alexa Fluor 488-conjugated goat anti-rabbit secondary antibody (green). The nuclei were stained with DAPI (blue). Cells infected with a recombinant baculovirus expressing an untagged version of the AHSV-4 NS2 protein (Bac-NS2) and BSR cells infected with AHSV-4 (AHSV-4/BSR) are shown for comparative purposes (images by Ms Litia Yssel, unpublished). Micrographs of mock-infected Sf-9 cells and cells infected with wild-type (WT) baculovirus are included, indicating the antibody did not bind to cellular or baculovirus-expressed proteins. Scale bars = 10 µm.

CHAPTER FIVE

DISCUSSION

Various members of the order *Reovirales* replicate in the cytoplasm of host cells by forming virus inclusion bodies (VIBs). These structures serve multiple purposes during infection that include the concentration of viral proteins and host factors to ensure the high efficiency of replication, sequestration of viral nucleic acids and proteins to prevent the activation of cell-intrinsic defenses and coordinate the assembly of progeny particles (Kar *et al.*, 2007; Tenorio *et al.*, 2019; Papa *et al.*, 2021; Fernández de Castro *et al*., 2021). Although knowledge about VIB biogenesis has been enhanced through ultrastructural and functional studies (Stuart and Grimes, 2006; Patton *et al*., 2006; Mumtsidu *et al.*, 2007; de Castro *et al.*, 2013; Garcés Suárez *et al.*, 2019), for many viruses, including African horse sickness virus (AHSV), the mechanism required for their formation remain largely unknown. The AHSV non-structural protein NS2, which is one of the first viral proteins synthesized in virus-infected cells, plays a crucial role in the formation of VIBs. Expression of NS2 alone results in the formation of VIB-like structures and therefore suggests that NS2 is the viral protein responsible for inclusion body (IB) formation (Brookes *et al.*, 1993; Uitenweerde *et al.*, 1995). Another distinguishing feature of NS2 is that it is the only virus-specified phosphoprotein (Huismans *et al.*, 1987; Thomas *et al.*, 1990), but the functional relevance of this post-translational modification for protein function is not well understood. Given the paucity of information on AHSV NS2 protein phosphorylation and the role of NS2 phosphorylation in the replication cycle of AHSV, this study specifically addressed the following questions: (i) which enzyme/s are responsible for NS2 protein phosphorylation, (ii) which site/s within the NS2 protein are phosphorylated, and (iii) what is the role of such phosphorylation on NS2 function, especially with regards to VIB formation?

To firstly elucidate the mechanism by which phosphorylation of AHSV NS2 occurs, the NS2 protein of AHSV-4 was expressed in *Escherichia coli* and its phosphorylation status was compared to that of NS2 expressed in *Spodoptera frugiperda* (Sf-9) insect cells by a baculovirus recombinant. The result from a phosphoprotein staining assay, which allows for the staining of phosphorylated proteins directly in SDS-polyacrylamide gels (Schulenberg *et al*, 2004), indicated that the bacterial-expressed NS2 was not phosphorylated, whereas the recombinant baculovirus-expressed NS2 was strongly phosphorylated. From these results it could therefore be concluded that the NS2 protein of AHSV lacks an autophosphorylation activity and is in agreement with results reported previously for the NS2 proteins of Bluetongue virus (BTV) (Thomas *et al.*, 1990; Taraporewala *et al.*, 2001) and Epizootic haemorrhagic diseases virus (EHDV) (Theron *et al.*, 1994). Moreover, it could also be concluded that a

protein kinase present in Sf-9 cells is responsible for AHSV NS2 phosphorylation. The protein kinase responsible for NS2 phosphorylation was subsequently identified by phosphorylation of purified *E. coli*-expressed NS2 preparations with casein kinase 2 (CK2) and by making use of the CK2 inhibitor TBB. It has been shown that TBB is highly specific for CK2 and does not affect the activities of more than 30 other protein kinases tested (Sarno *et al.*, 2001; Battistutta *et al.*, 2001). TBB inhibited the NS2 phosphorylating activity in Sf-9 cell lysates and that of purified CK2 to undetectable levels, as was evidenced by the lack of phosphorylation signal upon phosphoprotein staining of the treated NS2 protein samples. These results thus indicated that CK2 is responsible for AHSV-4 NS2 phosphorylation. Phosphorylation of BTV NS2 by CK2 has also been reported (Modrof *et al.*, 2005; Mohl and Roy, 2016) and may suggest that phosphorylation of different orbivirus NS2 proteins occurs through a common mechanism that involves the same protein kinase.

Having established that CK2 is responsible for NS2 phosphorylation and taking into consideration that an earlier study indicated that only C-terminal serine residues are phosphorylated in the NS2 proteins of BTV and AHSV (Devaney *et al.*, 1988), the NS2 protein of AHSV-4 was analyzed for the presence of CK2 target sites. Computer-assisted screening of the NS2 amino acid sequence revealed that four serine residues (*i.e.*, Ser-256, Ser-258, Ser-262 and Ser-270), clustered in the C-terminal region of AHSV-4 NS2, represented potential target sites for CK2. Closer inspection of these sites indicated that only Ser-256 and Ser-262 have the downstream signature sequence SDSD and SDED, respectively, which corresponds to the minimum consensus sequence recognized by CK2 (**S** X X E/D) (Meggio *et al.*, 1994). However, besides the minimal sequence, several other elements have been identified as important in determining phosphorylation by CK2. In general, additional acidic amino acids (Asp, D and Glu, E) act as positive determinants, especially downstream at positions up to n+7 relative to the target serine residue (Meggio and Pinna, 2003; Vilardell *et al.*, 2018). This configuration is evident in the amino sequence downstream of Ser-258, which contains five acidic amino acids. In contrast, the amino acid sequence downstream of Ser-270 comprised mostly of neutral amino acids and only two acidic amino acids are present, which may account for the low phosphorylation prediction score in each of the three prediction programmes used in this study (Table 4.1). Nevertheless, all four serine residues were selected and subsequently evaluated as potential phosphorylation sites of the NS2 protein.

Towards mapping of the phosphorylated sites within the NS2 protein of AHSV-4, NS2 mutant proteins in which the predicted CK2 target serine residues were substituted with either alanine (A) or aspartate (D) residues were expressed by means of the baculovirus-insect cell expression system. It was reported previously that BTV NS2 expressed transiently in mammalian cells and NS2 expressed in Sf-9 cells are phosphorylated at identical sites in the C terminus of these proteins (Modrof *et al.*, 2005; Mumtsidu *et al.*, 2007). Therefore, the use of recombinant AHSV-4 NS2 expressed in the baculovirus-insect cell expression system should allow for accurate mapping of phosphorylated residues in the NS2 protein. Analysis of cell lysates prepared from recombinant baculovirus-infected Sf-9 cells indicated that the NS2 mutant proteins displayed heterogeneous electrophoretic mobility in SDS-polyacrylamide gels that was especially noticeable for the serine-to-alanine NS2 mutant proteins. It is unlikely that the apparent difference in molecular mass of the NS2 mutant proteins was due to errors introduced during the construction and cloning of the mutated NS2 genes, since nucleotide sequence analysis confirmed that the sizes and sequences were identical, except for the site-specific mutations that were introduced to mutate selected serine residues (Appendix). It is also unlikely that the full-length NS2 protein was proteolytically cleaved by a ubiquitous cellular protease, since NS2 proteins in which selected serine residues were mutated to aspartate displayed identical electrophoretic mobility compared to the wild-type NS2 protein. Consequently, the most likely factor to influence the electrophoretic mobility of the serine-to-alanine NS2 mutant proteins may be due to differences in the basal phosphorylation levels (and thus by implication the net negative charge) of the various serine-to-alanine NS2 mutant proteins. In contrast, in the case of NS2 mutant proteins in which the phosphomimic amino acid aspartate (Lewellyn and Loeb, 2011) was used to replace the serine residues, the mutant NS2 proteins are expected to retain the electrochemical properties of the fully phosphorylated NS2 protein. This may therefore explain the uniform electrophoretic mobility of these NS2 mutant proteins and their identical migration to the wild-type NS2 protein in the SDS-polyacrylamide gels.

In support of the above, it has been reported that proteins containing dense clusters of negatively charged residues or proteins that have been post-translationally modified can display anomalies in electrophoretic mobility during SDS-PAGE (Lee *et al.*, 2013; Tiwari *et al.*, 2019). Moreover, phosphorylation of the rotavirus NSP5 protein results in widely variable migration patterns in SDS-PAGE (Afrikanova *et al.*, 1996; Blackhall *et al.*, 1998). The NSP5 protein, which together with NSP2 contributes to viroplasm formation (Criglar *et al.*, 2018), is

phosphorylated at its C terminus by a CK1α / CK2-dependent mechanism (Eichwald *et al.*, 2002; Eichwald *et al.*, 2004; Campagna *et al.*, 2007). The NS2 proteins of BTV (Taraporewela *et al.*, 2001; Butan *et al.*, 2004) and EHDV (Theron *et al.*, 1994) can also be presented as two bands upon electrophoresis in SDS-polyacrylamide gels, and it was suggested that these may represent differentially phosphorylated versions of the NS2 protein.

To identify which of the selected serine residues within the AHSV-4 NS2 protein are phosphorylated, a phosphoprotein staining assay was performed of the recombinant baculovirus-expressed wild-type NS2 and NS2 mutant proteins. It was demonstrated that wild-type NS2 and NS2 mutant proteins in which Ser-262 or Ser-270 was substituted with alanine were phosphorylated. Mutant NS2 proteins in which Ser-256 or Ser-258 were substituted stained less intensely compared to the above proteins, and substitution of both these serine residues with alanine yielded no phosphorylation signal. These results thus mapped the phosphorylation within NS2 to Ser-256 and Ser-258. Direct supporting evidence was obtained in a parallel, independent experiment in which the phosphorylation state of NS2 mutants with serine-to-aspartate mutations was evaluated. As above, the results confirmed that the substitution of either Ser-256 or Ser-258 with aspartate resulted in a faint phosphorylation signal, whereas no signal was detected for a dual NS2 mutant protein. These results furthermore suggest that NS2 is not phosphorylated by a hierarchical mechanism, *i.e.*, where the addition of phosphate through a phosphorylation event in the protein creates adequate sequence determinants for other nearby phosphorylation events to occur and thus results in processive phosphorylation events catalyzed by a single kinase (Roach *et al.*, 1991). Rather, the results of this study suggest that each Ser-256 and Ser-258 serve as independent target sites for CK2. This is supported by observations that the NS2 mutant proteins in which these serine residues were substituted individually with alanine or aspartate yielded near identical levels of phosphorylation.

Since NS2 is essential for the formation of cytoplasmic inclusion bodies, the role of NS2 phosphorylation in this process was assessed by immunofluorescence confocal microscopy with an antibody against NS2 of AHSV-4. It was readily apparent that IB formation was adversely affected by impaired NS2 phosphorylation, as evidenced by the intermediate distribution pattern of the NS2 mutant proteins in which Ser-256 (NS2 S-A256) or Ser-258 (NS2 S-A258) was mutated to alanine. Most strikingly, when both these serine residues were substituted with alanine, the dual NS2 mutant protein (NS2 S-A256,258) failed to form IBs in

the cytoplasm of recombinant baculovirus-infected Sf-9 cells. However, mutation of these serine residues to aspartate, which mimics a phosphorylated state, resulted in the formation of IBs similar to those formed by the wild-type NS2 protein. This, therefore, suggests that it is the negative charges introduced by NS2 phosphorylation rather than the serine residues that are important for IB formation. Taken together, the results indicate a phosphorylation-dependent mechanism for AHSV inclusion body formation that requires a cellular CK2 protein kinase and phosphorylation of NS2 to form these cytoplasmic structures.

In addition to the phosphorylation of the NS2 protein, a recent paper suggested that the ability of the BTV NS2 protein to bind to Ca^{2+} by means of an EF-hand-like motif (D X D X D) present in the C terminus of the protein affects the phosphorylation level of NS2 and, as such, has an important role in regulating VIB assembly (Rahman *et al.*, 2020). However, it should be noted that the Ca^{2+} binding motif mutated by Rahman *et al.* (2020) corresponds to the CK2 consensus sequences downstream of Ser-249 (**S**DDDDQ), which is one of two serine residues phosphorylated in the BTV NS2 protein (Modrof *et al.*, 2005). It, therefore, follows that mutagenesis of this Ca^{2+} binding site / CK2 phosphorylation site through substitution of the acidic amino acid residues with neutral alanine amino acid residues would prevent NS2 phosphorylation at this site, irrespective of Ca^{2+} binding or not. Moreover, EF-hand motifs often occur upstream of α-helices and are associated with regulating large conformational changes in helical domain function in a cooperative manner (Rigden and Galperin, 2004; Elíes *et al.*, 2020). Thus, in addition to mutating the CK2 phosphorylation site in BTV NS2, the mutation may also have affected the folding conformation of the protein and therefore the accessibility of the downstream Ser-259 for phosphorylation by CK2. Based on the aforementioned, it is not surprising that the NS2 protein of a recombinant BTV, obtained through reverse genetics, was reported to be phosphorylated at a lesser extent than the wild-type NS2 protein and that the formation of VIBs was impaired. It can therefore be posited that phosphorylation of NS2, and not its ability to bind Ca^{2+} as suggested by Rahman *et al.* (2020), is an important factor critical for VIB formation. In support of this, the results of this study indicated that differences in the level of NS2 phosphorylation impact the formation of VIB-like structures (Fig. 4.12). This was clearly observed by comparing the IBs formed by the partially phosphorylated mutant proteins NS2 S-A256 and NS2 S-A258 (cytoplasmic distribution of the mutant proteins), the unphosphorylated protein NS2 SA256,258 (lack of IB formation) and the fully phosphorylated wild-type NS2 (IBs were formed comparable to VIB-like structures in virus-infected cells). Consequently, whether Ca^{2+} is an important role player

in NS2 function or serves as a regulator of VIB formation requires further investigation before any definitive conclusions can be drawn.

In conclusion, non-structural proteins play a key role in the replication cycle of viruses. Prior investigations have established that the AHSV NS2 protein binds single-stranded RNA, is associated with the VIBs present in infected cells, and is the only phosphorylated AHSV protein (Theron *et al.*, 1994; Uitenweerde *et al.*, 1995). Although the first two properties of the NS2 protein suggest that it may be responsible for sequestering viral mRNAs at the sites of assembly of new viral particles, not much is known regarding the functional importance of AHSV NS2 protein phosphorylation. The results of this study showed that IB formation by the AHSV NS2 protein occurs by a phosphorylation-dependent mechanism that requires CK2 phosphorylation of NS2 at serine residues 256 and 258. Since protein phosphorylation impacts diverse processes and interactions, including protein-protein and protein-nucleic acid interactions (Cohen, 2000; Jakubiec and Jupin, 2007), it is possible that phosphorylation of the NS2 protein may govern its interaction with viral proteins and/or viral mRNA during the virus replication cycle. As such, the role and relevance of NS2 phosphorylation in the context of virus replication warrants further investigation.

CHAPTER SIX

CONCLUDING REMARKS

Previous studies on the NS2 protein of the African horse sickness virus (AHSV) have sought to characterize the properties of the protein. These studies, mostly dating back to the 1990s, have reported that NS2 is the major component of virus inclusion bodies (VIBs), is able to bind single-stranded (ss) RNA, and is phosphorylated (Devaney *et al.*, 1988; Theron *et al.*, 1994; Uitenweerde *et al.*, 1995). However, the functional importance of these properties during virus replication has received little attention. Consequently, towards the long-term goal of understanding the role of NS2 in the replication cycle of AHSV, this study aimed to elucidate the mechanism of NS2 phosphorylation and to evaluate the importance of NS2 phosphorylation on its ability to form VIB-like structures. In this conclusion, the main results emanating from this study are summarized briefly and suggestions regarding future research are made.

The results of this study indicated that the NS2 protein of AHSV-4 lacks autophosphorylation activity and is phosphorylated by Casein kinase 2 (CK2) at two serine residues (Ser-256 and Ser-258) in the C terminus of the protein. Moreover, it was established that NS2 phosphorylation is required for the protein to assemble into cytoplasmic inclusion bodies (IBs). These results are similar to that reported for the Bluetongue virus (BTV) NS2 protein (Modrof *et al.*, 2005; Mohl and Roy, 2016), suggesting that IB-formation by orbiviruses may occur through a common mechanism.

In orbiviruses-infected cells, the VIBs are considered to be the sites of virus replication and early virus assembly (Patel and Roy, 2014). As such, AHSV NS2 can be expected to interact with and recruit into VIBs, the various viral structural proteins as well as viral ssRNA transcripts that serve as the substrates for packaging into progeny virions. Therefore, in addition to its importance for IB formation, it may be reasonable to assume that phosphorylation of the NS2 protein may regulate its interaction with other viral proteins and viral ssRNA during the assembly of particles in the VIBs. It has been reported that phosphorylation of the BTV NS2 protein has no effect on its ssRNA binding activity (Thomas *et al.*, 1990; Modrof *et al.*, 2005), whereas phosphorylation of the Epizootic haemorrhagic disease virus (EHDV) NS2 protein was shown to down-regulate its ssRNA binding property (Theron *et al.*, 1996). Since it is not known whether the phosphorylation status of AHSV NS2 may influence its ssRNA binding ability, future studies could make use of the baculovirus-expressed wild-type NS2 and unphosphorylated NS2 mutant protein (NS2 S-A256,258) to assess their ability to bind to ssRNA in electrophoretic mobility shift assays (EMSA). These investigations can also be extended to perform the binding assays in the presence of specific or

non-specific competitor ssRNA in order to determine whether NS2 phosphorylation may regulate the preferential binding of NS2 to viral mRNA over non-specific ssRNA. Future studies to assess the influence of NS2 phosphorylation on NS2-viral protein interactions could comprise of co-localization studies of viral structural proteins co-expressed with wild-type phosphorylated NS2 or the unphosphorylated NS2 mutant protein. To confirm a direct interaction of NS2 with co-localized proteins, the purified viral and NS2 proteins can be incubated together, and an immunoprecipitation assay can be performed with the anti-NS2 antibody, followed by Western blot analysis using viral protein-specific antibodies. Such studies would not only provide greater insight into the functional importance of NS2 phosphorylation but may also generate information that contributes to the understanding of AHSV morphogenesis.

Although the importance of NS2 phosphorylation for the formation of VIB-like structures was established in this study, future studies should aim to elucidate the importance of these structures and NS2 phosphorylation for productive AHSV replication. Such studies may be undertaken by either treating AHSV-infected cells with CK2-specific inhibitors, such as the cell-permeable CK2-specific inhibitor TBB used in this study or by making use of siRNAs to silence the expression of CK2 in virus-infected cells. The effects of such treatments on the ability of NS2 to assemble into VIBs and on virus replication can then be assessed by immunofluorescent confocal microscopy and virus titration assays, respectively. However, CK2 is constitutively expressed and is the most pleiotropic kinase among individual members of the protein kinase superfamily with roles in transcription, signaling, proliferation, and in various steps of cell development (Olsten *et al.*, 2001; Meggio and Pina, 2003). By making use of these approaches and taking into account the transient nature of these treatments, it may not be possible to draw definitive conclusions from such experiments. Reverse genetics technology, however, could provide a more suitable approach to directly evaluate the role of NS2, NS2 phosphorylation, and VIBs in the virus replication cycle. An entirely plasmid DNA-based reverse genetics system has been developed for AHSV-4 and relies on the use of recombinant plasmid DNA constructs harbouring cloned cDNA copies of the ten AHSV-4 genome segments (Conradie *et al.*, 2016). Future studies could make use of this reverse genetics system to generate recombinant AHSV-4 that is unable to produce NS2 or that produces an unphosphorylated NS2, and these recombinant viruses can then be compared to wild-type AHSV-4 in infected cell cultures. A combination of transmission electron microscopy, immunofluorescent confocal microscopy, and virus titration assays can be used to

compare the VIBs and evaluate their importance for virus replication. These studies can also be extended to examine the location of viral structural proteins and viral mRNA transcripts in the respective infected cell cultures. For the latter, virus-infected cells can be treated with actinomycin D to arrest host replication and transcription, and newly synthesized viral transcripts can then be labelled by including 5-ethynyl uridine in the cell culture medium followed by detection with an azide-conjugated fluorophore (Papa *et al.*, 2020).

Interestingly, recent reports have indicated that BTV (Rahman *et al.*, 2022) and Rotavirus (Geiger *et al.*, 2021) appear to use liquid-liquid phase separation (LLPS) for the assembly of VIBs and viroplasms, respectively, at the early stages of infection. LLPS occurs when biomolecules, such as certain nucleic acids or proteins, preferentially interact with one another over others in an environment and then coalesce to form discreet compartments that separate from the surrounding environment. LLPS, therefore, facilitates intracellular compartmentalization in the absence of membrane enclosures and has been likened to the formation of oil droplets in water (Hyman *et al.*, 2014; Lee and Dermody, 2021). For Rotavirus, the interaction between NSP2, which serves as a chaperone of viral RNA, and NSP5 was shown to result in their condensation (droplet formation), which was suggested to provide a molecular environment for the establishment of inter-molecular contacts between the rotavirus mRNA transcripts, followed by their assortment and packaging (Geiger *et al.*, 2021). In the case of BTV, it was reported that the ability of NS2 to undergo LLPS is dependent on NS2 phosphorylation and its ability to bind ssRNA (Rahman *et al.*, 2022). Although it would be of interest to determine whether the AHSV NS2 protein is capable of driving LLPS, there does not appear to be a uniformly accepted methodology for these types of investigations. Nevertheless, current standards include microscopy to observe condensate morphology, qualitative assessment of condensate dynamics by observing fission and fusion events, quantitative analysis of condensate dynamics using fluorescence recovery after photobleaching (FRAP), determining the effect of LLPS-dissolving drugs on condensate stability, and building phase-transition diagrams to define minimal components that induce LLPS (Alberti *et al.*, 2019; Lee and Dermody, 2021).

In conclusion, the orbivirus NS2 phosphoprotein is a multifunctional protein and possesses different properties (ssRNA binding activity, formation of VIBs, and nucleotidyl phosphatase activity) that suggest it may play an important role in virus replication. This study has revealed the importance of AHSV NS2 protein phosphorylation for IB formation and identified two

serine residues within NS2 that serve as phosphorylation sites of the protein. This information can be used in future studies, as highlighted in the sections above, to better understand the role of VIBs in the replication cycle of AHSV and also to characterize the significance of phosphorylation on NS2 function. It can be envisaged that such information should contribute greatly to unravelling the role of NS2 in the processes of viral replication and morphogenesis.

REFERENCES

Afrikanova I, Miozzo MC, Giambiagi S & Burrone O (1996) Phosphorylation generates different forms of rotavirus NSP5. Journal of General Virology 77: 2059-2065.

Aklilu N, Batten C, Gelaye E, Jenberie S, Ayelet G, Wilson A, Belay A, Asfaw Y, Oura C, Maan S, Banchanek-Bankwoska K & Mertens PC. (2014) African horse sickness outbreaks caused by multiple virus types in Ethiopia. Transboundary and Emerging Diseases 61: 185-192.

Alberti S, Gladfelter A & Mittag T (2019) Considerations and challenges in studying liquid-liquid phase separation and biomolecular condensates. Cell 176: 419-434.

Assefa A, Tibebu A, Bihon A, Dagnachew A & Muktar Y (2022) Ecological niche modelling predicting the potential distribution of African horse sickness virus from 2020 to 2060. Scientific Reports 12: 1748.

Awad FI, Amin MM, Salama SA & Kinde S (1981) The role played by *Hylomma dromedarii* in transmission of African horse sickness virus in Egypt. Bulletin of Animal Health and Production in Africa 29E: 337-340.

Barnard B (1997) Antibodies against some viruses of domestic animals in southern African wild animals. Onderstepoort Journal of Veterinary Research 64: 95-110.

Barnard BJ, Bengis R, Keet D & Dekker EH (1994) Epidemiology of African horse sickness, duration of viraemia in zebra (*Equus burchelli*). Onderstepoort Journal of Veterinary Research 91: 391-393.

Basak A, Gouet P, Grimes J, Roy P & Stuart D (1996) Crystal structure of the top domain of African horse sickness virus VP7: Comparison with Bluetongue virus VP7. Journal of Virology 70: 3797-3806.

Basak A, Stuart D & Roy P (1992) Preliminary crystallographic study of bluetongue virus capsid protein, VP7. Journal of Molecular Biology 228: 687-689.

Battistutta R, De Moliner E, Sarno S, Zanotti G & Pinna LA (2001) Structural features underlying selective inhibition of protein kinase CK2 by ATP site-directed tetrabromo-2-benzotriazole. Protein Science 10: 2200-2206.

Beaton AR, Rodriguez J, Reddy YK & Roy P (2002) The membrane trafficking protein calpactin forms a complex with Bluetongue virus protein NS3 and mediates virus release. Proceedings of the National Academy of Sciences of the United States of America 99: 13154-13159.

Bekker S, Huismans H & van Staden V (2014) Factors that affect the intracellular localization and trafficking of African horse sickness virus core protein, VP7. Virology 456: 279-291.
Bekker S, Potgieter CA, van Staden V & Theron J (2022) Investigating the role of African horse sickness virus VP7 protein crystalline particles on virus replication and release. Viruses 14: 2193.

Belhouchet M, Mohd Jaafar F, Firth A, Grimes J, Mertens P & Attoui H (2011) Detection of a fourth orbivirus non-structural protein. PLoS ONE 6: e25697.

Bentley L, Fehrsen J, Jordaan F, Huismans H & du Plessis DH (2000) Identification of antigenic regions on VP2 of African horsesickness virus serotype 3 by using phage-displayed epitope libraries. Journal of General Virology 81: 993-1000.

Bergmans H, van Die I & Hoekstra W (1981) Transformation in *Escherichia coli*: Stages in the Process. Journal of Bacteriology 146: 564-570.

Bhattacharya B & Roy P (2008) Bluetongue virus outer capsid protein VP5 interacts with membrane lipid rafts via a SNARE domain. Journal of Virology 82: 10600-10612.

Bhattacharya B, Noad R & Roy P (2007) Interaction between Bluetongue virus outer capsid protein VP2 and vimentin is necessary for virus egress. Virology Journal 4: 7.

Blackhall J, Munoz M, Fuentes A & Magnusson G (1998) Analysis of rotavirus nonstructural protein NSP5 phosphorylation. Journal of Virology 72: 6398-6405.

Blom N, Sicheritz-Pontén T, Gupta R, Gammeltoft S & Brunak S (2004) Prediction of post-translational glycosylation and phosphorylation of proteins from the amino acid sequence. Proteomics 4: 1633-1649.

Boorman J, Mellor PS, Penn M & Jennings M (1975) The growth of African horse sickness virus in embryonated hen eggs and the transmission of virus by *Culicoides variipennis Coquillett* (Diptera: Ceratopogonidae). Archives of Virology 47: 343-349.

Bornhorst JA & Falke JJ (2000) Purification of proteins using polyhistidine affinity tags. Methods in Enzymology 326: 245-254.

Bosman P, Bruckner GH & Faul A (1995) African horse sickness surveillance systems and regionalisation/zoning, the case of South Africa. Revue Scientifique et Technique 14: 645-653.

Boughan S, Potgieter AC & van Staden V (2020) African horse sickness virus NS4 is a nucleocytoplasmic protein that localizes to PML nuclear bodies. Journal of General Virology 101: 366-374.

Boyce M, Celma C & Roy P (2012) Bluetongue virus non-structural protein 1 is a positive regulator of viral protein synthesis. Virology Journal 9: 178-189.
Boyce M, Wehrfritz J, Noad R & Roy P (2004) Purified recombinant bluetongue virus VP1 exhibits RNA replicase activity. Journal of Virology 78: 3994-4002.

Bradford M (1976) A rapid and sensitive method for quantification of microgram quantities of protein utilising the principle of protein-dye binding. Analytical Biochemistry 72: 248-254.

Breese SS, Ozawa Y & Dardiri AH (1969) Electron microscopic characterization of African horse-sickness virus. Journal of the American Veterinary Medical Association 155: 391-400.

Bremer C (1976) A gel electrophoretic study of the protein and nucleic acid components of African horse sickness virus. Onderstepoort Journal of Veterinary Research 43: 193-199.

Brookes S, Hyatt A & Eaton B (1993) Characterization of virus inclusion bodies in Bluetongue virus-infected cells. Journal of General Virology 74: 525-530.

Brown M & Faulkner P (1977) A plaque assay for nuclear polyhedrosis viruses using a solid overlay. Journal of General Virology 36: 361-364.

Burkhardt C, Sung P-Y, Celma CC & Roy P (2014) Structural constraints in the packaging of Bluetongue virus genomic segments. Journal of General Virology 95: 2240-2250.

Burroughs J, O'Hara R, Smale C, Hamblin C, Walton A, Armstrong R & Mertens P (1994) Purification and properties of virus particles, infectious subviral particles, cores and VP7 crystals of African horse sickness virus serotype 9. Journal of General Virology 75: 1849-1857.

Butan C, Van Der Zandt H &Tucker PA (2004) Structure and assembly of the RNA binding domain of bluetongue virus non-structural protein 2. Journal of Biological Chemistry 279: 37613-37621.

Calvo-Pinilla E, Marín-López A, Utrilla-Trigo S, Jiménez-Cabello L & Ortego J (2020) Reverse genetics approaches: A novel strategy for African horse sickness virus vaccine design. Current Opinions in Virology 44: 49-56.

Campagna M, Budini M, Arnoldi F, Desselberger U, Allende JE & Burrone O (2007) Impaired hyperphosphorylation of rotavirus NSP5 in cells depleted of casein kinase 1a is associated with the formation of viroplasms with altered morphology and a moderate decrease in virus replication. Journal of General Virology 88: 2800-2810.

Carpenter S, Mellor P, Fall A, Garros C & Venter G (2017) African horse sickness virus: History, transmission, and current status. Annual Review of Entomology 62: 343-358.

Celma C & Roy P (2009) A viral nonstructural protein regulates bluetongue virus trafficking and release. Journal of General Virology 83: 6806-6816.

Celma CC & Roy P (2011) Interaction of calpactin light chain (S100A10/p11) and a viral NS protein is essential for intracellular trafficking of nonenveloped Bluetongue virus. Journal of Virology 85: 4783-4791.

Chauveau E, Doceul V, Lara E, Breard E, Sailleau C, Vidalain P-O, Meurs EF, Dabo S, Schwartz-Cornil I & Zientara S (2013) NS3 of Bluetongue virus interferes with the induction of type I interferon. Journal of Virology 87: 8241-8246.

Chiam R, Sharp E, Maan S, Rao S, Mertens P, Blacklaws B, Davis-Poynter N, Wood J & Castillo-Olivares J (2009) Induction of antibody responses to African horse sickness virus (AHSV) in ponies after vaccination with recombinant modified vaccinia Ankara (MVA). PLoS ONE 4: e5997.

Chuma T, Le Blois H, Sanchez-Vizcaíno J, Diaz-Laviada M & Roy P (1992) Expression of the major core antigen VP7 of African horse sickness virus by a recombinant baculovirus and its use as a group-specific diagnostic reagent. Journal of General Virology 73: 925-931.

Clemmons E, Alfson K & Dutton J (2021) Transboundary animal diseases, an overview of 17 diseases with potential for global spread and serious consequences. Animals 11: 2039.

Coetzer J & Guthrie A (2004) African horse sickness. Infectious Diseases of Livestock, 2nd Edition, Vol. 4 (Coetzer J & Trustin R, eds.), pp. 1231-1246. Oxford University Press, Cape Town, South Africa.

Cohen P (2000) The regulation of protein function by multisite phosphorylation - a 25-year update. Trends in Biochemical Sciences 25: 596-601.

Conradie AM, Stassen L, Huismans H, Potgieter CA & Theron J (2016) Establishment of different plasmid only-based reverse genetics systems for the recovery of African horse sickness virus. Virology 499: 144-155.

Cowley JA & Gorman BM (1987) Genetic reassortants for identification of the genome segment coding for the Bluetongue virus hemagglutinin. Journal of Virology 61: 2304-2306.

Criglar JM, Anish R, Hu L, Crawford SE, Sankaran B, Prasad BVV & Estes MK (2018) Phosphorylation cascade regulates the formation and maturation of rotaviral replication factories. Proceedings of the National Academy of Sciences of the United States of America 115: e12015-e12023.

De Castro IF, Volonte L & Risco C (2013) Virus factories: Biogenesis and structural design. Cellular Microbiology 15: 24-34.

De Vos CJ, Hoek CA & Nodelijk G (2012) Risk of introducing African horse sickness virus into the Netherlands by international equine movements. Preventive Veterinary Medicine 106: 108-122.

De Waal P & Huismans H (2005) Characterization of the nucleic acid binding activity of inner core protein VP6 of African horse sickness virus. Archives of Virology 150: 2037-2050.

Dennis SJ, Meyers AE, Guthrie AJ, Hitzeroth II & Rybicki EP (2018a) Immunogenicity of plant-produced African horse sickness virus-like particles: Implications for a novel vaccine. Plant Biotechnology Journal 16: 442-450.

Dennis SJ, O'Kennedy MM, Rutkowska D, Tsekoa T, Lourens CW, Hitzeroth II, Meyers AE & Rybicki EP (2018b) Safety and immunogenicity of plant-produced African horse sickness virus-like particles in horses. BMC Veterinary Research 49: 105.

Devaney M, Kenall J & Grubman M (1988) Characterization of a nonstructural phosphoprotein of two Orbiviruses. Virus Research 11: 151-164.

Diouf ND, Etter E, Lo MM & Akakpo AJ (2013) Outbreaks of African horse sickness in Senegal, and methods of control of the 2007 epidemic. Veterinary Research 172: 152.

Drews M, Paalme T & Vilu R (1995) The growth and nutrient utilization of the insect cell line *Spodoptera frugiperda* Sf9 in batch and continuous culture. Journal of Biotechnology 40: 187-198.

du Plessis M, Cloete M, Aitchison H & van Dyk A (1998) Protein aggregation complicates the development of baculovirus-expressed African horse sickness virus serotype 5 VP2 subunit vaccines. Onderstepoort Journal of Veterinary Research 65: 321-329.

du Toit R (1944) The transmission of blue-tongue and horse-sickness by *Culicoides*. Onderstepoort Journal of Veterinary Science and Animal Industry 19: 7-16.

Dufour Á, Moutou F, Hattenberger A & Rodhain F (2008) Global change: Impact, management, risk approach and health measures - the case of Europe. Revue Scientifique et Technique 27: 529-550.

Eaton B, Hyatt A & Brookes S (1990) The replication of bluetongue virus. Current Topics in Microbiology and Immunology 162: 89-118.

Eaton B, Hyatt A & White J (1988) Localization of the nonstructural protein NS1 in bluetongue virus-infected cells and its presence in virus particles. Virology 163: 527-537.

Eichwald C, Jacob G, Muszynski B, Allende JE & Burrone OR (2004) Uncoupling substrate and activation functions of rotavirus NSP5: Phosphorylation of Ser-67 by casein kinase 1 is essential for hyperphosphorylation. Proceedings of the National Academy of Sciences of the United States of America 101: 16304-16309.

Eichwald C, Vascotto F, Fabbretti E & Burrone OR (2002) Rotavirus NSP5: Mapping phosphorylation sites and kinase activation and viroplasm localization domains. Journal of Virology 76: 3461-3470.

El Garch H, Crafford JE, Amouyal P, Durand PY, Edlund Toulemonde C, Lemaitre L, Cozette V, Guthrie A & Minke JM (2012) An African horse sickness virus serotype 4 recombinant canarypox virus vaccine elicits specific cell-mediated immune responses in horses. Veterinary Immunology and Immunopathology 149: 76-85.

El Hasnaoui H, El Harrak M, Zientara S, Laviada M & Hamblin C (1998) Serological and virological responses in mules and donkeys following inoculation with African horse sickness virus serotype 4. Archives of Virology 14: 29-36.

Elíes J, Yáñez M, Pereira TMC, Gil-Longo J, MacDougall DA & Campos-Toimil M (2020) An update to calcium binding proteins. Advances in Experimental Medicine and Biology 1131: 183-213.

Erasmus BJ, Young E, Pieterse LM & Boshoff ST (1978) The susceptibility of zebra and elephants to African horsesickness virus. Equine Medicine, Surgery and Reproduction 1: 409-413.

Fajardo T, Sung P-Y & Roy P (2015) Disruption of specific RNA-RNA interactions in a double-stranded RNA virus inhibits genome packaging and virus infectivity. PLoS Pathogens 11: e1005321.

Fassi-Fihri O, El Harrak M & Fassi-Fehri MM (1998) Clinical, virological, and immune responses of normal and immunosuppressed donkeys (*Equus asinus africanus*) after inoculation with African horse sickness virus. Archives of Virology 14: 49-56.

Fawcett T (1999) Isolation of high-quality large plasmid DNA. Focus 21: 20-21.

Feenstra F, Van Gennip R, Van de Water S & Van Rijn P (2014) RNA elements in open reading frames of the bluetongue virus genome are essential for virus replication. PLoS ONE 9: e92377.

Fernández de Castro I, Tenorio R & Risco C (2021) Virus Factories. Encyclopaedia of Virology,4th Edition (Bamford D & Zuckerman M, eds.), pp. 495-500. Cambridge, Massachusetts, USA.

Fillmore G, Lin H & Li J (2002) Localization of the single-stranded RNA-binding domains of bluetongue virus nonstructural protein NS2. Journal of Virology 76: 499-506.
Firth A (2008) Bioinformatic analysis suggests that the orbivirus VP6 cistron encodes an overlapping gene. Virology Journal 5: 48.

Forzan M, Marsh M & Roy P (2007) Bluetongue virus entry into cells. Journal of Virology 81: 4819-4827.

French T, Marshall J & Roy P (1990) Assembly of double-shelled, virus-like particles of Bluetongue virus by the simultaneous expression of four structural proteins. Journal of Virology 64: 5695-5700.

Gale P, Brouwer A, Ramnial V, Kelly L, Kosmider R, Fooks A & Snary E (2010) Assessing the impact of climate change on vector-borne viruses in the EU through the elicitation of expert opinion. Epidemiology and Infection 138: 214-225.

Garcés Suárez Y, Martínez JL, Torres Hernández D, Hernández HO, Pérez-Delgado A, Méndez M, Wood CD, Rendon-Mancha JM, Silva-Ayala D, López S, Guerrero A & Arias CF (2019) Nanoscale organization of rotavirus replication machineries. eLife 8.

Geiger F, Acker J, Papa G, Wang X, Arter WE, Saar KL, Erkamp NA, Qi R, Bravo JP, Strauss S, Krainer G, Burrone OR, Jungmann R, Knowles TP, Engelke H & Borodavka A (2021) Liquid-liquid phase separation underpins the formation of replication factories in rotaviruses. EMBO Journal 40: e107711.

Gold S, Monaghan P, Mertens P & Jackson T (2010) A clathrin independent macropinocytosis-like entry mechanism used by bluetongue virus-1 during infection of BHK cells. PLoS ONE 5: e11360.

Gorman BM, Taylor J & Walker PJ (1983) Orbiviruses. Plenum Press, New York.

Guthrie AJ, Quana M, Lourensa CW, Audonnet J, Minkeb JM, Yao J, He L, Nordgren R, Gardner IA & MacLachlan NJ (2009) Protective immunisation of horses with a recombinant canarypox virus

vectored vaccine co-expressing genes encoding the outer capsid proteins of African horse sickness virus. Vaccine 16: 4434-4438.

Hamblin G, Salt JS, Mellor PS, Graham SD, Smith PR & Wohlsein P (1998) Donkeys as reservoirs of African horse sickness virus. Archives of Virology 14: 37-47.

Han Z & Harty RN (2004) The NS3 protein of Bluetongue virus exhibits viroporin-like properties. Journal of Biological Chemistry 279: 43092-43097.

Hassan S & Roy P (1999) Expression and characterization of bluetongue virus VP2 protein: Role in cell entry. Journal of Virology 73: 9832-9842.

Hassan S, Wirblich C, Forzan M & Roy P (2001) Expression and functional characterization of bluetongue virus VP5 protein: Role in cellular permeabilization. Journal of Virology 75: 8356-8367.

Hayama E & Li J (1994) Mapping and characterization of antigenic epitopes and the nucleic acid-binding domains of the VP6 protein of bluetongue viruses. Journal of Virology 68: 3604-3611.

He Y, Shivakoti S, Ding K, Cui Y, Roy P & Zhou ZH (2019) *In situ* structures of RNA-dependent RNA polymerase inside Bluetongue virus before and after uncoating. Proceedings of the National Academy of Sciences of the United States of America 116: 16535-16540.

Hewat EA, Booth TF & Roy P (1992b) Structure of Bluetongue virus particles by cryoelectron microscopy. Journal of Structural Biology 109: 61-69.

Hewat EA, Booth TF, Wade RH & Roy P (1992a) 3-D reconstruction of Bluetongue virus tubules using cryoelectron microscopy. Journal of Structural Biology 108: 35-48.

Horscroft N & Roy P (2000) NTP binding and phosphohydrolase activity associated with purified bluetongue virus non-structural protein NS2. Journal of General Virology 81: 1961-1965.

Howell P (1960) The 1960 epizootic of African horsesickness in the Middle East and SW Asia. Journal of the South African Veterinary Medical Association 31: 329-334.

Howell P (1963) African horse sickness. Emerging diseases of animals, Vol. 61, pp. 71-108. FAO Agricultural Studies FAO, Rome.

Huismans H & Els H (1979) Characterization of the tubules associated with the replication of three different orbiviruses. Virology 92: 379-406.

Huismans H & Erasmus B (1981) Identification of the serotype-specific and group-specific antigens of Bluetongue virus. Onderstepoort Journal of Veterinary Research 48: 51-58.

Huismans H & van Dijk A (1990) Bluetongue virus structural components. Current Topics in Microbiology and Immunology 162: 21-37.

Huismans H (1979) Protein synthesis in Bluetongue virus-infected cells. Virology 92: 385-396.

Huismans H, van Dijk A & Bauskin A (1987) *In vitro* phosphorylation and purification of a nonstructural protein of bluetongue virus with affinity for single-stranded RNA. Journal of Virology 61: 3589-3595.

Hyatt A & Eaton B (1988) Ultrastructural distribution of the major capsid proteins within bluetongue virus-infected cells. Journal of Molecular Evolution 69: 805-815.

Hyatt A, Eaton B & Brookes S (1989) The release of bluetongue virus from infected cells and their superinfection by progeny virus. Virology 173: 21-34.

Hyatt AD, Zhao Y & Roy P (1993) Release of Bluetongue virus-like particles from insect cells is mediated by BTV nonstructural protein NS3/NS3A. Virology 193: 592-603.

Hyman AA, Weber CA & Jülicher F (2014) Liquid-liquid phase separation in biology. Annual Reviews in Cell Developmental Biology 30: 39-58.

Inumaru S, Ghiasi H & Roy P (1987) Expression of Bluetongue virus group-specific antigen VP3 in insect cells by a baculovirus vector: Its use for the detection of Bluetongue virus antibodies. Journal of General Virology 68: 1627-1635.

Iwata H, Yamagawa M & Roy P (1992) Evolutionary relationships among the gnat-transmitted orbiviruses that cause African horse sickness, bluetongue and epizootic haemorrhagic disease as evidenced by their capsid protein sequences. Virology 191: 251-261.

Jakubiec A & Jupin I (2007) Regulation of positive-strand RNA virus replication: The emerging role of phosphorylation. Virus Research 129: 73-79.

Kanai Y, van Rijn P, Maris-Veldhuis M, Kaname Y, Athmaram Y & Roy P (2014) Immunogenicity of recombinant VP2 proteins of all nine serotypes of African horse sickness virus. Vaccine 32: 4932-4937.

Kar A, Ghosh M & Roy P (2004) Mapping the assembly pathway of bluetongue virus scaffolding protein VP3. Virology 324: 387-399.

Kar AK & Roy P (2003) Defining the structure-function relationships of Bluetongue virus helicase protein VP6. Journal of Virology 77: 11347-11356.

Kar AK, Bhattacharya B & Roy P (2007) Bluetongue virus RNA binding protein NS2 is a modulator of viral replication and assembly. BMC Molecular Biology 8: 4-17.

Kerviel A, Ge P, Lai M, Jih J, Boyce M, Zhang X, Zhou ZH & Roy P (2019) Atomic structure of the translation regulatory protein NS1 of Bluetongue virus. Nature Microbiology 4: 837-845.

King S, Rajko-Nenow P, Ashby M, Frost L, Carpenter S & Batten C (2020) Outbreak of African horse sickness in Thailand. Transboundary and Emerging Diseases 67 (5): 1751-2267.

Kundlacz C, Pourcelot M, Fablet A, Da Silba Moraes RA, Léger T, Morlet B, Viarouge C, Sailleau C, Turpaud M, Gorlier A, Breard E, Lecollinet S, van Rijn PA, Zientara S, Vitour D & Caignard C. (2019) Novel function of Bluetongue virus NS3 protein in regulation of the MAPK/ERK signalling pathway. Journal of Virology 93: e00336.

Labadie T & Roy P (2020) A non-enveloped arbovirus released in lysosome-derived extracellular vesicles induces super-infection exclusion. PLoS Pathogens 16: e1009015.

Laegreid WW, Skowronek A, Stone-Marschat M & Burrage T (1993) Characterisation of virulence variants of African horsesickness virus. Virology 195: 836-839.

Laemmli UK (1970) Cleavage of structural proteins during the assembly of the head of bacteriophage T4. Nature 227: 680-685.

Lee CH & Dermody TS (2021) Some viruses need to phase-separate to replicate. EMBO Journal 40: e109558.

Lee C-R, Park Y-H, Kim Y-R, Peterkofsky A & Seok Y-J (2013) Phosphorylation-dependent mobility shift of proteins on SDS-PAGE is due to decreased binding of SDS. Bulletin of the Korean Chemical Society 34: 2063-2066.

Leta S, Fetene E, Mulatu T, Amenu K, Jaleta MB, Beyene TJ, Negussie H, Kriticos D & Revie CW (2019) Updating the global occurrence of *Culicoides imicola*, a vector for emerging viral diseases. Scientific Data 6: 185.

Lewellyn E & Loeb D (2011) Serine phosphoacceptor sites within the core protein of hepatitis B virus contribute to genome replication pleiotropically. PloS ONE 6: e17202.

Li Z, Lu D, Yang H, Li Z, Zhu P, Xie J, Liao D, Zheng Y & Li H (2021) Bluetongue virus non-structural protein 3 (NS3) and NS4 coordinatively antagonize type interferon signaling by targeting STAT1. Veterinary Microbiology 254: 108986.

Loudon PT & Roy P (1992) Assembly of five Bluetongue virus proteins expressed by recombinant baculoviruses, inclusion of the largest protein VP1 in the core and virus-like proteins. Virology 180: 798-802.

Luckow VA, Lee SC, Barry GF & Olins PO (1993) Efficient generation of infectious recombinant baculoviruses by site-specific transposon-mediated insertion of foreign genes into a baculovirus genome propagated in *Escherichia coli.* Journal of Virology. 67: 4566-4579.

Lulla V, Losada A, Lecollinet S, Kerviel A, Lilin T, Sailleau C, Beck C, Zientara S & Roy P (2017) Protective efficacy of multivalent replication-abortive vaccine strains in horses against African horse sickness challenge. Vaccine 35: 4262-4269.

Lulla V, Lulla A, Wernike K, Aebischer A, Beer M & Roy P (2016) Assembly of replication-incompetent African horse sickness virus particles: Rational design of vaccines for all serotypes. Journal of Virology 90: 7405-7414.

Lymperopoulos K, Noad R, Tosi S, Nethisinghe S, Brierley I & Roy P (2006) Specific binding of Bluetongue virus NS2 to different viral plus-strand RNAs. Virology 353: 17-26.

Lymperopoulos K, Wirblich C, Brierley I & Roy P (2003) Sequence specificity in the interaction of bluetongue virus non-structural protein 2 (NS2) with viral RNA. Journal of Biological Chemistry 278: 31722-31730.

MacLachlan N, Balasuriya U, Davis N, Collier M, Johnston R, Ferraro G & Guthrie A (2007) Experiences with new generation vaccines against equine viral arteritis, West Nile disease and African horse sickness. Vaccine 25: 5577-5582.

MacLachlan NJ & Guthrie AJ (2010) Re-emergence of Bluetongue, African horse sickness, and other orbivirus diseases. Veterinary Research 41: 35.

Manning NM, Bachanek-Bankowska K, Mertens PPC & Castillo-Olivares J (2017) Vaccination with recombinant Modified Vaccinia Ankara (MVA) viruses expressing single African horse sickness virus VP2 antigens induced cross-reactive virus neutralising antibodies (VNAb) in horses when administered in combination. Vaccine 35: 6024-6029.

Manole V, Pasi L, Van Wyngaardt W, Potgieter C, Wright I, Venter G, Van Dijk A & Sewell B (2012) Structural insight into African horse sickness virus infection. Journal of Virology 86: 7858-7866.

Maree F & Huismans H (1997) Characterization of tubular structures composed on nonstructural protein NS1 of African horse sickness virus expressed in insect cells. Journal of General Virology 78: 1077-1082.

Maree S & Paweska JT (2005) Preparation of recombinant African horse sickness virus VP7 antigen via a simple method and validation of a VP7-based indirect ELISA for the detection of group-specific IgG antibodies in horse sera. Journal of Virological Methods 125: 55-65.

Maree S, Durbach S & Huismans H (1998) Intracellular production of African horse sickness virus core-like particles by expression of two major core proteins, VP3 and VP7, in insect cells. Journal of General Virology 79: 333-337.

Maree S, Maree FF, Putterill JF, de Beer TA, Huismans H & Theron J (2016) Synthesis of empty African horse sickness virus particles. Virus Research 213: 184-194.

Markotter W, Theron J & Nel L (2004) Segment-specific inverted repeat sequences in bluetongue virus mRNA are required for interaction with the virus non-structural protein NS2. Virus Research 105: 1-9.

Marshall JJ & Roy P (1990) High level expression of the two outer capsid proteins of Bluetongue virus serotype 10: Their relationship with the neutralization of virus infection. Virus Research 15: 189-195.

Martinez-Costas J, Sutton G, Ramadevi N & Roy P (1998) Guanylyltransferase and RNA 5'-triphosphatase activities of the purified expressed VP4 protein of Bluetongue virus. Journal of Molecular Biology 280: 859-866.

Martínez-López B, Perez A & Sánchez-Vizcaíno J (2011) Identifying equine premises at high risk of introduction of vector-borne diseases using geo-statistical and space-time analyses. Preventive Veterinary Medicine 100: 100-108.

Martínez-Torrecuadrada JL & Casal JI (1995) Identification of a linear neutralization domain in the protein VP2 of African horse sickness virus. Virology 210: 391-399.

Martínez-Torrecuadrada JL, Langeveld JP, Meloen RH & Casal JI (2001) Definition of neutralizing sites on African horse sickness virus serotype 4 VP2 at the level of peptides. Journal of General Virology 82: 2415-2424.

Martínez-Torrecuadrada JL, Langeveld JP, Venteo A, Sanz A, Dalsgaard K, Hamilton WD, Meloen RH & Casal JI (1999) Antigenic profile of African horse sickness virus serotype 4 VP5 and identification of a neutralizing epitope shared with Bluetongue virus and epizootic haemorrhagic disease virus. Virology 257: 449-459.

Matsuo E & Roy P (2009) Bluetongue virus VP6 acts early in the replication cycle and can form the basis of chimeric virus formation. Journal of Virology 83: 8842-8848.

Matsuo E & Roy P (2011) Bluetongue virus VP1 polymerase activity *in vitro*: Template dependency, dinucleotide priming, and cap dependency. PLoS ONE 6: e27702.

Matsuo E & Roy P (2013) Minimum requirements for Bluetongue virus primary replication *in vivo*. Journal of Virology 87: 882-889.

Matsuo E, Leon E, Matthews SJ & Roy P (2014) Structure-based modification of Bluetongue virus helicase protein VP6 to produce a viable VP6-truncated BTV. Biochemical and Biophysical Research Communications 451: 603-608.

Matsuo E, Yamazaki K, Tsuruta H & Roy P (2018) Interaction between a unique minor protein and a major capsid protein of Bluetongue virus controls virus infectivity. Journal of Virology 92: e01784.

Matthijnssens J, Attoui H, Bányai K, Brussaard CPD, Danthi P, del Vas M, Dermody TS, Duncan, R, Fang Q, Johne R, Mertens PPC, Jaafar FM, Patton J, Sasaya T, Suzuki N, Wei T, & ICTV Report Consortium (2022a) ICTV Virus Taxonomy Profile: *Sedoreoviridae*. Journal of General Virology 103: 001782.

Matthijnssens J, Attoui H, Bányai K, Brussaard CPD, Danthi P, del Vas M, Dermody TS, Duncan, R, Fang Q, Johne R, Mertens PPC, Jaafar FM, Patton J, Sasaya T, Suzuki N, Wei T, & ICTV Report Consortium (2022b) ICTV Virus Taxonomy Profile: *Spinareoviridae*, Journal of General Virology 103: 001781.

McIntosh B (1958) Immunological types of horse sickness virus and their significance in immunization. Onderstepoort Journal of Veterinary Research 27: 465-539.

Mecham JO & McHolland LE (2010) Measurement of Bluetongue virus binding to a mammalian cell surface receptor by an *in situ* immune fluorescent staining technique. Journal of Virological Methods 165: 112-115.

Meggio F & Pinna LA (2003) One-thousand-and-one substrates of protein kinase CK2? FASEB Journal 17: 349-368.

Meggio F, Marin O & Pinna LA (1994) Substrate specificity of protein kinase CK2. Cellular and Molecular Biological Research 40: 401-409.

Meiswinkel R, Baylis M & Labuschagne K (2000) Stabling and the protection of horses from *Culicoides bolitinos* (Diptera, Ceratopogonidae), a recently identified vector of African horse sickness virus. Bulletin of Entomological Research 90: 509-515.

Mellor P & Hamblin C (2004) African horse sickness. Veterinary Research 35: 445-466.

Mellor P (1993) African horse sickness: Transmission and epidemiology. Veterinary Research 24: 199-212.

Mellor P (1994) Epizootiology and vectors of African horse sickness virus. Comparative Immunology, Microbiology, and Infectious Diseases 17: 287-296.

Mellor PS, Boned J, Hamblin C & Graham S (1990) Isolations of African horse sickness virus from vector insects made during the 1988 epizootic in Spain. Epidemiology and Infection 105: 447-454.

Mellor PS, Boorman J, Wilkinson PJ & Martinez-Gomez F (1983) Potential vectors of Bluetongue and African horse sickness viruses in Spain. Veterinary Research 112: 229-230.

Mertens P & Diprose J (2004) The bluetongue virus core: A nano-scale transcription machine. Virus Research 101: 29-43.

Mertens P (2004) The dsRNA viruses. Virus Research 101: 3-13.

Modrof J, Lymperopoulos K & Roy P (2005) Phosphorylation of bluetongue virus nonstructural protein 2 is essential for formation of viral inclusion bodies. Journal of Virology 79: 10023-10031.

Mohl B & Roy P (2016) Cellular casein kinase 2 and protein phosphatase 2A modulate replication site assembly of bluetongue virus. Journal of Biological Chemistry 291: 14566-14574.

Mohl B-P, Kerviel A, Labadie T, Matsuo E & Roy P (2020) Differential localization of structural and non-structural proteins during the Bluetongue virus replication cycle. Viruses 12: 343.

Mortola E, Noad R & Roy P (2004) Bluetongue virus outer capsid proteins are sufficient to trigger apoptosis in mammalian cells. Journal of Virology 78: 2875-2883.

Mumtsidu E, Makhov A, Roessle M, Bathke A & Tucker P (2007) Structural features of the Bluetongue virus NS2 protein. Journal of Structural Biology 160: 157-167.

Muthukrishnan S, Both G, Furuichi Y & Shatkin A (1975) 5'-Terminal 7-methylguanosine in eukaryotic mRNA is required for translation. Nature 255: 33-37.

Noriko M, Kenichi S, Akira I, Takeshi T, Susumu U, Bunchong A, Masanobu K & Akio F (1993) The complete nucleotide sequence of African horsesickness virus serotype 4 (vaccine strain) segment 4, which encodes the minor core protein VP4. Virus Research 28: 299-306.

O'Kennedy MM, Coetzee P, Koekemoer O, du Plessis L, Lourens CW, Kwezi L, du Preez I, Mamputha S, Mokoena NB, Rutkowska DA, Verschoor JA, Lemmer Y (2022) Protective immunity of plant-produced African horse sickness virus serotype 5 chimaeric virus-like particles (VLPs) and viral protein 2 (VP2) vaccines in IFNAR$^{-/-}$mice. Vaccine 40: 5160-5169.

Oellermann R, Els H & Erasmus B (1970) Characterization of African horse sickness virus. Archiv fur die Gesamte Virusforchung 29: 163-174.

Olsten MEK. & Litchfield DW (2004) Order or chaos? An evaluation of the regulation of protein kinase CK2. Biochemistry and Cell Biology 82: 681-693.

Oura CA, Ivens PA, Bachanek-Bankowska K, Bin-Tarif A, Jallow DB, Sailleau C, Maan S, Mertens PC & Batten CA (2012) African horse sickness in The Gambia: Circulation of a live-attenuated vaccine-derived strain. Epidemiology and Infection 140: 462-465.

Owens R, Limn C & Roy P (2004) Role of an arbovirus nonstructural protein in cellular pathogenesis and virus release. Journal of Virology 78: 6649-6656.

Papa G, Borodavka A, Desselberger U (2021) Viroplasms: Assembly and functions of rotavirus replication factories. Viruses 13: 1349.

Papa G, Venditti L, Arnoldi F, Schraner EM, Potgieter C, Borodavka A, Eichwald C & Burrone OR (2020) Recombinant rotaviruses rescued by reverse genetics reveal the role of NSP5 hyperphosphorylation in the assembly of viral factories. Journal of Virology 94: e01110-19.

Patel A & Roy P (2014) The molecular biology of Bluetongue virus replication. Virus Research 182: 5-20.

Patton J, Silversri L, Tortorici M, Vasquez-Del Carpio R & Taraporewala Z (2006) Rotavirus genome replication and morphogenesis: Role of the viroplasm. Current Topics in Microbiology and Immunology 309: 169-187.

Porath J (1992) Immobilized metal ion affinity chromatography. Protein Expression and Purification 3: 263-281.

Potgieter AC, Cloete M, Pretorius P & van Dijk AA (2003) A first full outer capsid protein sequence dataset in the *Orbivirus* genus (family *Reoviridae*): Cloning, sequencing, expression and analysis of a complete set of full-length outer capsid VP2 genes of the nine African horsesickness virus serotypes. Journal of General Virology 84: 1317-1326.

Potgieter C, Wright I & van Dijk A (2015) Consensus sequence of 27 African horse sickness virus genomes from viruses collected over a 76-year period (1933 to 2009). Genome Announcements 3: e00921.

Pourcelot M, Moraes RA, Fablet A, Bréard E, Sailleau C, Viarouge C, Postic L, Zientara S, Caignard G & Vitour D (2021) The VP3 protein of Bluetongue virus associates with the MAVS complex and interferes with the RIG-I-signalling pathway. Viruses 13: 230.

Pritlove DC, Fodor E, Seong BL & Brownlee GG (1995) *In vitro* transcription and polymerase binding studies of the termini of influenza A virus cRNA: Evidence for a cRNA panhandle. Journal of General Virology 9: 2205-2213.

Purse B, Brown H, Harrup L, Mertens P & Rogers D (2008) Invasion of Bluetongue and other orbivirus infections into Europe: The role of biological and climatic processes. Revue Scientifique et Technique 27: 427-442.

Rahman SK, Ampah KK & Roy P (2022) Role of NS2 specific RNA binding and phosphorylation in liquid-liquid phase separation and virus assembly. Nucleic Acids Research 50: 11273-11284.

Rahman SK, Kerviel A, Mohl B-P, He Y, Zhou ZH & Roy P (2020) A calcium sensor discovered in Bluetongue virus nonstructural protein 2 is critical for virus replication. Journal of Virology 94: e01099.

Ramadevi N & Roy P (1998) Bluetongue virus core protein VP4 has nucleoside trisphosphate phosphohydrolase activity. Journal of General Virology 79: 2475-2480.

Ramadevi N, Burroughs J, Mertens P, Jones I & Roy P (1998) Capping and methylation of mRNA by purified recombinant VP4 protein of bluetongue virus. Proceedings of the National Academy of Sciences of the United States of America 95: 13537-13542.

Rao C, Kiuchi A & Roy P (1983) Homologous terminal sequences of the genome double-stranded RNAs of Bluetongue virus. Journal of Virology 46: 378-383.

Ratinier M, Caporale M, Golder M, Franzoni G, Allan K, Nunes SF, Armezzani A, Bayoumy A, Rixon F & Shaw A (2011) Identification and characterization of a novel non-structural protein of Bluetongue virus. PLoS Pathogens 7: e1002477.

Ratinier M, Shaw A, Barry G, Gu Q, Di Gialleonardo L, Janowicz A, Varela M, Randall R, Caporale M & Palmarini M (2016) Bluetongue virus NS4 protein is an interferon antagonist and a determinant of virus virulence. Journal of Virology 90: 5427-5439.

Reddy YV, Ding Q, Lees-Miller SP, Meek K & Ramsden DA (2004) Non-homologous end joining requires that the DNA-PK complex undergo an autophosphorylation-dependent rearrangement at DNA ends. Journal of Biological Chemistry 279: 39408-39413.

Rigden D J &Galperin MY (2004) The DxDxDG motif for calcium binding: multiple structural contexts and implications for evolution. Journal of Molecular Biology 343: 971-984.

Roach PJ (1991) Multisite and hierarchal protein phosphorylation. The Journal of Biological Chemistry 266: 14139-14142.

Robin M, Page P, Archer D & Baylis M (2016) African horse sickness: The potential for an outbreak in disease-free regions and current disease control and elimination techniques. Equine Veterinary Journal 48: 659-669.

Rodriguez M, Hooghuis H & Castaño M (1992) African horse sickness in Spain. Veterinary Microbiology 33: 129-142.

Rojas J, Avia M, Martin V & Sevilla N (2021) Inhibition of the IFN response by Bluetongue virus: The story so far. Frontiers in Microbiology 12: 692069.

Roy P (1989) Bluetongue virus genetics and genome structure. Virus Research 13: 179-206.

Roy P (2013) Orbiviruses. Lippincott & Wilkins, Philadelphia.

Roy P, Adachi A, Urakawa T, Booth T & Thomas C (1990) Identification of bluetongue virus VP6 protein as a nucleic acid-binding protein and the localization of VP6 in virus-infected vertebrate cells. Journal of Virology 64: 1-8.

Roy P, Fukusho A, Ritter G & Lyon D (1988) Evidence for genetic relationship between RNA and DNA viruses from the sequence homology of a putative polymerase gene of bluetongue virus with that of vaccinia virus: Conservation of RNA polymerase genes from diverse species. Nucleic Acids Research 16: 11759-11767.

Roy P, Mertens P & Casal I (1994) African horse sickness virus structure. Comparative Immunology, Microbiology, and Infectious Diseases 17: 243-273.

Rutkowska DA, Mokoena NB, Tsekoa TL, Dibakwane VS & O'Kennedy MM (2019) Plant-produced chimeric virus-like particles - a new generation vaccine against African horse sickness. BMC Veterinary Research 15: 432.

Sambrook J & Russell D (2001) Molecular Cloning: A laboratory manual. Cold Spring Habor Laboratory Press, New York, USA.

Sarno S, Reddy H, Meggio F, Ruzzene M, Davies SP, Donella-Deana A, Shugar D & Pinna LA (2001) Selectivity of 4,5,6,7-tetrabromobenzotriazole, an ATP site-directed inhibitor of protein kinase CK2 (casein kinase-2). FEBS Letters 496: 44-48.

Scanlen M, Paweska JT, Verschoor JA & van Dijk AA (2002) The protective efficacy of a recombinant VP2-based African horsesickness vaccine candidate is determined by adjuvant. Vaccine 20: 1079-1088.

Schulenberg B, Goodman T, Aggeler R, Capaldi R & Patton W (2004) Characterization of dynamic and steady-state protein phosphorylation using a fluorescent phosphoprotein gel stain and mass spectrometry. Electrophoresis 25: 2526-2532.

Sealfon RS, Lin MF, Jungreis I, Wolf MY, Kellis M & Sabeti PC (2015) FRESCo: Finding regions of excess synonymous constraint in diverse viruses. Genome Biology 16: 38.

Shults P, Cohnstaedt L, Adelman Z & Brelsford C (2021) Next-generation tools to control biting midge populations and reduce pathogen transmission. Parasites Vectors 14: 31.

Stassen L, Huismans H & Theron J (2011) Membrane permeabilization of the African horse sickness virus VP5 protein is mediated by two N-terminal amphipathic α-helices. Archives of Virology 156: 711-715.

Stauber N, Martinez-Costas J, Sutton G, Monastyrskaya K & Roy P (1997) Bluetongue virus VP6 protein binds ATP and exhibits an RNA-dependent ATPase function and a helicase activity that catalyse the unwinding of double-stranded RNA substrates. Journal of Virology 71: 7220-7226.

Steinberg T, Agnew B, Gee K, Leung W-Y, Goodman T, Schulenberg B, Hendrickson J, Beechem J, Haugland R & Patton W (2003) Global quantitative phosphoprotein analysis using Multiplexed Proteomics Technology. Proteomics 3: 1128-1144.

Stevens LM, Moffat K, Cooke L, Nomikou K, Mertens PPC, Jackson T & Darpel KE (2019) A low-passage insect-cell isolate of Bluetongue virus uses a macropinocytosis-like entry pathway to infect natural target cells derived from the bovine host. Journal of General Virology 100: 568-582.

Stewart ME & Roy P (2015) Structure-based identification of functional residues in the nucleoside-2'-O-methylase domain of Bluetongue virus VP4 capping enzyme. FEBS Open Bio 5: 138-146.

Stewart ME, Hardy A, Barry G, Pinto RM, Caporale M, Melzi E, Hughes J, Taggart A, Janowicz A & Varela M (2015) Characterization of a second open reading frame in genome segment 10 of Bluetongue virus. Journal of General Virology 96: 3280-3293.

Stoltz M, van der Merwe C, Coetzee J & Huismans H (1996) Subcellular localization of the nonstructural protein NS3 of African horse sickness virus. Onderstepoort Journal of Veterinary Research 63: 57-61.

Stuart DI & Grimes JM (2006) Structural studies of orbivirus proteins and particles. Current Topics in Microbiology and Immunology 309: 221-244.

Sullivan S, Lecollinet S, Kerviel A, Hue E, Pronost S, Beck C, Dumarest M, Zientara S & Roy P (2021) Entry-competent-replication-abortive African horse sickness virus strains elicit robust immunity in ponies against all serotypes. Vaccine 39: 3161-3168.

Sung P-Y & Roy P (2014) Sequential packaging of RNA genomic segments during the assembly of Bluetongue virus. Nucleic Acids Research 42: 13824-13838.

Sung P-Y, Vaughan R, Rahman S, Yi G, Kerviel A, Kao C & Roy P (2019) The interaction of bluetongue virus VP6 and genomic RNA is essential for genome packaging. Journal of Virology 93: e02023.

Sutton G, Grimes J, Stuart D & Roy P (2007) Bluetongue virus VP4 is an RNA-capping assembly line. Nature Structural and Molecular Biology 14: 449-451.

Tan B, Nason R, Stäuber N, Jiang W, Monastyrskaya K & Roy P (2001) RGD tripeptide of bluetongue virus VP7 protein is responsible for attachment to *Culicoides* cells. Journal of Virology 75: 3937-3947.

Taraporewala Z, Chen D & Patton J (2001) Multimers of the bluetongue virus nonstructural protein, NS2, possess nucleotidyl phosphatase activity: Similarities between NS2 and rotavirus NSP2. Virology 280: 21-31.

Tenorio R, Fernández de Castro I, Knowlton JJ, Zamora PF, Sutherland DM, Risco C, Dermody TS. (2019) Function, architecture, and biogenesis of Reovirus replication neoorganelles. Viruses 11: 288.

Theron J & Nel L (1997) Stable protein-RNA interaction involves the terminal domains of bluetongue virus mRNA, but not the terminally conserved sequences. Virology 229: 134-142.

Theron J, Huismans H & Nel LH (1996) Identification of a short domain within the non-structural protein NS2 of epizootic haemorrhagic disease virus that is important for single strand RNA-binding activity. Journal of General Virology 77: 129-137.

Theron J, Uitenweerde JM, Huismans H &Nel LH (1994) Comparison of the expression and phosphorylation of the non-structural protein NS2 of three different orbiviruses, evidence for the involvement of an ubiquitous cellular kinase. Journal of General Virology 75: 3401-3411.

Thomas C, Booth T & Roy P (1990) Synthesis of bluetongue virus-encoded phosphoprotein and formation of inclusion bodies by recombinant baculovirus in insect cells: It binds the single-stranded RNA species. Journal of General Virology 71: 2073-2083.

Thompson G, Jess S & Murche A (2012) A review of African horse sickness and its implications for Ireland. Irish Veterinary Journal 65 (9): 1-8.

Tiwari P, Kaila P & Guptasarma P (2019) Understanding anomalous mobility of proteins on SDS-PAGE with special reference to the highly acidic extracellular domains of human E- and N-cadherins. Electrophoresis 40: 1273-1281.

Turnbull P, Cormack S & Huismans H (1996) Characterization of the gene encoding core protein VP6 of two African horse sickness virus serotypes. Journal of General Virology 77: 1421-1423.

Uitenweerde JM, Theron J, Stoltz MA &Huismans H (1995) The multimeric nonstructural NS2 proteins of bluetongue virus, African horse sickness virus, and epizootic hemorrhagic disease virus differ in their single-stranded RNA-binding ability. Virology 209: 624-632.

Urakawa T, Ritter D & Roy P (1989) Expression of the largest RNA segment and synthesis of VP1 protein of Bluetongue virus in insect cells by recombinant baculovirus: Association of VP1 protein with RNA polymerase activity. Nucleic Acids Research 17: 7395-7401.

van de Water SG, van Gennip RG, Potgieter CA, Wright IM & van Rijn PA (2015) VP2 exchange and NS3/NS3a deletion in African horse sickness virus (AHSV) in development of disabled infectious single animal vaccine candidates for AHSV. Journal of Virology 89: 8764-8772.

van Dijk AA & Huismans H (1980) The *in vitro* activation and further characterisation of the Bluetongue virus-associated transcriptase. Virology 104: 347-356.

van Gennip R, van de Water S & van Rijn P (2014) Bluetongue virus non-structural protein NS3/NS3a is not essential for virus replication. PLoS ONE 9: e85788.

van Gennip R, van de Water S, Potgieter C & van Rijn P (2017) Structural protein VP2 of African horse sickness virus is not essential for virus replication *in vitro*. Journal of Virology 91: e01328.

van Niekerk M, Smit C, Fick W, Van Staden V & Huismans H (2001) Membrane association of African horse sickness virus nonstructural protein NS3 determines its cytotoxicity. Virology 279: 499-508.

van Rensberg I, De Clerk J, Groenewald H & Botha W (1981) An outbreak of African horsesickness in dogs. Journal of the South African Veterinary Medical Association 52: 323-325.

van Sittert SJ, Drew TM, Kotze JL, Strydom T, Weyer CT & Guthrie AJ (2013) Occurrence of African horse sickness in a domestic dog without apparent ingestion of horse meat. Journal of the South African Veterinary Medical Association 84: 1-5.

van Staden V & Huismans H (1991) A comparison of the genes which encode nonstructural protein NS3 of different orbiviruses. Journal of General Virology 72: 1073-1079.

van Staden V, Stoltz M & Huismans H (1995) Expression of nonstructural protein NS3 of African horse sickness virus (AHSV): Evidence for a cytotoxic effect of NS3 in insect cells, and characterization of the gene products in AHSV-infected Vero cells. Archives of Virology 140: 289-306.

Venter G, Graham S & Hamblin C (2000) African horse sickness epidemiology: Vector competence of South African *Culicoides* species for virus serotypes 3, 5 and 8. Medical and Veterinary Entomology 14: 245-250.

Vermaak E & Theron J (2015) Virus uncoating is required for apoptosis induction in cultured mammalian cells infected with African horse sickness virus. Journal of General Virology 96: 1811-1820.

Vermaak E, Conradie A, Maree F & Theron J (2016) African horse sickness virus infects BSR cells through macropinocytosis. Virology 497: 217-232.

Vermaak E, Patterson D, Conradie A & Theron J (2015) Directed genetic modification of African horse sickness virus by reverse genetics. South African Journal of Science 1111: 1-8.

Verwoerd DW & Huismans H (1972) Studies on the *in vitro* and the *in vivo* transcription of the Bluetongue virus genome. Onderstepoort Journal of Veterinary Research 39: 185-191.

Vilardell J, Girardi C, Marin O, Cozza G, Pinna LA & Ruzzene M (2018) The importance of negative determinants as modulators of CK2 targeting. The lesson of Akt2 S131. PloS ONE 13: e0193479.

von Teichman B, Dungu B & Smit T (2010) *In vivo* cross-protection to African horse sickness serotypes 5 and 9 after vaccination with serotypes 8 and 6. Vaccine 28: 6505-6517.

Wall G, Wright I, Barnardo C, Erasmus B, van Staden V & Potgieter C (2021) African horse sickness virus NS4 protein is an important virulence factor and interferes with JAK-STAT signalling during viral infection. Virus Research 298: 198407.

Wehrfritz JM, Boyce M, Mirza S & Roy P (2007) Reconstitution of Bluetongue virus polymerase activity from isolated domains based on a three-dimensional structural model. Biopolymers 86: 83-94.

Wellby MP, Baylis M, Rawlings P & Mellor PS (1996) Effect of temperature on survival and rate of virogenesis of African horse sickness virus in *Culicoides variipennis sonorensis* (Diptera:

Ceratopogonidae) and its significance in relation to the epidemiology of the disease. Bulletin of Entomological Research 86: 715-720.

Weyer C, Grewar J, Burger P, Rossouw E, Lourenst C, Joone C, le Grange M, Coetzee P, Venter EH, Martin DP, MacLachlan NJ & Guthrie A. (2016) African horse sickness caused by genome reassortment and reversion to virulence of live, attenuated vaccine viruses. Emerging Infectious Diseases 22: 2087-2096.

Wirblich C, Bhattacharya B & Roy P (2006) Nonstructural protein 3 of Bluetongue virus assists virus release by recruiting ESCRT-I protein Tsg101. Journal of Virology 80: 460-473.

Wu W & Roy P (2022) Sialic acid binding sites in VP2 of Bluetongue virus and their use during virus entry. Journal of Virology 96: e0167721.

Wu W, Celma CC, Kerviel A & Roy P (2019) Mapping the pH sensors critical for host cell entry by a complex nonenveloped virus. Journal of Virology 93: e01897.

Wu X, Chen S, Iwata H, Compans R & Roy P (1992) Multiple glycoproteins synthesized by the smallest RNA segment (S10) of bluetongue virus. Journal of Virology 66: 7104-7112.

Xia X, Weining Wu W, Cui Y, Roy P & Zhou ZH (2021) Bluetongue virus capsid protein VP5 perforates membranes at low endosomal pH during viral entry. Nature Microbiology 6: 1424-1432.

Xu G, Wilson W, Mecham J, Murphy K, Zhou E-M & Tabachnick W (1997) VP7: An attachment protein of bluetongue virus for cellular receptors in *Culicoides variipennis*. Journal of General Virology 78: 1617-1623.

Xue Y, Ren J, Gao X, Jin C, Wen L & Yao X (2008) GPS 2.0: Prediction of kinase-specific phosphorylation sites in hierarchy. Molecular and Cellular Proteomics 7: 1598-1608.

Zhang X, Boyce M, Bhattacharya B, Zhang X, Schein S, Roy P & Zhou Z (2010) Bluetongue virus coat protein VP2 contains sialic acid-binding domains, and VP5 resembles enveloped virus fusion proteins. Proceedings of the National Academy of Sciences of the United States of America 107: 6292-6297.

Zhang X, Patel A, Celma CC, Yu X, Roy P & Zhou ZH (2016) Atomic model of a nonenveloped virus reveals pH sensors for a coordinated process of cell entry. Nature Structural and Molecular Biology 23: 74-80.

Zhao Y, Thomas C, Bremer C & Roy P (1994) Deletion and mutational analyses of Bluetongue virus NS2 protein indicate that the amino but not the carboxy terminus of the protein is critical for RNA-protein interactions. Journal of Virology 68: 2179-2185.

Zientara S, Weyer C & Lecollinet S (2015) African horse sickness. International Office of Epizootics 34: 315-327.

Zwart L, Potgieter C, Clift S & van Staden V (2015) Characterising non-structural protein NS4 of African horse sickness virus. PLoS ONE 10: e0124281.

APPENDIX

- **NUCLEOTIDE SEQUENCE ALIGNMENT OF A TRUNCATED AHSV-4 NS2 GENE USED IN THE CONSTRUCTION OF pET-NS2**

The sequences provided in this part of the Appendix represent the nucleotide and deduced amino acid sequences of a truncated version of the AHSV-4 NS2 gene, lacking a TGA stop codon, that was cloned into the pET26b(+) bacterial expression vector for expression of the NS2 protein with a hexahistidine tag sequence to facilitate protein purification. Shown are the sequences of the wild-type NS2 gene (pJET-S8), the sequences of the truncated NS2 gene cloned into the pJET/blunt 2.1 cloning vector (pJET-NS2) and the sequences of the truncated NS2 gene cloned in frame with the hexahistidine tag sequence present in pET26b(+) (pET-NS2). The recognition sequences for *Nde*I and *Xho*I, as well as the 6xHis tag sequence are highlighted in turquoise.

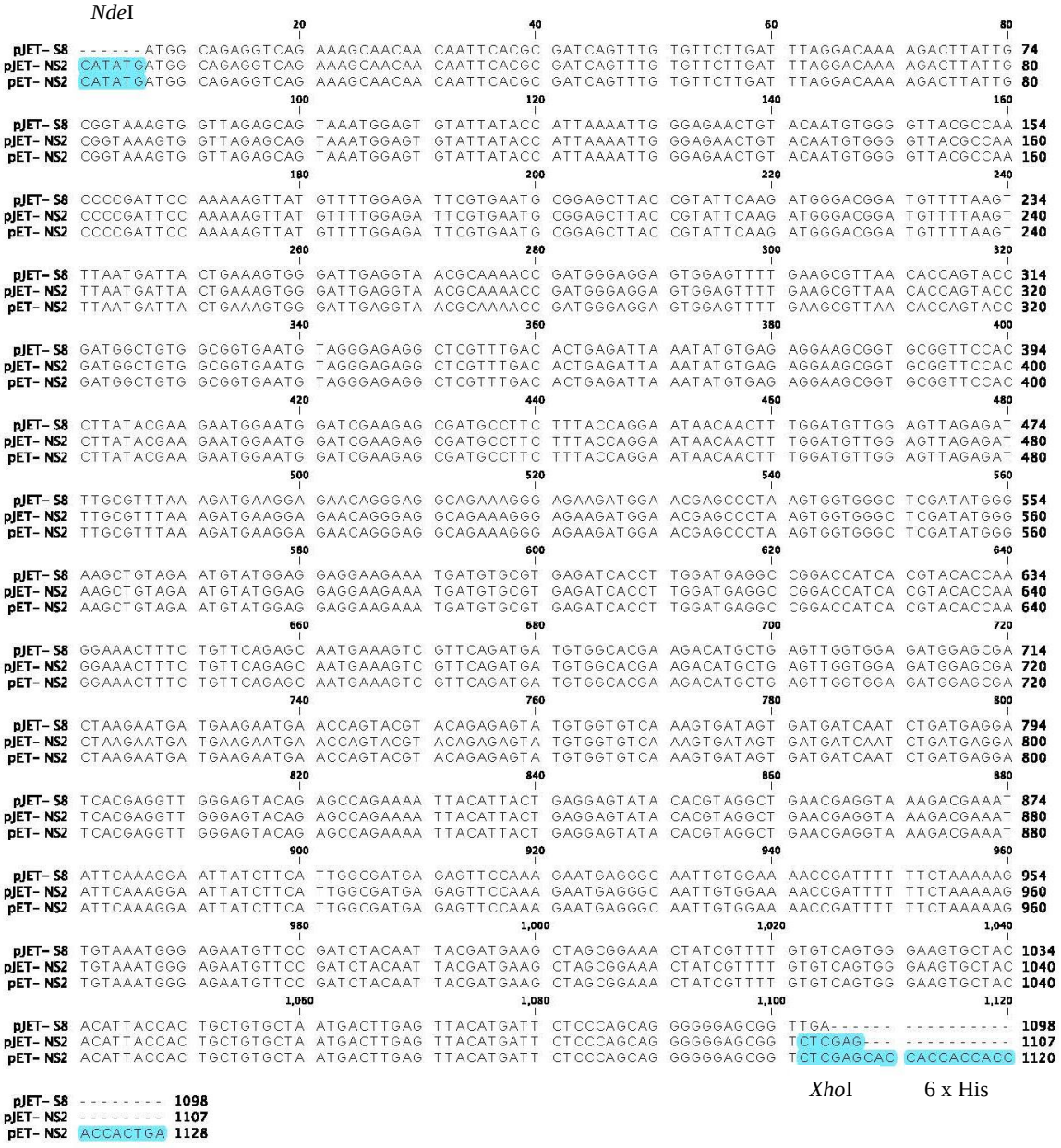

- **AMINO ACID SEQUENCE ALIGNMENT OF A TRUNCATED AHSV-4 NS2 GENE USED IN THE CONSTRUCTION OF pET-NS2**

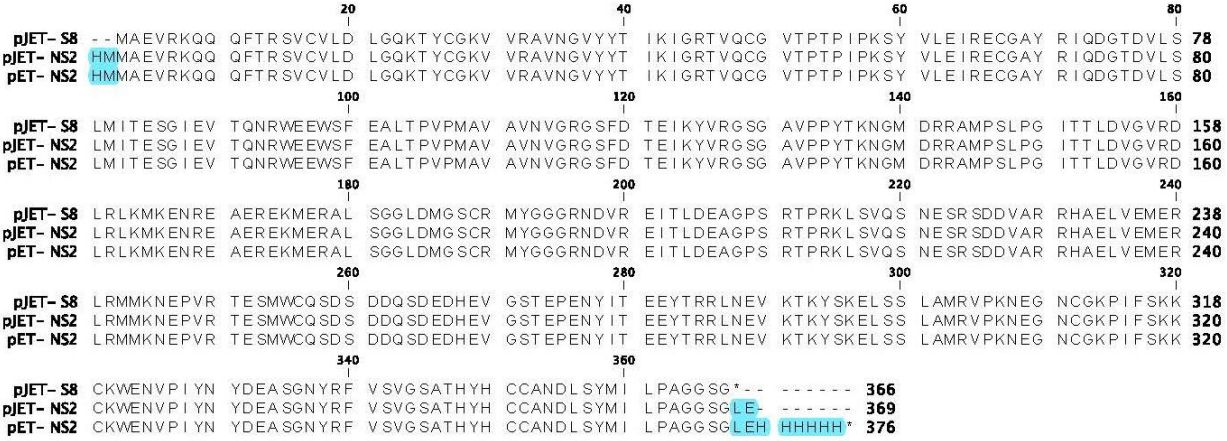

- **NUCLEOTIDE SEQUENCE ALIGNMENT OF AHSV-4 WILD-TYPE AND MUTATED NS2 GENES**

The sequences provided in this part of the Appendix represent the nucleotide and deduced amino acid sequences of the AHSV-4 wild-type and mutated NS2 genes; the latter of which were generated by making use of an inverse PCR-based approach to substitute selected C-terminal serine residues with either alanine or aspartate. These mutations are highlighted in turquoise.

```
                                20                  40                  60                  80
                                |                   |                   |                   |
pJET-S8          ATGGCAGAGG TCAGAAAGCA ACAACAATTC ACGCGATCAG TTTGTGTTCT TGATTTAGGA CAAAAGACTT ATTGCGGTAA 80
pJET-NS2 S-A256  ATGGCAGAGG TCAGAAAGCA ACAACAATTC ACGCGATCAG TTTGTGTTCT TGATTTAGGA CAAAAGACTT ATTGCGGTAA 80
pJET-NS2 S-A258  ATGGCAGAGG TCAGAAAGCA ACAACAATTC ACGCGATCAG TTTGTGTTCT TGATTTAGGA CAAAAGACTT ATTGCGGTAA 80
pJET-NS2 S-A262  ATGGCAGAGG TCAGAAAGCA ACAACAATTC ACGCGATCAG TTTGTGTTCT TGATTTAGGA CAAAAGACTT ATTGCGGTAA 80
pJET-NS2 S-A270  ATGGCAGAGG TCAGAAAGCA ACAACAATTC ACGCGATCAG TTTGTGTTCT TGATTTAGGA CAAAAGACTT ATTGCGGTAA 80
pJET-NS2 S-D256  ATGGCAGAGG TCAGAAAGCA ACAACAATTC ACGCGATCAG TTTGTGTTCT TGATTTAGGA CAAAAGACTT ATTGCGGTAA 80
pJET-NS2 S-D258  ATGGCAGAGG TCAGAAAGCA ACAACAATTC ACGCGATCAG TTTGTGTTCT TGATTTAGGA CAAAAGACTT ATTGCGGTAA 80
pJET-NS2 S-A256,258 ATGGCAGAGG TCAGAAAGCA ACAACAATTC ACGCGATCAG TTTGTGTTCT TGATTTAGGA CAAAAGACTT ATTGCGGTAA 80
pJET-NS2 S-D256,258 ATGGCAGAGG TCAGAAAGCA ACAACAATTC ACGCGATCAG TTTGTGTTCT TGATTTAGGA CAAAAGACTT ATTGCGGTAA 80
                               100                 120                 140                 160
                                |                   |                   |                   |
pJET-S8          AGTGGTTAGA GCAGTAAATG GAGTGTATTA TACCATTAAA ATTGGGAGAA CTGTACAATG TGGGGTTACG CCAACCCCGA 160
pJET-NS2 S-A256  AGTGGTTAGA GCAGTAAATG GAGTGTATTA TACCATTAAA ATTGGGAGAA CTGTACAATG TGGGGTTACG CCAACCCCGA 160
pJET-NS2 S-A258  AGTGGTTAGA GCAGTAAATG GAGTGTATTA TACCATTAAA ATTGGGAGAA CTGTACAATG TGGGGTTACG CCAACCCCGA 160
pJET-NS2 S-A262  AGTGGTTAGA GCAGTAAATG GAGTGTATTA TACCATTAAA ATTGGGAGAA CTGTACAATG TGGGGTTACG CCAACCCCGA 160
pJET-NS2 S-A270  AGTGGTTAGA GCAGTAAATG GAGTGTATTA TACCATTAAA ATTGGGAGAA CTGTACAATG TGGGGTTACG CCAACCCCGA 160
pJET-NS2 S-D256  AGTGGTTAGA GCAGTAAATG GAGTGTATTA TACCATTAAA ATTGGGAGAA CTGTACAATG TGGGGTTACG CCAACCCCGA 160
pJET-NS2 S-D258  AGTGGTTAGA GCAGTAAATG GAGTGTATTA TACCATTAAA ATTGGGAGAA CTGTACAATG TGGGGTTACG CCAACCCCGA 160
pJET-NS2 S-A256,258 AGTGGTTAGA GCAGTAAATG GAGTGTATTA TACCATTAAA ATTGGGAGAA CTGTACAATG TGGGGTTACG CCAACCCCGA 160
pJET-NS2 S-D256,258 AGTGGTTAGA GCAGTAAATG GAGTGTATTA TACCATTAAA ATTGGGAGAA CTGTACAATG TGGGGTTACG CCAACCCCGA 160
                               180                 200                 220                 240
                                |                   |                   |                   |
pJET-S8          TTCCAAAAAG TTATGTTTTG GAGATTCGTG AATGCGGAGC TTACCGTATT CAAGATGGGA CGGATGTTTT AAGTTTAATG 240
pJET-NS2 S-A256  TTCCAAAAAG TTATGTTTTG GAGATTCGTG AATGCGGAGC TTACCGTATT CAAGATGGGA CGGATGTTTT AAGTTTAATG 240
pJET-NS2 S-A258  TTCCAAAAAG TTATGTTTTG GAGATTCGTG AATGCGGAGC TTACCGTATT CAAGATGGGA CGGATGTTTT AAGTTTAATG 240
pJET-NS2 S-A262  TTCCAAAAAG TTATGTTTTG GAGATTCGTG AATGCGGAGC TTACCGTATT CAAGATGGGA CGGATGTTTT AAGTTTAATG 240
pJET-NS2 S-A270  TTCCAAAAAG TTATGTTTTG GAGATTCGTG AATGCGGAGC TTACCGTATT CAAGATGGGA CGGATGTTTT AAGTTTAATG 240
pJET-NS2 S-D256  TTCCAAAAAG TTATGTTTTG GAGATTCGTG AATGCGGAGC TTACCGTATT CAAGATGGGA CGGATGTTTT AAGTTTAATG 240
pJET-NS2 S-D258  TTCCAAAAAG TTATGTTTTG GAGATTCGTG AATGCGGAGC TTACCGTATT CAAGATGGGA CGGATGTTTT AAGTTTAATG 240
pJET-NS2 S-A256,258 TTCCAAAAAG TTATGTTTTG GAGATTCGTG AATGCGGAGC TTACCGTATT CAAGATGGGA CGGATGTTTT AAGTTTAATG 240
pJET-NS2 S-D256,258 TTCCAAAAAG TTATGTTTTG GAGATTCGTG AATGCGGAGC TTACCGTATT CAAGATGGGA CGGATGTTTT AAGTTTAATG 240
                               260                 280                 300                 320
                                |                   |                   |                   |
pJET-S8          ATTACTGAAA GTGGGATTGA GGTAACGCAA AACCGATGGG AGGAGTGGAG TTTTGAAGCG TTAACACCAG TACCGATGGC 320
pJET-NS2 S-A256  ATTACTGAAA GTGGGATTGA GGTAACGCAA AACCGATGGG AGGAGTGGAG TTTTGAAGCG TTAACACCAG TACCGATGGC 320
pJET-NS2 S-A258  ATTACTGAAA GTGGGATTGA GGTAACGCAA AACCGATGGG AGGAGTGGAG TTTTGAAGCG TTAACACCAG TACCGATGGC 320
pJET-NS2 S-A262  ATTACTGAAA GTGGGATTGA GGTAACGCAA AACCGATGGG AGGAGTGGAG TTTTGAAGCG TTAACACCAG TACCGATGGC 320
pJET-NS2 S-A270  ATTACTGAAA GTGGGATTGA GGTAACGCAA AACCGATGGG AGGAGTGGAG TTTTGAAGCG TTAACACCAG TACCGATGGC 320
pJET-NS2 S-D256  ATTACTGAAA GTGGGATTGA GGTAACGCAA AACCGATGGG AGGAGTGGAG TTTTGAAGCG TTAACACCAG TACCGATGGC 320
pJET-NS2 S-D258  ATTACTGAAA GTGGGATTGA GGTAACGCAA AACCGATGGG AGGAGTGGAG TTTTGAAGCG TTAACACCAG TACCGATGGC 320
pJET-NS2 S-A256,258 ATTACTGAAA GTGGGATTGA GGTAACGCAA AACCGATGGG AGGAGTGGAG TTTTGAAGCG TTAACACCAG TACCGATGGC 320
pJET-NS2 S-D256,258 ATTACTGAAA GTGGGATTGA GGTAACGCAA AACCGATGGG AGGAGTGGAG TTTTGAAGCG TTAACACCAG TACCGATGGC 320
                               340                 360                 380                 400
                                |                   |                   |                   |
pJET-S8          TGTGGCGGTG AATGTAGGGA GAGGCTCGTT TGACACTGAG ATTAAATATG TGAGAGGAAG CGGTGCGGTT CCACCTTATA 400
pJET-NS2 S-A256  TGTGGCGGTG AATGTAGGGA GAGGCTCGTT TGACACTGAG ATTAAATATG TGAGAGGAAG CGGTGCGGTT CCACCTTATA 400
pJET-NS2 S-A258  TGTGGCGGTG AATGTAGGGA GAGGCTCGTT TGACACTGAG ATTAAATATG TGAGAGGAAG CGGTGCGGTT CCACCTTATA 400
pJET-NS2 S-A262  TGTGGCGGTG AATGTAGGGA GAGGCTCGTT TGACACTGAG ATTAAATATG TGAGAGGAAG CGGTGCGGTT CCACCTTATA 400
pJET-NS2 S-A270  TGTGGCGGTG AATGTAGGGA GAGGCTCGTT TGACACTGAG ATTAAATATG TGAGAGGAAG CGGTGCGGTT CCACCTTATA 400
pJET-NS2 S-D256  TGTGGCGGTG AATGTAGGGA GAGGCTCGTT TGACACTGAG ATTAAATATG TGAGAGGAAG CGGTGCGGTT CCACCTTATA 400
pJET-NS2 S-D258  TGTGGCGGTG AATGTAGGGA GAGGCTCGTT TGACACTGAG ATTAAATATG TGAGAGGAAG CGGTGCGGTT CCACCTTATA 400
pJET-NS2 S-A256,258 TGTGGCGGTG AATGTAGGGA GAGGCTCGTT TGACACTGAG ATTAAATATG TGAGAGGAAG CGGTGCGGTT CCACCTTATA 400
pJET-NS2 S-D256,258 TGTGGCGGTG AATGTAGGGA GAGGCTCGTT TGACACTGAG ATTAAATATG TGAGAGGAAG CGGTGCGGTT CCACCTTATA 400
                               420                 440                 460                 480
                                |                   |                   |                   |
pJET-S8          CGAAGAATGG AATGGATCGA AGAGCGATGC CTTCTTTACC AGGAATAACA ACTTTGGATG TTGGAGTTAG AGATTTGCGT 480
pJET-NS2 S-A256  CGAAGAATGG AATGGATCGA AGAGCGATGC CTTCTTTACC AGGAATAACA ACTTTGGATG TTGGAGTTAG AGATTTGCGT 480
pJET-NS2 S-A258  CGAAGAATGG AATGGATCGA AGAGCGATGC CTTCTTTACC AGGAATAACA ACTTTGGATG TTGGAGTTAG AGATTTGCGT 480
pJET-NS2 S-A262  CGAAGAATGG AATGGATCGA AGAGCGATGC CTTCTTTACC AGGAATAACA ACTTTGGATG TTGGAGTTAG AGATTTGCGT 480
pJET-NS2 S-A270  CGAAGAATGG AATGGATCGA AGAGCGATGC CTTCTTTACC AGGAATAACA ACTTTGGATG TTGGAGTTAG AGATTTGCGT 480
pJET-NS2 S-D256  CGAAGAATGG AATGGATCGA AGAGCGATGC CTTCTTTACC AGGAATAACA ACTTTGGATG TTGGAGTTAG AGATTTGCGT 480
pJET-NS2 S-D258  CGAAGAATGG AATGGATCGA AGAGCGATGC CTTCTTTACC AGGAATAACA ACTTTGGATG TTGGAGTTAG AGATTTGCGT 480
pJET-NS2 S-A256,258 CGAAGAATGG AATGGATCGA AGAGCGATGC CTTCTTTACC AGGAATAACA ACTTTGGATG TTGGAGTTAG AGATTTGCGT 480
pJET-NS2 S-D256,258 CGAAGAATGG AATGGATCGA AGAGCGATGC CTTCTTTACC AGGAATAACA ACTTTGGATG TTGGAGTTAG AGATTTGCGT 480
                               500                 520                 540                 560
                                |                   |                   |                   |
pJET-S8          TTAAAGATGA AGGAGAACAG GGAGGCAGAA AGGGAGAAGA TGGAACGAGC CCTAAGTGGT GGGCTCGATA TGGGAAGCTG 560
pJET-NS2 S-A256  TTAAAGATGA AGGAGAACAG GGAGGCAGAA AGGGAGAAGA TGGAACGAGC CCTAAGTGGT GGGCTCGATA TGGGAAGCTG 560
pJET-NS2 S-A258  TTAAAGATGA AGGAGAACAG GGAGGCAGAA AGGGAGAAGA TGGAACGAGC CCTAAGTGGT GGGCTCGATA TGGGAAGCTG 560
pJET-NS2 S-A262  TTAAAGATGA AGGAGAACAG GGAGGCAGAA AGGGAGAAGA TGGAACGAGC CCTAAGTGGT GGGCTCGATA TGGGAAGCTG 560
pJET-NS2 S-A270  TTAAAGATGA AGGAGAACAG GGAGGCAGAA AGGGAGAAGA TGGAACGAGC CCTAAGTGGT GGGCTCGATA TGGGAAGCTG 560
pJET-NS2 S-D256  TTAAAGATGA AGGAGAACAG GGAGGCAGAA AGGGAGAAGA TGGAACGAGC CCTAAGTGGT GGGCTCGATA TGGGAAGCTG 560
pJET-NS2 S-D258  TTAAAGATGA AGGAGAACAG GGAGGCAGAA AGGGAGAAGA TGGAACGAGC CCTAAGTGGT GGGCTCGATA TGGGAAGCTG 560
pJET-NS2 S-A256,258 TTAAAGATGA AGGAGAACAG GGAGGCAGAA AGGGAGAAGA TGGAACGAGC CCTAAGTGGT GGGCTCGATA TGGGAAGCTG 560
pJET-NS2 S-D256,258 TTAAAGATGA AGGAGAACAG GGAGGCAGAA AGGGAGAAGA TGGAACGAGC CCTAAGTGGT GGGCTCGATA TGGGAAGCTG 560
                               580                 600                 620                 640
                                |                   |                   |                   |
pJET-S8          TAGAATGTAT GGAGGAGGAA GAAATGATGT GCGTGAGATC ACCTTGGATG AGGCCGGACC ATCACGTACA CCAAGGAAAC 640
pJET-NS2 S-A256  TAGAATGTAT GGAGGAGGAA GAAATGATGT GCGTGAGATC ACCTTGGATG AGGCCGGACC ATCACGTACA CCAAGGAAAC 640
pJET-NS2 S-A258  TAGAATGTAT GGAGGAGGAA GAAATGATGT GCGTGAGATC ACCTTGGATG AGGCCGGACC ATCACGTACA CCAAGGAAAC 640
pJET-NS2 S-A262  TAGAATGTAT GGAGGAGGAA GAAATGATGT GCGTGAGATC ACCTTGGATG AGGCCGGACC ATCACGTACA CCAAGGAAAC 640
pJET-NS2 S-A270  TAGAATGTAT GGAGGAGGAA GAAATGATGT GCGTGAGATC ACCTTGGATG AGGCCGGACC ATCACGTACA CCAAGGAAAC 640
pJET-NS2 S-D256  TAGAATGTAT GGAGGAGGAA GAAATGATGT GCGTGAGATC ACCTTGGATG AGGCCGGACC ATCACGTACA CCAAGGAAAC 640
pJET-NS2 S-D258  TAGAATGTAT GGAGGAGGAA GAAATGATGT GCGTGAGATC ACCTTGGATG AGGCCGGACC ATCACGTACA CCAAGGAAAC 640
pJET-NS2 S-A256,258 TAGAATGTAT GGAGGAGGAA GAAATGATGT GCGTGAGATC ACCTTGGATG AGGCCGGACC ATCACGTACA CCAAGGAAAC 640
pJET-NS2 S-D256,258 TAGAATGTAT GGAGGAGGAA GAAATGATGT GCGTGAGATC ACCTTGGATG AGGCCGGACC ATCACGTACA CCAAGGAAAC 640
```


660 680 700 720
pJET-S8 TTTCTGTTCA GAGCAATGAA AGTCGTTCAG ATGATGTGGC ACGAAGACAT GCTGAGTTGG TGGAGATGGA GCGACTAAGA 720
pJET-NS2 S-A256 TTTCTGTTCA GAGCAATGAA AGTCGTTCAG ATGATGTGGC ACGAAGACAT GCTGAGTTGG TGGAGATGGA GCGACTAAGA 720
pJET-NS2 S-A258 TTTCTGTTCA GAGCAATGAA AGTCGTTCAG ATGATGTGGC ACGAAGACAT GCTGAGTTGG TGGAGATGGA GCGACTAAGA 720
pJET-NS2 S-A262 TTTCTGTTCA GAGCAATGAA AGTCGTTCAG ATGATGTGGC ACGAAGACAT GCTGAGTTGG TGGAGATGGA GCGACTAAGA 720
pJET-NS2 S-A270 TTTCTGTTCA GAGCAATGAA AGTCGTTCAG ATGATGTGGC ACGAAGACAT GCTGAGTTGG TGGAGATGGA GCGACTAAGA 720
pJET-NS2 S-D256 TTTCTGTTCA GAGCAATGAA AGTCGTTCAG ATGATGTGGC ACGAAGACAT GCTGAGTTGG TGGAGATGGA GCGACTAAGA 720
pJET-NS2 S-D258 TTTCTGTTCA GAGCAATGAA AGTCGTTCAG ATGATGTGGC ACGAAGACAT GCTGAGTTGG TGGAGATGGA GCGACTAAGA 720
pJET-NS2 S-A256,258 TTTCTGTTCA GAGCAATGAA AGTCGTTCAG ATGATGTGGC ACGAAGACAT GCTGAGTTGG TGGAGATGGA GCGACTAAGA 720
pJET-NS2 S-D256,258 TTTCTGTTCA GAGCAATGAA AGTCGTTCAG ATGATGTGGC ACGAAGACAT GCTGAGTTGG TGGAGATGGA GCGACTAAGA 720
740 760 780 800
pJET-S8 ATGATGAAGA ATGAACCAGT ACGTACAGAG AGTATGTGGT GTCAAAGTGA TAGTGATGAT CAATCTGATG AGGATCACGA 800
pJET-NS2 S-A256 ATGATGAAGA ATGAACCAGT ACGTACAGAG AGTATGTGGT GTCAAGCCGA TAGTGATGAT CAATCTGATG AGGATCACGA 800
pJET-NS2 S-A258 ATGATGAAGA ATGAACCAGT ACGTACAGAG AGTATGTGGT GTCAAAGTGA TGCCGATGAT CAATCTGATG AGGATCACGA 800
pJET-NS2 S-A262 ATGATGAAGA ATGAACCAGT ACGTACAGAG AGTATGTGGT GTCAAAGTGA TAGTGATGAT CAAGCCGATG AGGATCACGA 800
pJET-NS2 S-A270 ATGATGAAGA ATGAACCAGT ACGTACAGAG AGTATGTGGT GTCAAAGTGA TAGTGATGAT CAATCTGATG AGGATCACGA 800
pJET-NS2 S-D256 ATGATGAAGA ATGAACCAGT ACGTACAGAG AGTATGTGGT GTCAAGACGA TAGTGATGAT CAATCTGATG AGGATCACGA 800
pJET-NS2 S-D258 ATGATGAAGA ATGAACCAGT ACGTACAGAG AGTATGTGGT GTCAAAGTGA TGACGATGAT CAATCTGATG AGGATCACGA 800
pJET-NS2 S-A256,258 ATGATGAAGA ATGAACCAGT ACGTACAGAG AGTATGTGGT GTCAAGCCGA TGCCGATGAT CAATCTGATG AGGATCACGA 800
pJET-NS2 S-D256,258 ATGATGAAGA ATGAACCAGT ACGTACAGAG AGTATGTGGT GTCAAGACGA TGACGATGAT CAATCTGATG AGGATCACGA 800
820 840 860 880
pJET-S8 GGTTGGGAGT ACAGAGCCAG AAAATTACAT TACTGAGGAG TATACACGTA GGCTGAACGA GGTAAAGACG AAATATTCAA 880
pJET-NS2 S-A256 GGTTGGGAGT ACAGAGCCAG AAAATTACAT TACTGAGGAG TATACACGTA GGCTGAACGA GGTAAAGACG AAATATTCAA 880
pJET-NS2 S-A258 GGTTGGGAGT ACAGAGCCAG AAAATTACAT TACTGAGGAG TATACACGTA GGCTGAACGA GGTAAAGACG AAATATTCAA 880
pJET-NS2 S-A262 GGTTGGGAGT ACAGAGCCAG AAAATTACAT TACTGAGGAG TATACACGTA GGCTGAACGA GGTAAAGACG AAATATTCAA 880
pJET-NS2 S-A270 GGTTGGGGCC ACAGAGCCAG AAAATTACAT TACTGAGGAG TATACACGTA GGCTGAACGA GGTAAAGACG AAATATTCAA 880
pJET-NS2 S-D256 GGTTGGGAGT ACAGAGCCAG AAAATTACAT TACTGAGGAG TATACACGTA GGCTGAACGA GGTAAAGACG AAATATTCAA 880
pJET-NS2 S-D258 GGTTGGGAGT ACAGAGCCAG AAAATTACAT TACTGAGGAG TATACACGTA GGCTGAACGA GGTAAAGACG AAATATTCAA 880
pJET-NS2 S-A256,258 GGTTGGGAGT ACAGAGCCAG AAAATTACAT TACTGAGGAG TATACACGTA GGCTGAACGA GGTAAAGACG AAATATTCAA 880
pJET-NS2 S-D256,258 GGTTGGGAGT ACAGAGCCAG AAAATTACAT TACTGAGGAG TATACACGTA GGCTGAACGA GGTAAAGACG AAATATTCAA 880
900 920 940 960
pJET-S8 AGGAATTATC TTCATTGGCG ATGAGAGTTC CAAAGAATGA GGGCAATTGT GGAAAACCGA TTTTTTCTAA AAAGTGTAAA 960
pJET-NS2 S-A256 AGGAATTATC TTCATTGGCG ATGAGAGTTC CAAAGAATGA GGGCAATTGT GGAAAACCGA TTTTTTCTAA AAAGTGTAAA 960
pJET-NS2 S-A258 AGGAATTATC TTCATTGGCG ATGAGAGTTC CAAAGAATGA GGGCAATTGT GGAAAACCGA TTTTTTCTAA AAAGTGTAAA 960
pJET-NS2 S-A262 AGGAATTATC TTCATTGGCG ATGAGAGTTC CAAAGAATGA GGGCAATTGT GGAAAACCGA TTTTTTCTAA AAAGTGTAAA 960
pJET-NS2 S-A270 AGGAATTATC TTCATTGGCG ATGAGAGTTC CAAAGAATGA GGGCAATTGT GGAAAACCGA TTTTTTCTAA AAAGTGTAAA 960
pJET-NS2 S-D256 AGGAATTATC TTCATTGGCG ATGAGAGTTC CAAAGAATGA GGGCAATTGT GGAAAACCGA TTTTTTCTAA AAAGTGTAAA 960
pJET-NS2 S-D258 AGGAATTATC TTCATTGGCG ATGAGAGTTC CAAAGAATGA GGGCAATTGT GGAAAACCGA TTTTTTCTAA AAAGTGTAAA 960
pJET-NS2 S-A256,258 AGGAATTATC TTCATTGGCG ATGAGAGTTC CAAAGAATGA GGGCAATTGT GGAAAACCGA TTTTTTCTAA AAAGTGTAAA 960
pJET-NS2 S-D256,258 AGGAATTATC TTCATTGGCG ATGAGAGTTC CAAAGAATGA GGGCAATTGT GGAAAACCGA TTTTTTCTAA AAAGTGTAAA 960
980 1,000 1,020 1,040
pJET-S8 TGGGAGAATG TTCCGATCTA CAATTACGAT GAAGCTAGCG GAAACTATCG TTTTGTGTCA GTGGGAAGTG CTACACATTA 1040
pJET-NS2 S-A256 TGGGAGAATG TTCCGATCTA CAATTACGAT GAAGCTAGCG GAAACTATCG TTTTGTGTCA GTGGGAAGTG CTACACATTA 1040
pJET-NS2 S-A258 TGGGAGAATG TTCCGATCTA CAATTACGAT GAAGCTAGCG GAAACTATCG TTTTGTGTCA GTGGGAAGTG CTACACATTA 1040
pJET-NS2 S-A262 TGGGAGAATG TTCCGATCTA CAATTACGAT GAAGCTAGCG GAAACTATCG TTTTGTGTCA GTGGGAAGTG CTACACATTA 1040
pJET-NS2 S-A270 TGGGAGAATG TTCCGATCTA CAATTACGAT GAAGCTAGCG GAAACTATCG TTTTGTGTCA GTGGGAAGTG CTACACATTA 1040
pJET-NS2 S-D256 TGGGAGAATG TTCCGATCTA CAATTACGAT GAAGCTAGCG GAAACTATCG TTTTGTGTCA GTGGGAAGTG CTACACATTA 1040
pJET-NS2 S-D258 TGGGAGAATG TTCCGATCTA CAATTACGAT GAAGCTAGCG GAAACTATCG TTTTGTGTCA GTGGGAAGTG CTACACATTA 1040
pJET-NS2 S-A256,258 TGGGAGAATG TTCCGATCTA CAATTACGAT GAAGCTAGCG GAAACTATCG TTTTGTGTCA GTGGGAAGTG CTACACATTA 1040
pJET-NS2 S-D256,258 TGGGAGAATG TTCCGATCTA CAATTACGAT GAAGCTAGCG GAAACTATCG TTTTGTGTCA GTGGGAAGTG CTACACATTA 1040
1,060 1,080
pJET-S8 CCACTGCTGT GCTAATGACT TGAGTTACAT GATTCTCCCA GCAGGGGGGA GCGGTTGA 1098
pJET-NS2 S-A256 CCACTGCTGT GCTAATGACT TGAGTTACAT GATTCTCCCA GCAGGGGGGA GCGGTTGA 1098
pJET-NS2 S-A258 CCACTGCTGT GCTAATGACT TGAGTTACAT GATTCTCCCA GCAGGGGGGA GCGGTTGA 1098
pJET-NS2 S-A262 CCACTGCTGT GCTAATGACT TGAGTTACAT GATTCTCCCA GCAGGGGGGA GCGGTTGA 1098
pJET-NS2 S-A270 CCACTGCTGT GCTAATGACT TGAGTTACAT GATTCTCCCA GCAGGGGGGA GCGGTTGA 1098
pJET-NS2 S-D256 CCACTGCTGT GCTAATGACT TGAGTTACAT GATTCTCCCA GCAGGGGGGA GCGGTTGA 1098
pJET-NS2 S-D258 CCACTGCTGT GCTAATGACT TGAGTTACAT GATTCTCCCA GCAGGGGGGA GCGGTTGA 1098
pJET-NS2 S-A256,258 CCACTGCTGT GCTAATGACT TGAGTTACAT GATTCTCCCA GCAGGGGGGA GCGGTTGA 1098
pJET-NS2 S-D256,258 CCACTGCTGT GCTAATGACT TGAGTTACAT GATTCTCCCA GCAGGGGGGA GCGGTTGA 1098

- **AMINO ACID SEQUENCE ALIGNMENT OF AHSV-4 WILD-TYPE AND MUTANT NS2 PROTEINS**

```
                                20                  40                  60                  80
                                |                   |                   |                   |
          WT NS2 MAEVRKQQQF TRSVCVLDLG QKTYCGKVVR AVNGVYYTIK IGRTVQCGVT PTPIPKSYVL EIRECGAYRI QDGTDVLSLM 80
    NS2 S-A256 MAEVRKQQQF TRSVCVLDLG QKTYCGKVVR AVNGVYYTIK IGRTVQCGVT PTPIPKSYVL EIRECGAYRI QDGTDVLSLM 80
    NS2 S-A258 MAEVRKQQQF TRSVCVLDLG QKTYCGKVVR AVNGVYYTIK IGRTVQCGVT PTPIPKSYVL EIRECGAYRI QDGTDVLSLM 80
    NS2 S-A262 MAEVRKQQQF TRSVCVLDLG QKTYCGKVVR AVNGVYYTIK IGRTVQCGVT PTPIPKSYVL EIRECGAYRI QDGTDVLSLM 80
    NS2 S-A270 MAEVRKQQQF TRSVCVLDLG QKTYCGKVVR AVNGVYYTIK IGRTVQCGVT PTPIPKSYVL EIRECGAYRI QDGTDVLSLM 80
    NS2 S-D256 MAEVRKQQQF TRSVCVLDLG QKTYCGKVVR AVNGVYYTIK IGRTVQCGVT PTPIPKSYVL EIRECGAYRI QDGTDVLSLM 80
    NS2 S-D258 MAEVRKQQQF TRSVCVLDLG QKTYCGKVVR AVNGVYYTIK IGRTVQCGVT PTPIPKSYVL EIRECGAYRI QDGTDVLSLM 80
NS2 S-A256,258 MAEVRKQQQF TRSVCVLDLG QKTYCGKVVR AVNGVYYTIK IGRTVQCGVT PTPIPKSYVL EIRECGAYRI QDGTDVLSLM 80
NS2 S-D256,258 MAEVRKQQQF TRSVCVLDLG QKTYCGKVVR AVNGVYYTIK IGRTVQCGVT PTPIPKSYVL EIRECGAYRI QDGTDVLSLM 80
                               100                 120                 140                 160
                                |                   |                   |                   |
          WT NS2 ITESGIEVTQ NRWEEWSFEA LTPVPMAVAV NVGRGSFDTE IKYVRGSGAV PPYTKNGMDR RAMPSLPGIT TLDVGVRDLR 160
    NS2 S-A256 ITESGIEVTQ NRWEEWSFEA LTPVPMAVAV NVGRGSFDTE IKYVRGSGAV PPYTKNGMDR RAMPSLPGIT TLDVGVRDLR 160
    NS2 S-A258 ITESGIEVTQ NRWEEWSFEA LTPVPMAVAV NVGRGSFDTE IKYVRGSGAV PPYTKNGMDR RAMPSLPGIT TLDVGVRDLR 160
    NS2 S-A262 ITESGIEVTQ NRWEEWSFEA LTPVPMAVAV NVGRGSFDTE IKYVRGSGAV PPYTKNGMDR RAMPSLPGIT TLDVGVRDLR 160
    NS2 S-A270 ITESGIEVTQ NRWEEWSFEA LTPVPMAVAV NVGRGSFDTE IKYVRGSGAV PPYTKNGMDR RAMPSLPGIT TLDVGVRDLR 160
    NS2 S-D256 ITESGIEVTQ NRWEEWSFEA LTPVPMAVAV NVGRGSFDTE IKYVRGSGAV PPYTKNGMDR RAMPSLPGIT TLDVGVRDLR 160
    NS2 S-D258 ITESGIEVTQ NRWEEWSFEA LTPVPMAVAV NVGRGSFDTE IKYVRGSGAV PPYTKNGMDR RAMPSLPGIT TLDVGVRDLR 160
NS2 S-A256,258 ITESGIEVTQ NRWEEWSFEA LTPVPMAVAV NVGRGSFDTE IKYVRGSGAV PPYTKNGMDR RAMPSLPGIT TLDVGVRDLR 160
NS2 S-D256,258 ITESGIEVTQ NRWEEWSFEA LTPVPMAVAV NVGRGSFDTE IKYVRGSGAV PPYTKNGMDR RAMPSLPGIT TLDVGVRDLR 160
                               180                 200                 220                 240
                                |                   |                   |                   |
          WT NS2 LKMKENREAE REKMERALSG GLDMGSCRMY GGGRNDVREI TLDEAGPSRT PRKLSVQSNE SRSDDVARRH AELVEMERLR 240
    NS2 S-A256 LKMKENREAE REKMERALSG GLDMGSCRMY GGGRNDVREI TLDEAGPSRT PRKLSVQSNE SRSDDVARRH AELVEMERLR 240
    NS2 S-A258 LKMKENREAE REKMERALSG GLDMGSCRMY GGGRNDVREI TLDEAGPSRT PRKLSVQSNE SRSDDVARRH AELVEMERLR 240
    NS2 S-A262 LKMKENREAE REKMERALSG GLDMGSCRMY GGGRNDVREI TLDEAGPSRT PRKLSVQSNE SRSDDVARRH AELVEMERLR 240
    NS2 S-A270 LKMKENREAE REKMERALSG GLDMGSCRMY GGGRNDVREI TLDEAGPSRT PRKLSVQSNE SRSDDVARRH AELVEMERLR 240
    NS2 S-D256 LKMKENREAE REKMERALSG GLDMGSCRMY GGGRNDVREI TLDEAGPSRT PRKLSVQSNE SRSDDVARRH AELVEMERLR 240
    NS2 S-D258 LKMKENREAE REKMERALSG GLDMGSCRMY GGGRNDVREI TLDEAGPSRT PRKLSVQSNE SRSDDVARRH AELVEMERLR 240
NS2 S-A256,258 LKMKENREAE REKMERALSG GLDMGSCRMY GGGRNDVREI TLDEAGPSRT PRKLSVQSNE SRSDDVARRH AELVEMERLR 240
NS2 S-D256,258 LKMKENREAE REKMERALSG GLDMGSCRMY GGGRNDVREI TLDEAGPSRT PRKLSVQSNE SRSDDVARRH AELVEMERLR 240
                               260                 280                 300                 320
                                |                   |                   |                   |
          WT NS2 MMKNEPVRTE SMWCQSDSDD QSDEDHEVGS TEPENYITEE YTRRLNEVKT KYSKELSSLA MRVPKNEGNC GKPIFSKKCK 320
    NS2 S-A256 MMKNEPVRTE SMWCQADSDD QSDEDHEVGS TEPENYITEE YTRRLNEVKT KYSKELSSLA MRVPKNEGNC GKPIFSKKCK 320
    NS2 S-A258 MMKNEPVRTE SMWCQSDADD QSDEDHEVGS TEPENYITEE YTRRLNEVKT KYSKELSSLA MRVPKNEGNC GKPIFSKKCK 320
    NS2 S-A262 MMKNEPVRTE SMWCQSDSDD QADEDHEVGS TEPENYITEE YTRRLNEVKT KYSKELSSLA MRVPKNEGNC GKPIFSKKCK 320
    NS2 S-A270 MMKNEPVRTE SMWCQSDSDD QSDEDHEVGA TEPENYITEE YTRRLNEVKT KYSKELSSLA MRVPKNEGNC GKPIFSKKCK 320
    NS2 S-D256 MMKNEPVRTE SMWCQDDSDD QSDEDHEVGS TEPENYITEE YTRRLNEVKT KYSKELSSLA MRVPKNEGNC GKPIFSKKCK 320
    NS2 S-D258 MMKNEPVRTE SMWCQSDDDD QSDEDHEVGS TEPENYITEE YTRRLNEVKT KYSKELSSLA MRVPKNEGNC GKPIFSKKCK 320
NS2 S-A256,258 MMKNEPVRTE SMWCQADADD QSDEDHEVGS TEPENYITEE YTRRLNEVKT KYSKELSSLA MRVPKNEGNC GKPIFSKKCK 320
NS2 S-D256,258 MMKNEPVRTE SMWCQDDDDD QSDEDHEVGS TEPENYITEE YTRRLNEVKT KYSKELSSLA MRVPKNEGNC GKPIFSKKCK 320
                               340                 360
                                |                   |
          WT NS2 WENVPIYNYD EASGNYRFVS VGSATHYHCC ANDLSYMILP AGGSG* 366
    NS2 S-A256 WENVPIYNYD EASGNYRFVS VGSATHYHCC ANDLSYMILP AGGSG* 366
    NS2 S-A258 WENVPIYNYD EASGNYRFVS VGSATHYHCC ANDLSYMILP AGGSG* 366
    NS2 S-A262 WENVPIYNYD EASGNYRFVS VGSATHYHCC ANDLSYMILP AGGSG* 366
    NS2 S-A270 WENVPIYNYD EASGNYRFVS VGSATHYHCC ANDLSYMILP AGGSG* 366
    NS2 S-D256 WENVPIYNYD EASGNYRFVS VGSATHYHCC ANDLSYMILP AGGSG* 366
    NS2 S-D258 WENVPIYNYD EASGNYRFVS VGSATHYHCC ANDLSYMILP AGGSG* 366
NS2 S-A256,258 WENVPIYNYD EASGNYRFVS VGSATHYHCC ANDLSYMILP AGGSG* 366
NS2 S-D256,258 WENVPIYNYD EASGNYRFVS VGSATHYHCC ANDLSYMILP AGGSG* 366
```